

UNIVERSITAT DE BARCELONA

FACULTAT DE FARMÀCIA

DEPARTAMENT DE FARMÀCIA I TECNOLOGIA FARMACÈUTICA
Unitat de Farmàcia i Tecnologia Farmacèutica

TARGETING OF ANTILEISHMANIAL DRUGS PRODUCED BY
NANOTECHNOLOGIES

GEORGINA PUJALS I NARANJO

Barcelona, 2007

EXPERIMENTAL SECTION

5. DEVELOPMENT OF MEGLUMINE ANTIMONIATE FORMULATION

5.1. INTRODUCTION

The present development of a new dosage form of MGA starts with the elaboration of emulsions, self-emulsifying drug delivery systems and nanosuspensions. However, the main part is centralized by the microencapsulation of MGA by spray drying using the preliminary studies as reference and the polymer chitosan as the main excipient. Spray drying technique has been used to elaborate two kinds of nano/microspheres, on one side those which come from emulsions and on the other side those which come from solutions. Both cases have been morphologically characterized and their effectiveness has been studied *in vitro* against *Leishmania* parasites. Moreover, the ability to be phagocytosed by macrophages cells has been investigated using quantum dots assisted imaging in the Department of Pharmaceutical Sciences of the University of Connecticut during a stage.

Lipidic microspheres are developed following an experimental design which leads to study the influence of lipid concentration, inlet temperature and emulsification method on morphological properties, residual moisture, and yield of the process and efficiency of encapsulation. Some lipidic components used in these formulations have been selected with the intention to reverse antimony resistance mediated by P-glycoprotein. In order to elucidate the influence of these P-glycoprotein inhibitors on effectiveness, a specific group of formulations have been developed and tested *in vitro* against *Leishmania*.

Nano/microspheres which come from solutions are studied using a fractional experimental design where dissolution studies and effectiveness against *Leishmania* are also included.

The *in vitro* parasitological studies of each group of microspheres are described in the last part of the effort and they have been organized according to the same structure of the technological sections.

The results and their discussions are exposed together in order to facilitate the understanding of the process or formulation modifications during the investigation line.

Those microspheres selected for the treatment of leishmaniasis which produced activity against *Leishmania in vitro*, showed a good ability to be phagocytosed by macrophages,

were not cytotoxic, it would be an ideal candidate for a continuation of the investigation line in a near future. For example, it would be interesting to include this primary MGA delivery device into a second pharmaceutical dosage form which could be tested *in vivo* such as capsules, tablets, etc. by oral route or implants by parenteral route..

5.2. MATERIALS

In this section, the materials used in this investigation are listed according to if they are chemicals, parasite strains, cultures, equipments or software's.

Among the chemicals, one of the excipients utilized to develop the new MGA dosage form, chitosan, polymer used to microencapsulate the drug by spray drying, is considered the compound most important of this effort. For this reason, before to list all the material used, it is believed necessary to describe chitosan interesting properties that lead us to select it as main biopolymer.

5.2.1. Chitosan

5.2.1.1. Physicochemical properties

Chitosan is a cationic polysaccharide comprising copolymers of glucosamine and N-acetylglucosamine and can be derived by partial deacetylation of chitin from crustacean shells (figure 28) (Illum L., 1998). It is also naturally present in some microorganisms, insects and fungi such as *Aspergillus niger* (Singla A.K. and Chawla M., 2001). The term chitosan is used to describe a series of chitosan polymers with different molecular weights (50 kDa-2000 kDa), viscosity (1% chitosan in 1% acetic acid, < 2000 mPaS), and degree of deacetylation (40 % - 98 %). Chitosan is insoluble at neutral and alkaline pH values but forms salts with inorganic and organic acids such as acetic acid. Upon dissolution, the amine groups are protonated and the resultant soluble polysaccharide is positively charged. However, chitosan salts are soluble in water, the solubility being dependent on the degree of deacetylation. The viscosity of a chitosan solution increases in viscosity with rise in chitosan concentration and decrease in temperature. The viscosity also increases with rising degree of deacetylation (Illum L., 1998, Singla A.K. and Chawla M., 2001).

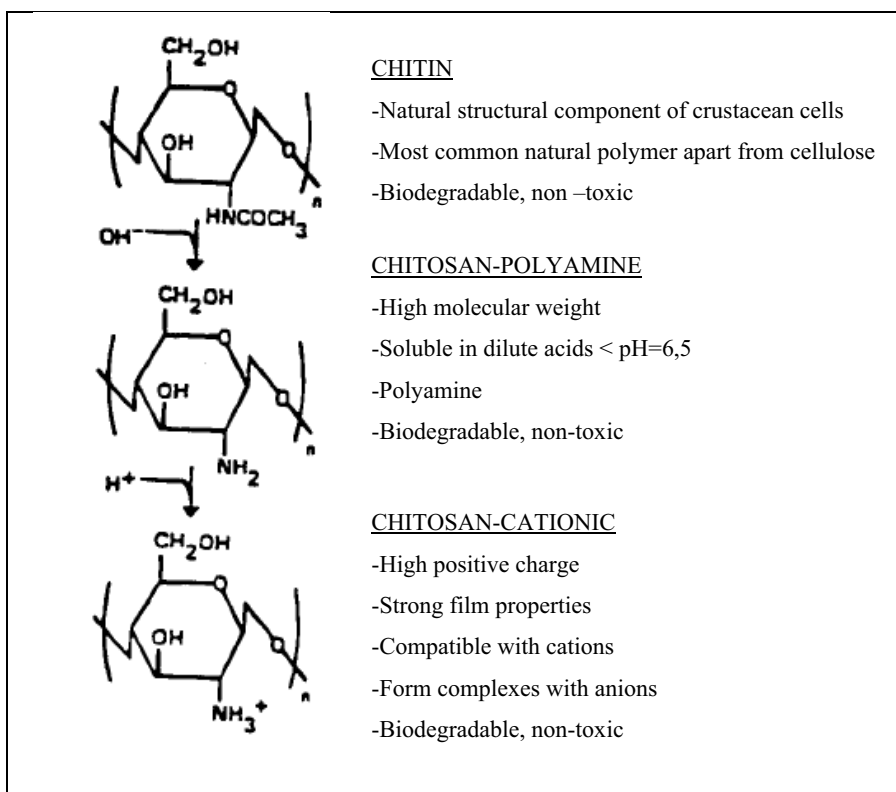


Figure 28: Chitin and chitosan (Illum L., 1998)

5.2.1.1. Biological properties

Chitosan possess low toxicity, is only slightly allergenic, exerts moderate immunostimulating effects and is also metabolised by lysosomes. *In vivo* toxicity studies show chitosan to be inert, non-toxic and biodegradable. The LD₅₀ (lethal dose 50) of chitosan in mice was determined greater than 16 g·kg⁻¹ (Singla A.K. and Chawla M, 2000). A summary of the biomedical properties of chitosan is given in table 8.

Application	Reference
Haemostatic	Hoekstra A. et al.,1998, Gustafson SB. et al., 2007
Antibacterial	Suzuki K. et al., 1984, Guo Z. et al.,2006, Jumaa M. et al., 2002, Felt O. et al., 2000, Gerasimenko D.V. et al., 2004.
Immunitization	Porporatto C. et al., 2003, 2005.
Anticarcinogen	Qi L. et al., 2007.
Anticholesterolemic	Jing S.B. et al., 1997, Gallaher D.D. et al., 2002
Contact lens care	Hong B.-S. et al.,2004
Renal failure	Jing S.B. et al., 1997
Wound healing-absorbable sutures	Kim J., 1999, Gustafson S.B. et al., 2007
Eye bandages-forms tough protective coating	Paul W.and Sharma C.P., 2000
Dental-bioadhesive	Aksungur P. et al., 2004
Orthopaedic-temporary bioengineering material	Andersson M., 2006

Table 8: Biomedical properties of chitosan

Studies in dogs reflected that suspensions of chitin and chitosan induced chemokinetic migrations of the neutrophils and produced accumulation of them to chitin-chitosan implanted regions (Usami Y. et al. 1994, 1998). If it is also considered that chitosan has the capacity to interact with mannosyl receptors of macrophages, it is logically to deduce that the process of recognition of the MGA delivery system will be facilitated if chitosan is used in microparticles forms. Moreover, it is believed that the binding of chitosan to the specific receptor is thought to be a prerequisite for enhancing macrophages activation (Porporatto C. et al., 2003, Feng J. et al., 2004, Mori T. et al., 2005, Han Y. et al., 2005).

5.2.1.2. Chitosan as pharmaceutical excipient

Several important applications of chitosan as an excipient in pharmaceutical products are being investigated (listed in table 9), however few registered pharmaceutical products have been found. The 3M company in UK has marketed TegisorbTM a wound healing product containing chitosan. For veterinary wound healing, the company Sunfive Inc. (Japan) has now developed and marketed cotton of chitosan (Chitopak TMC) and chitosan suspension (Chitofine TMS).

Chitosan has been extensively examined in the pharmaceutical industry for its potential in the development of controlled release drug delivery systems due to its unique polymeric cationic character and its gel and film properties. Chitosan is considered an absorption enhancer for hydrophilic drugs across the intestinal (Schipper N.G.M. et al., 1996, Hejazi R. and Amiji M., 2003, Prego. C. et al., 2005) and nasal mucosa (Fernandez-Urrusuno R. et al. 1999, Yang M. et al., 2007)) due to its positive charge which changes the permeability of the epithelia (Fang N., 2001). Chitosan also enhances the absorption of drugs in buccal (Sandri G. et al., 2006) and pulmonary mucosal surfaces (Huang Y.C. et al., 2002, Grenha A. et al., 2005) and through the ophthalmic epithelium (Genta I. et al., 1997).

As chitosan has good film forming properties, it has been used as a coating material for the production of microparticles of an extensive quantity of drugs for many purposes and by different techniques. Taking into account all the properties mentioned above, it is thought convenient to select chitosan as the biopolymer to encapsulate MGA.

<u>Conventional formulations</u>	<u>Novel applications</u>
Directly compressible vehicle for tablets Controlled release matrix tablets Tablet binder Wet granulation Gels Films Emulsions Wetting agent Coating agent Microspheres and microcapsules	Bioadhesion Transmucosal drug transport Vaccine delivery DNA delivery
Table 9: Pharmaceutical applications of chitosan (Illum L., 1998; Singla A.K., 2001)	

5.2.2. Chemicals

Antimonials

- Antimony atomic absorption standard solution, 1,000 µg/mL Sb in 8 wt. % HCl. Lot num. 03826 EF. Aldrich (Milwaukee, USA).
- Meglumine antimoniate (Glucantime[®]): in preformulation experiments: 1: human lot num 04003/1, lot num. 04003 from Aventis Pharma (Barcelona, Spain) and 2: veterinarian lot: 647 E. MERIAL Lab. (Lyon,France), the last one used in parasitic assays too.
- Meglumine antimoniate powder: lot num. 0425200 from Aventis. Inspection lot num. 4145236.

Excipients and auxiliary material

- Medium-chain Triglycerides (MCT): Triglycerides of caprylic/capric acid:
 1. Estasan[®]: lot num. 0017591, Uniquema, comercial Química Massó, (Barcelona,Spain).
 2. Labrafac CC[®]: lot num. 45050325, Gattefossé (Saint Priest Cedex, France).
 3. Captex 300[®]: lot num. 060709-7, Abitec Corporation (Northampton, US).

- Polyoxyethylen (20)-sorbitan mono-oleat (Tween 80[®]): lot num. 0306150, Roig Farma,S.A. (Terrassa, Spain).
- Polyoxyl 40 hydrogenated Castor Oil (P40HCO):
 1. Cremophor RH-40[®]: lot num. 0305133, Roig Farma, S.A. (Terrassa, Spain).
 2. Lipocol LAV HCO-40[®]: lot num. P-216G4, Lipo chemicals (New Jersey, US).
- Deoiled soy lecithin:
 1. Lecimuthin 100[®]: sample Degussa Texturant Systems, Cargill (Hamburg, Deutschland).
 2. Lecimulthin 150[®]: sample Degussa Texturant Systems, Cargill (Minneapolis, US).
- Fluid lecithin: Topcithin NGM[®]: lot num 2360432. Degussa Texturant Systems, Cargill (Hamburg, Deutschland).
- Maltodextrin:
 1. Glucidex[®] 19D and 6D: sample of Roquette, (Lestrem, France).
 2. Maltodextrin dextrose equivalent: 16,5-19,5: lot num 1416D: Aldrich Chemical Company,Inc, (St.Louis, US).
- Chitosan:
 1. Deacetylation degree > 85%, viscosity < 500 mPaS. lot num: ACID 268/14, Bioiberica (Palafolls, Spain) from Primex (Siglufjordur, Iceland).
 2. Chito Clear[®]. Deacetylation degree 95%, viscosity 80 mPaS: lot num: TM2570, Primex (Siglufjordur, Iceland).
- Sorbitan monooleate (Span 85[®]): Uniquema, Comercial Química Massó (Barcelona, Spain).
- Potassium sorbate: lot num 0304033, Roig Farma, S.A. (Terrassa, Spain).
- Coloidal Silica Dioxide (Aerosil 200[®]): lot num 50420110. Degussa-Hüls (Barcelona, Spain).
- Butylhydroxytoluene: lot num 0306174. Roig Farma (Terrassa, Spain).
- PLGA (poly(lactic-co-glycolic acid): (50:50; MW:60.000; Resomer RG504). Boehringer Ingelheim (Ridgefield, CT, USA).
- PVA (Polyvinyl acetate): (MW, 30 000-70 000). Sigma Chemical Co. (St Louis, MO, USA).

- Dialysis sacs: Dialysis tubing, high retention seamless cellulose tubing avg. flat width 32 mm (1.3 in.), Sigma-Aldrich (Steinheim, Germany).
- PVDF filters of 25 mm of diameter and 0,45 µm of porous. Millipore. (Billerica, USA).
- Quantum dots (QDs): CdSe/ZnS (core/shell) hydrophobic QDs in a 80:20 mixture of polyethylene glycol (PEG)-functionalized phospholipids, 1,2-distearoyl-sn-glycero-3-phosphoethanolamine-N-[methoxy(polyethyleneglycol)-2000] (ammonium salt) (PEG-PE2000) (Storrs, US).

Reagents

All solutions were prepared from analytical grade chemicals and only distilled/deionised water was used.

- Glutaraldehyde solution 25 % .Panreac (Castellar del Vallès, Spain)
- Glacial acetic acid. Quality Chemicals (Palafolls, Spain)
- Hydrochloric acid 37 %. Panreac (Castellar del Vallès, Spain)
- Dimethyl sulfoxide (DMSO). Sigma D-2650 (Steinheim, Germany).
- 1N NaOH. Panreac (Castellar del Vallès, Spain)
- NaS.H₂O. Panreac (Castellar del Vallès, Spain)
- Sulfuric acid. Panreac (Castellar del Vallès, Spain)
- Potassium chloride. Roig Farma (Terrassa, Spain)
- 1% TRITON X-100. Dow Chemical (Michigan, USA).
- p-Nitrophenyl phosphate Sigma N-6260 (Steinheim, Germany).
- Potassium dihydrogenphosphate. Panreac (Castellar del Vallès, Spain).
- Trypan blue dye. Merck (Darmstadt, Germany).
- Giemsa dye. Merck (Darmstadt, Germany).

5.2.3. Parasite strains and cultures

- *L.infantum* strain MCAN/ES/92/BCN83 (BCN83). (*Leishmania* Criobanc of “Grup de Parasitologia Clínica de la Universitat de Barcelona”, Barcelona, Spain).
- Schneider’s insect medium (Sigma G-1397), (Steinheim, Germany), pH 7, containing 20 % previously tested heat-inactivated fetal calf serum (Gibco lot

40Q1735X), Invitrogen (California, USA), 25 µg/ml gentamicin solution (Sigma G-1397), (Steinheim, Germany), and 1 % penicillin (100 U/ml)-streptomycin (100 µg/ml) solution (Gibco BRL 15140-114), Invitrogen (California, USA).

- Peritoneal murine (SWISS) macrophage cells (Barcelona, Spain).
- RPMI-1640 (Bio-Whittaker 12-115) supplemented with 10% heat inactivated fetal calf serum, Invitrogen (California, USA).
- Chamber slide system (Nunc 177402), Nalge Nunc International (Rochester, USA).
- 96-well microtitre plates (Costar 3595), Corning Inc. (NY, USA).
- 8-well LabTekII chamber glass slides Nalge Nunc International (Rochester, USA).
- Neubauer count chamber, Labor Optic (Friedrichsdorf, Germany).
- MHA cells (Storrs, USA).
- RAW cells (Storrs, USA).
- Hanks Balanced salt solution, Sigma-Aldrich (St.Louis, USA).
- Lipofectin[®], Invitrogen (California, USA).

5.2.4. Equipments

5.2.4.1. Equipments for development

- Telstar Liolabor 3 freeze-drier apparatus (Terrassa, Spain).
- Balances: Precisa 600C (Dietikon, Switzerland), Sartorius BP211D (Goettingen, Germany).
- Helix mixer Heidolph[®] (Cambridgeshire, US).
- High speed mixer Janke & Kunkel, IKA[®], Labortechnik (Staufen, Germany).
- High speed mixer Powergen[®] 700 D, Fischer scientific (Pittsburg, US).
- High pressure homogenizer Emulsiflex[®] -C3 apparatus, Avestin (Manheim, Germany).
- High pressure homogenizer Microfluidizer[®], Microfluidics (Massachusetts, US).
- Büchi[®] Mini Spray Dryer B-290 apparatus (Postfach, Switzerland)
- Büchi[®] Dehumidifier B-296 apparatus (Postfach, Switzerland)
- Büchi[®] Mini Spray Dryer B-190 apparatus (Postfach, Switzerland)

5.2.4.2. Equipments for pharmaceutical products characterization

- Antimony richness: ICP-OES (Inductively Coupled Plasma Optical Emission Spectroscopy) Perkin Elmer Elan Optima 3200 RLs (Massachusetts, USA).
- Infrareds: Spectroscopometer Perkin Elmer FT-IR (Massachusetts, USA).
- X-rays: Diffractometer PANalytical X'Pert PRO (Almelo, The Netherlands).
- Differential Scanning Calorimeter (DSC) 822e Mettler Toledo apparatus (Greifensee, Switzerland).
- Particle sizer: Beckman[®] Coulter model LS 13, 320 (California, USA) and Accusizer[®] 780 A Autodiluter. Particle sizing system (California, USA).
- pH metre Crison[®] (Herisau, Switzerland).
- Viscosimeter Brookfield RVT (Massachusetts, USA).
- Optical microscope JENA[®] 421021 (USA)
- Scanning Electronic Microscope: Hitachi[®] 2300 (Krefeld, Germany), Hitachi S-4100 (Krefeld, Germany).
- Phillips environmental scanning electron microscope (ESEM). FEI Company (Hillsboro, US).
- Karl-Fisher 703 TiStand apparatus. Metrohm (Buckingham, UK).
- Z-potential: Zetasizer Nano S, Malvern Instruments (Worcestershire, UK), Zetaplus apparatus. Brookhaven Instruments (Hotsville, NY).
- Leica SP2 Spectral Confocal Microscope (Bannockburn, USA).
- Spectrofluorometer SPEX Fluorolog 3, Horiba (New Jersey, USA).
- Dissolution apparatus: Turu Grau T-6. (Barcelona, Spain).

5.2.4.3. Equipments for biological assays

- Thermostatic bath SBS and P. Selecta precistern (Barcelona, Spain).
- OVAN vibra mix. Lovango (Barcelona, Spain).
- Tittertek Multiscan Plus. 405nm (Helsinki, Finland).
- Heater P. Selecta Mod.207 n° 141949, V220, W280 (Barcelona, Spain).
- Heater Heraeus 6000, 5% CO₂, 37° C (Hanau, Germany).
- Climatic room 24-26° C.
- Hood Telstar AV-30/70 (parasitic cultures) (Terrassa, Spain).
- Hood Telstar Bio II-AR (macrophages cultures) (Terrassa, Spain).

- Microscope Olympus CH-2 (Barcelona, Spain).
- Inverted microscope Leica (Barcelona, Spain).
- Balances Precisa 160M and Sartorius (Goettingen, Germany).

5.2.5. Specific software

- Statgraphics Plus 5.1. (Statistical Graphics Corp., USA).
- SPSS 12.0 for windows (SPSS Inc., Chicago, IL).
- WinNonlin 4.1., Pharsight (California, USA).
- Image J 1.38x. (National Institutes of Health, USA).

5.3. METHODS

5.3.1. Obtention of meglumine antimoniate by lyophilization

Freeze drying (also known as lyophilisation) works by freezing the material and then reducing the surrounding pressure and adding enough heat to allow the frozen water in the material to sublime directly from the solid phase to gas.

Two boxes of 10 vials of 5 ml (lot 04003/1) and one box (lot 04003) of Glucantime[®] to humane use from Aventis Pharma lab, and 2 boxes of 5 vials of 5 ml (lot 675E) of Glucantime[®] to vet use from Merial lab were lyophilized.

Conditions of lyophilization :

- 3 hours freezing at -40 °C.
- Starting heating liquid at +30 °C (for 21 hours).
- Final drying at +40 °C (for 17 hours).
- Final vacuum at 100 μ column Hg.

Once the lyophilized product is obtained, it is passed through a sieve of 0,6 mm and followed through 0,1 mm.

5.3.2. Characterization of meglumine antimoniate

Drug characterization is necessary to know properly the possible difficulties which can disturb the development processes of the new formulations. The properties between MGA obtained by lyophilisation and the pure drug obtained as a gift by Sanofi-Aventis are compared.

5.3.2.1. Antimony purity

The antimony purity is analysed in order to verify the Sb^V declared value in Glucantime[®] vials, which is 28,3 % for humans and it is not declared in the veterinarian form. Declared Sb^V content in pure MGA from Sanofi-Aventis is 27,1 % and $Sb^{III} < 0,01$ %. The variability of Sb^V and Sb^{III} in different batches of Glucantime[®] and generic drugs in the market has been reported by Franco M.A. et al., 1995, Rath S. et al., 1997 and Guerin P.J. et al., 2002.

The technique used is ICP-OES (Inductively Coupled Plasma Optical Emission Spectrometry). It is a type of emission spectroscopy that uses a plasma (e.g. inductively coupled plasma) to produce excited atoms that emit electromagnetic radiation at a wavelength characteristic of a particular element. The intensity of this emission is indicative of the concentration of the element within the sample. The limitation of this technique is not to differentiate the oxidation state of Sb.

Methodology used:

Preparation of the sample in powder state (lyophilised Glucantime[®] vials): Digestion of 0,05 g of sample, weighted in balance with sensibility 0,01 mg, with HNO_3 and H_2O_2 (“Baker Instra”) in high pressure teflon reactors, in microwave “Milestone Ethos Plus”, at 220 °C. The digested sample is diluted with HCl 1 ml and milli-Q water to 50 ml. Digestions were done with three different samples.

Preparation of the pure MGA sample: Weight of 10,00 mg of MGA in balance with sensibility 0,01 mg which will be dissolved in 0,1M HCl 50 ml or distilled water. Sonicate for 1 minute, then pass it through filter 0,45 mm. Three different calibration curves were measured:

1. External calibration in dilution medium (1 % HNO₃ + 0,5 % HF (solution A)).
2. Standard addition in problem aqueous solution diluted 1/5 with solution A.
3. Standard addition in problem HCl aqueous solution diluted 1/5 with solution A.

In case that meglumine structure affected in the quantification of Sb, different slopes of the curves would be obtained and then, the values of Sb resulted of each equation would be different.

Determination: Determination of total Sb by ICP-OES is carried out in PERKIN ELMER ELAN Optima 3200 RLs apparatus (figure 29) in standard conditions and calibrated with four standards prepared with solution A. 1/5 sample dilutions with solution A are done. Lectures were made by triplicate, at two different wavelengths (206,836 nm and 217,582 nm) for improving the precision, although the first one is where Sb has the maximum pick of emission.



Figure 29: Perkin Elmer Elan Optima 3200 RLs (left). Flame obtained by ICP_OES (right).

5.3.2.2. IR Assay

Using infrared spectroscopy technique by a Perkin Elmer FT-IR spectrometer-RX1, lyophilised and pure substance sample are analysed. Their spectrums will be compared to the available spectrum from Demichelli C. et al., 1999 (figure 30).

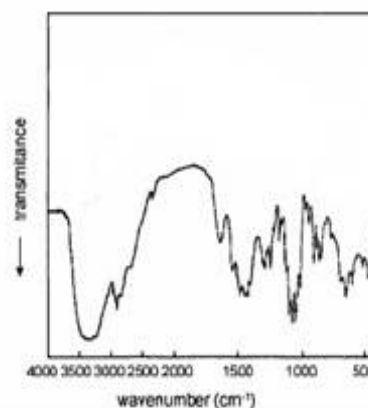


Figure 30: IR spectrum MGA (Demichelli C. et al., 1999).

Infrared vibrational spectroscopy is a technique which can be used to identify molecules by analysis of their constituent bonds. Each chemical bond in a molecule vibrates at a frequency which is characteristic of that bond. This can be used to gain information about the sample composition in terms of chemical groups present and also its purity, not desirable reactions during some processes as hydrolysis or oxidation.



Figure 31: Perkin Elmer Spectrum RX I.

Methodology used:

Preparation of the sample: A small quantity of powder is grinded up with anhydrous KBr (previously dried and stored at 60 °C). Then, the mixture is compressed at 10 tones of pressure and 16 consecutives lectures are made by Perkin Elmer Spectrum RX I (figure 31).

5.3.2.3. X-rays diffraction assay

MGA is defined as an amorphous solid (Demicheli C. et al., 2003). Subjecting the samples under x-rays diffraction will be verified this characteristic and will be known if the lyophilisation process produce any change in the morphological structure. The x-ray diffraction technique is used mainly for the structural characterization of solids by a diffractometer measuring the scattering produced when a beam of x-rays interacts with it. It's based in the Bragg law

$$2d(\sin\theta) = \lambda$$

Where,

d = lattice interplanar spacing of the crystal

θ = x-ray incidence angle (Bragg angle)

λ = wavelength of the characteristics x-rays (Bragg, W.L. 1914).

The basic geometry of an X-ray diffractometer involves a source of monochromatic radiation and an X-ray detector situated on the circumference of a graduated circle centered on the powder specimen. Divergent slits, located between the X-ray source and the specimen, and receiving slits, located between the specimen and the detector, limit scattered (non-diffracted) radiation, reduce background noise, and collimate the radiation. The detector and specimen holder are mechanically coupled with a goniometer so that a rotation of the detector through 2θ degrees occurs in conjunction with the rotation of the specimen through θ degrees, a fixed 2:1 ratio (figure 32) (U.S. Geological Survey, 2001).

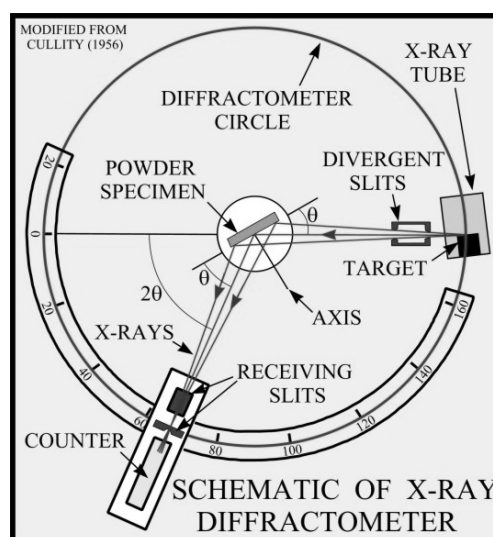


Figure 32: Schematic illustration of a X-ray diffractometer (U.S. Geological Survey, 2001).

Methodology used:

Sample preparation: Introduction of the powder material into glass capillaries (Hilgenberg Mark tube glass type number 0140) of 0.5 millimetres of diameter.

Instrument and experimental conditions: PANalytical X'Pert PRO MPD θ/θ powder diffractometer of 240 millimetres of radius, parallel beam optics with a hybrid monochromator and transmission geometry with a spinner glass capillary sample holder. Cu $K\alpha_1$ radiation ($\lambda = 1,5406 \text{ \AA}$), work power: 45 kV – 40 mA, incident beam slits defining a beam height of 0,19 millimetres, incident and diffracted beam 0,02 radians Soller slits, X'Celerator Detector: Active length = 2,122 °, 2θ scans from 2,5 to 50 ° 2θ with step size of 0,017° and measuring time of 200 seconds per step.

5.3.2.4. Particle size distribution

The determination of the particle size in pharmaceutical development is essential due to the dosage form and route of administration may necessitate the use of particles with unique characteristics (Burgess J. et al., 2004). Moreover, drug particle size has a critical effect on the content uniformity of solid dosage forms, where poor content uniformity would result if a drug powder were not dispersed evenly throughout a mixture with excipients (Burgess J. et al., 2004). In the present effort is important to study the volume mean diameter (VMD) because of being one of the most significant factors for phagocytotic activity of macrophages (Yoshida A. et al., 2006).

One of the most used techniques is laser diffraction which is based on the phenomenon that particles scatter light in all directions with an intensity pattern that is dependent on particle size. All present instruments assume a spherical shape for the particles. By using an optical model to compute scattering patterns for unit volumes of particles in selected size classes and by using a mathematical deconvolution procedure, a volumetric particle size distribution is calculated, the scattering pattern of which fits best with the measured pattern.

A typical light scattering instrument consists of a light beam (usually a laser), a particulate dispersion device, a detector for measuring the scattering pattern and a computer for both control of the instrument and calculation of the particle size distribution.

Methodology used:

The product was sized using a Beckman Coulter (model LS 13, 320) particle size laser analyser (figure 33), determining the VMD and polydispersity. Each sample of MGA was suspended in ethanol. The dynamic range of the LS230 is from 0,04 micron to 2000 micron.



Figure 33: Beckman Coulter (model LS 13, 320) particle size laser analyser.

5.3.2.5. Scanning Differential Calorimetry

Differential scanning calorimetry or DSC is a thermoanalytical technique in which the difference in the amount of heat required to increase the temperature of a sample and reference are measured as a function of temperature.

Methodology used:

Differential Scanning Calorimeter 822e, Mettler Toledo (figure 34) is used to determine the fusion temperature of MGA and possible interactions with excipients. Preparation of samples:

Drug + excipient: 50 % -50 %

Drug + excipient: 1:1 (proportion in formulation)

Drug + excipient: 1:2 (proportion in formulation)

Aluminium capsules of 40 μ l are used and they are heated from 30 $^{\circ}$ C to 300 $^{\circ}$ C with a heat speed of 10 $^{\circ}$ C/min in nitrogen atmosphere (50 ml/min).



Figure 34: DSC 822e Mettler Toledo

5.3.2.6. Solubility

MGA is defined in the bibliography (Brazilian Pharmacopea (F.Bras. IV, 2002), The Merck Index, 2001) as soluble in water. Solubility assay is done following the 5th edition European Pharmacopeia (5.8), where a product is considered easily soluble if 1 to 10 ml of diluent is needed to dissolve a gram of this product.

5.3.2.7. pH in aqueous solution

The pH declared values of MGA in the Analytical Certificate of Aventis Lab. are from 5,0 to 8,0. The limits by Brazilian Pharmacopea (F.Bras.IV, 2002) are from 5,5 to 7,5. Different samples are prepared and analysed by pH Crison:

- 5 % w/v MGA solution.
- 5 % w/v Glucantime[®] lyophilized powder solution
- 30 % w/v MGA solution with 0,16 % w/v sodium metabisulfite.
- Glucantime[®] vials.

5.3.3. Development of a new dosage form for meglumine antimoniate

After MGA characterization, the study of different pharmaceutical forms as possible candidates to develop a new oral or parenteral dosage form is started. The characteristics of all the excipients used in any formulation are previously studied and selected following some aspects:

- Theoretical compatibility between components.
- Possible administration by oral or parenteral route.
- Absence of toxicity in the planned doses.
- Likely disrupter of intestinal or/and *Leishmania* PGPA.
- Absorption enhancer.

At the beginning, emulsions (O/W and W/O), self-emulsifying delivery systems and nanosuspensions are selected to be developed. Normally, the use of lipidic excipients in oral forms is for improving the bioavailability of lipophilic drugs which would be in dissolution in the intestinal tract and they would enhance the absorption. Although MGA is a hydrophilic drug it would be in a lipidic dispersion which would increase the permeability of the intestinal membrane and the absorption would be also improved (Pouton C.W., 2000).

Besides some good results were obtained with these first formulations studied, solid dosage forms were taken in consideration. From this purpose, it was believed that the encapsulation of MGA into micro/nanoparticles could be one of the best options to target the drug to macrophages.

5.3.3.1 Emulsions, self-emulsifying drug delivery systems and nanosuspensions

An **emulsion** is a mixture of two immiscible substances. One substance (the dispersed phase) is dispersed in the other (the continuous phase). The drop size can oscillate from hundred nanometers to few micrometers. Emulsions are generally based on a continuous liquid phase surrounds droplets of water (W/O) or oil (O/W).

This system led to control drug release, protects from hydrolysis and oxidation and led to disguise the undesirable organoleptic characteristics of the drug (Faulí C., 1993).

In order to protect MGA and improve its absorption different W/O emulsions were studied (table 10) using MCT1 and Polyoxyethylen (20)-sorbitan mono-oleat which are

considered as likely disrupters of intestinal PGPA (Zhang H. et al, 2003, Cornaire G. et al., 2004):

Components	Emulsion W/O n° 1	Emulsion W/O n° 2	Emulsion W/O n° 3
MGA ¹	20 g	20 g	15 g
MCT1	50 g	50 g	50 g
Polyoxyethylen (20)-sorbitan mono-oleat	3,6 g	2 g	3,6 g
Sorbitan monooleate	8,4 g	10 g	8,4 g
Fluid lecithin	0 g	0,4g	0 g
Potassium sorbate	0,2 g	0,2 g	0,2 g
Water	qs 100 ml	qs 100 ml	qs 100 ml

Table 10: Different composition of MGA W/O emulsions prepared. ¹MGA in emulsions W/O n°1 and n°2 is that obtained from lyophilisation of Glucantime[®] and pure MGA in n° 3.

Method of preparation:

Components are weighted separately in two bakers one for each kind of phase. Both glasses are heated at 70-80 °C, and then aqueous phase is added into oil phase under stirring at 50 rpm. When the temperature is around 25 °C, MGA, which has been previously passed through a 50 µm sieve, is added until be homogenised.

Controls:

An amount of drops of the emulsions are taken either into a baker full of HCl solution (pH 1,5) and or into a baker full of phosphate buffer solution (pH 8). It will be observed if some change of colour appears and the behaviour of the drop through the solution to the bottom.

A **self-emulsifying drug delivery system (SEDDS)** is a class of emulsion that has received particular attention as a means of enhancing oral bioavailability of poorly absorbed drugs. These systems are essentially mixes of oil and surfactant (sometimes with added cosurfactant) that form emulsions on mixing with water with little or no energy input (Nielloud F. and Marti-Mestres G., 2000). An emulsifying system is likely to result in more rapid absorption and higher peak plasmatic concentrations of drug (Pouton C.W., 2000). Two different formulations are studied (table 11) where Polyoxyl 40 hydrogenated Castor Oil (another likely disrupter of PGPA) (Tayrouz Y. et al., 2003, Cornaire G. et al., 2004) has been included.

Components	SEDDS O/W	SEDDS W/O
MGA	20 g	20 g
Polyoxyethylen (20)-sorbitan mono-oleat	5 g	0 g
Sorbitan monooleate	0 g	5 g
Polyoxyl 40 hydrogenated Castor Oil	5 g	0 g
MCT1	qs 100 ml	qs 100 ml

Table 11: Composition of SEDDS studied.

Method of preparation:

Sift MGA with 50 μm sieve, weight it and take it into a mortar. Once the excipients are weighted, those that are in more quantity are first added into the mortar and then they are mixed manually. Finally, the rest of excipients are added and mixed.

Controls:

- Autoemulsion test: 1 ml of the SEDD is added in two different test tubes that contain 9 ml of water or HCl solution (pH 1,5). The test tubes are manually shaken.
- pH 10 %: 1g of SEDD is mixed with 10 ml of water. pH is determined.

Nanosuspensions can be defined as colloidal dispersions of nano-sized drug particles that are produced by a suitable method and stabilized by a suitable stabilizer (Patravale V.B. et al., 2004). The method elected was high pressure homogenization which is used for drugs with low solubility or high variability of biodisponibility. Lipidic suspensions are formulated to stabilize the drug and protect it from moisture. Moreover, chitosan starts to be used in these formulations because of its properties of absorption enhancer (Schipper N.G.M. et al., 1996) and its interactions with mannose receptors in macrophages (Han Y., 2005).

High pressure homogenization technique

The 'macro'-suspension is passed through a high pressure homogenizer applying typically 1500 bar and three to ten up to a maximum of 20 homogenisation cycles. The suspension passes a very small homogenization gap in the homogenizer. Due to the narrowness of the gap the streaming velocity of the suspension increases tremendously, that means the dynamic fluid pressure increases. Simultaneously the static pressure on the fluid decreases below the boiling point of water at room temperature. In consequence, water starts boiling at room temperature due to the high pressure, gas

bubbles are formed which implode (=cavitation) when the fluid leaves the homogenisation gap. These cavitation forces are strong enough to break the drug microparticles to drug nanoparticles (figure 35) (Jenning V. et al., 2002). For intravenous administration, larger nanosuspensions are preferred for targeting to the MPS cells (Mononuclear Phagocyte System cells) to avoid complete dissolution of the particles before they reach the macrophages (Müller R.H.et al., 2001).

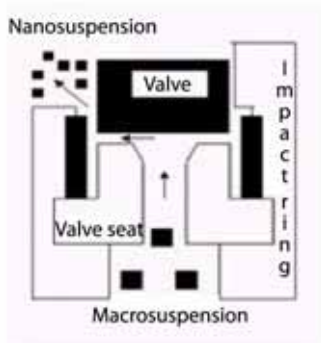


Figure 35: Schematic representation of the high-pressure homogenization process (Patravale V.B.,et al.2004)

It has been reported that oral administration of nanosuspensions of antileishmanial drugs such as atovaquone and amphotericin B improve bioavailability because of the high adhesiveness of drug particles sticking on biological surfaces (epithelial gut wall) and prolonging the absorption time (Müller R.H. et al., 2001). Moreover, nanosuspensions are efficiently taken up by phagocytic cells (Kayser O., 2000).

The two formulations studied are shown in the table 12.

Moreover, drug-free suspensions are also prepared.

Components	Suspension n° 1	Suspension n° 2
MGA	27,4 g	27,4 g
Polyoxyl 40 hydrogenated Castor Oil	6 g	6 g
MCT1	67,34 g	67,34 g
Colloidal Silica dioxide	2,16 g	2,16 g
Fluid lecithin	0,8 g	0,8 g
Butylhydroxitoluene	0,02 g	0,02 g
Chitosan	0 g	1 g

Table 12: Composition of ‘macro’-suspensions prepared

Method of preparation:

Once all the components are weighted, MCT1 is heated in thermostatic bath at 90 °C. Colloidal silica dioxide is suspended under stirring for 15 minutes. When the temperature is 70 °C, polyoxyl 40 hydrogenated castor oil is added under mixing for 10 minutes, after MGA will be dispersed slowly under stirring for 30 minutes in room temperature. Then, butylhydroxitoluene is taken into the glass and mixed for 2 minutes. Finally, fluid lecithin is homogenised for 20 minutes. In suspension n° 2, chitosan is added slowly and mixed at 10000 rpm for 20 minutes with high speed mixer. Once

macrosuspension is prepared, 50 ml are passed through a high pressure homogenizer Emulsiflex C3 at 15000 psi (1470 mPa) for 7 cycles.

Controls 'macro'-suspension:

- Aspect
- Particle size: It is determined by optical microscope JENA 421021 with an incorporate micrometer. Three different fields are observed and 300 particles analysed in each one. The results will be expressed as the mean percentage of particles in each range of sizes.
- Viscosity: Viscosimeter Brookfield was used to determine the viscosity at 24 °C, spindle number 3 and 50 rpm.
- Density: 10 ml of the suspension, measured in a graduated cylinder, are weighted. Density will be calculated dividing the weight obtained (subtracting cylinder tare) by 10 ml.

5.3.3.2. Nano/microspheres by spray-drying

Spray drying method is widely used to dry aqueous or organic solutions, emulsions etc., in industrial chemistry, cosmetic and food industry. Some current available products are dry milk powder, detergents, dyes and encapsulated volatile or essential oils such as lemon oil (Bhandari B.R. et al., 1999), *l*-menthol (Liu X-D. et al., 2000), orange oil (Edris A. and Bergnstahl B., 2001), linoleic acid (Minemoto Y. et al., 2002) or tuna oil (Klinkerson U. et al., 2005).

In pharmaceutical industry, spray drying has mainly three applications: a) spray-drying where the final product is a fine, amorphous or crystallized material (i.e. albumin, blood plasma, peptides, enzymes, combination vaccines, hormones and cell suspensions (Bacterial cultures) (Santivarangkna C. et al., 2007)), b) micronization or structural changes (lactose or corn starch) (Yu L., 2001), and c) microencapsulation.

For long time pharmaceutical industries have been widely applying this technique because of its numerous advantages over other methods of microencapsulation; the advantage of spray drying technique is that it is reproducible, rapid, easy scale up compatible with thermolabile products such as enzymes or antibiotics (Johansen P. et

al., 2000), and leads to spray solvents, emulsions or suspensions (Kala H. et al., 1979, Christensen K.L. et al. 2001a,b, Dollo G. et al., 2003). For all these reasons, it is thought to use it for the microencapsulation of MGA. The apparatus used is a mini spray drier B-290, with a maximum drying capacity of up to 1,0 l/h of water, connected with a dehumidifier B-296 which leads to define the drying conditions exactly and make them reproducible by removing the water content with a cold trap at 5 °C. The complete process of spray drying using this kind of atomizer basically consists of a sequence of four processes (figure 36):

1) Dispersion of the feed sample in small droplets using a pressure nozzle. As higher the energy for the dispersion is, the smaller are the generated droplets.

2) Mixing of spray and drying medium (air) with heat and mass transfer. The material is sprayed in the same direction as the flow of hot air through the apparatus (co-current flow). The droplets come into contact with the hot drying air (heated electrically) when they are the moistest.

3) As soon as droplets of the spray come into contact with the drying air, evaporation takes place from the saturated vapour film which is quickly established at the droplet surface. Due to the high specific surface area and the existing temperature and moisture gradients, an intense heat and mass transfer result in an efficient drying. The evaporation leads to a cooling of the droplet and thus to a small thermal load. Drying chamber design and air flow rate provide a droplet residence time in the chamber, so that the desired droplet moisture removal is completed and product removed from the dryer before product temperatures can rise to the outlet drying air temperature. Hence, there is little likelihood of heat damage to the product. This is an open-cycle system because the air stream is exhausted to atmosphere.

4) Based on inertial forces, the particles are separated to the cyclone wall as a down-going strain and removed (www.buchi.com).

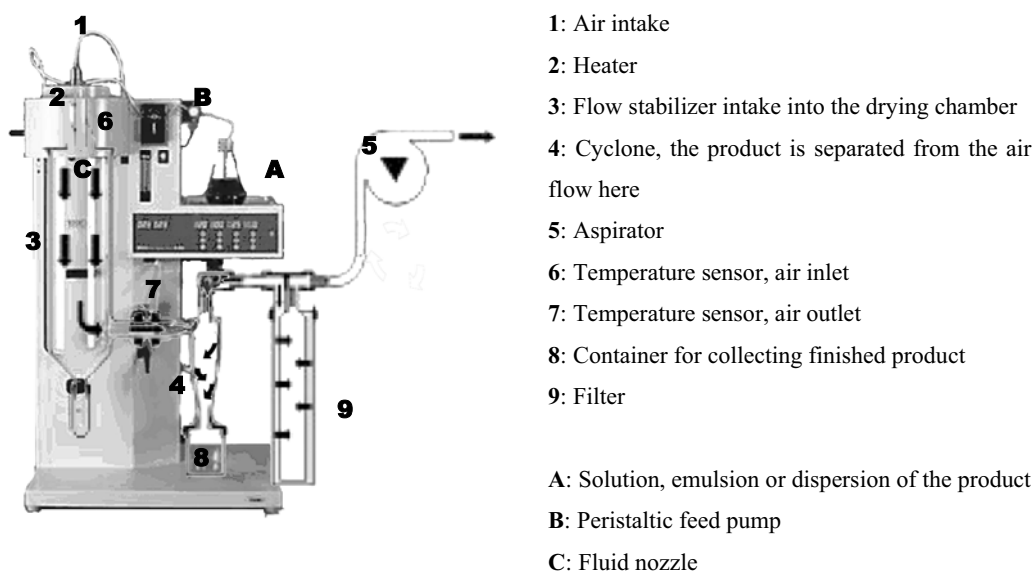
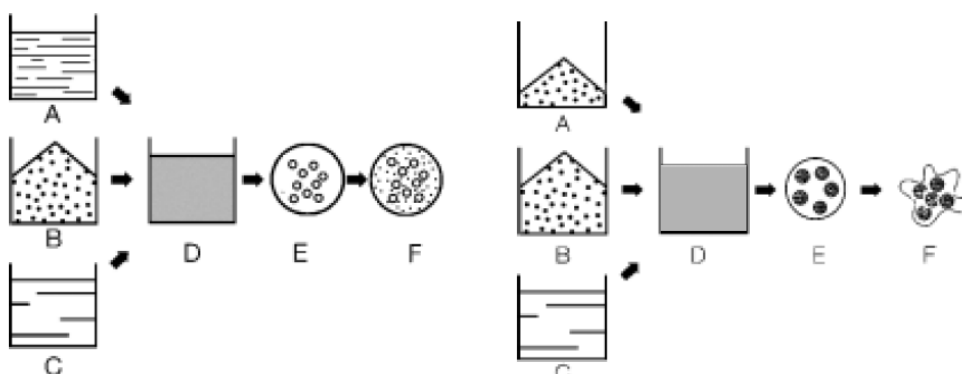


Figure 36: Schematic illustration of spray-drying process using mini spray drier B-290.

The diagrams of the processes using an emulsion or a solution are shown in the figure 37.



An emulsion (D) is created from the liquid product to be treated (A), a carrier substance (B) such as maltodextrin and a filmogen solution (C) such as chitosan in acidic water. This emulsion is then sprayed into small droplets (E). The solvent evaporates leading to a solid matrix around the dispersed second phase (F). The result is that the small droplets of the product (A) are stored in the carrier substance (B) and embedded in the filmogen (C).

A solution or suspension (D) is created from the product to be treated (A), a matrix (B) and water with additional filmogen (C). This solution is then sprayed into small droplets (E). The matrix and / or filmogen lead to an agglomeration or coating of the suspended particles (F).

Figure 37: Schematic illustrations of the microencapsulation process by spray-drying from an emulsion (left) and a solution or suspension (right) (www.buchi.com).

The instrument settings are named inlet temperature, feed rate, spray air flow and aspirator flow, as spray drying is a method where the result strongly depends upon the material properties, the instrumental settings are in a combined system influencing the product parameters such as temperature load, final humidity, particle size and yield. As a rule of thumb the influence on these parameters can be summarized in the table 13.

Inlet temperature is understood as the temperature of the heated drying air. It is noteworthy that the temperature of the air flow does not have to be higher than the boiling point of water to evaporate the individual drops during the short residence time. The gradient between wet surface and not saturate gas leads to evaporate at low temperatures.

Outlet temperature is the temperature of the air with the solid particles before entering the cyclone. This temperature is the resulting temperature of the heat and mass balance in the drying cylinder and thus cannot be regulated. Due to the intense heat and mass transfer and the loss of humidity, the particles can be regarded to have the same temperature as the gas. Thus, as a rule of thumb is that the outlet temperature is the same than the maximum product temperature. The outlet temperature is the result of the combination of the following parameters: inlet temperature, aspirator flow rate, peristaltic pump setting and concentration of the material being sprayed.

The drying air is blown or sucked through the device by the aspirator motor creating under pressure conditions. By regulating the aspirator rate, the amount of heated drying air can be increased or decreased.

The peristaltic pump feeds the spray solution to the nozzle. The pump's speed affects the temperature difference between the inlet temperature and the outlet temperature. The pump rate directly corresponds to the inlet mass. The higher the throughput of solution, the more energy is needed to evaporate the droplet to particles. Thus, the outlet temperature decreases. The limitation of the pump is when the particles are not dry enough resulting in sticky product or wet walls in the cylinder. The pump throughput is also dependent upon various factors such as the viscosity of the spray solution and tubing diameter.

The spray flow rate is the amount of compressed air needed to disperse the solution, emulsion or suspension. A gas other than compressed air can be used. The spray flow rate can be set to between 300 and 800 l/h on the device.

Parameter /Dependence	aspirator rate ↑	air humidity ↑	inlet temperature ↑	spray air flow ↑	feed rate ↑	solvent instead of water	concentration↑
Outlet temperature	↑↑less heat losses based on total inlet of energy	↑more energy stored in humidity	↑↑↑direct proportion	↓ more cool air to be heated up	↓↓more solvent to be evaporated	↑↑↑less heat of energy of solvent	↑↑↑less water to be evaporated
particle size	-	-	-	↓↓↓more energy for fluid dispersion	↑more fluid to disperse	↓less surface tension	↑↑↑ more remaining product
final humidity of product	↑↑lower partial pressure of evaporated water	↑↑higher partial pressure of drying air	↓↓lower relative humidity in air		↑↑more water leads to higher particel pressure	↓↓↓no water in feed leads to very dry product	↓less water evaporated, lower partial pressure
yield	↑↑better separation rate in cyclone	↓more humidity can lead to sticking product	↑eventually dryer product prevent sticking		↑↑depends on application	↑↑no hygroscopic behaviour leads to easier drying	↑bigger particles lead to higher separation

Table 13: Influence of instrumental setting on product parameters

A number of articles have been published describing the preparation of controlled release chitosan microparticles by such a spray drying technique (He P. et al., 1999a, 1999b, Huang Y.C. et al., 2002, Kumbar S.G. 2002, Dini E. et al., 2003, Grenha A. et al, 2005, Oliveira B.F. et al., 2005, Desai K.G. and Park H.J., 2005, 2006, Gupta K.C. et al., 2006). Ideally, a delivery system might be developed to release a drug at precisely the rate it is required for different application. However, as an unfavourable factor, spray dried chitosan microspheres swell quickly in water and release the encapsulated drug immediately (Desai K.G. and Park H.J., 2005). The drug release kinetics from spray dried chitosan microspheres is affected by the concentration and molecular weight of the chitosan, solubility of the drugs, especially the chitosan matrix (cross-linked or non-cross-linked). Therefore, non-cross-linked spray dried chitosan microspheres are unsuitable for sustained drug delivery (He P. et al., 1999a). In order to stabilize the spray dried chitosan microspheres, cross-linking agents such as glutaraldehyd (He P. et al. 1999a, 1999b, Monteiro O.A.C. and Airoidi C., 1999, Dini E. et al. 2003, Desai K.G. and Park H.J., 2005, Gupta K.C. et al., 2006), formaldehyd (He P. et al.,1999a, Desai

K.G. and Park H.J., 2005), Pluronic[®] (F68) and gelatine (Huang Y.C. et al., 2002), pentasodium tripolyphosphate (TPP) (Grenha A. et al., 2005, Desai K.G. and Park H.J., 2006), D,L-glyceraldehyde (Oliveira B.F. et al., 2005) and glyoxal (Gupta K.C. et al., 2006) have been used. Other study uses heat treatments as crosslinking method obtaining the fastest release if it is compared with glutaraldehyd cross-linking (Kumbar S.G. et al., 2002). However, the effect of different cross-linking agents on the properties of spray drying chitosan microspheres is not studied so far. In this work has been selected glutaraldehyd as cross-linking agent.

5.3.3.2.1. Spray-dried nano/microspheres characterization

A) Morphological analysis by Scanning Electron Microscope

The Scanning Electron Microscope (SEM) is a microscope that uses electrons rather than light to form an image and also produces images of high resolution. A beam of electrons is produced at the top of the microscope by heating of a metallic filament (the most common is the Tungsten hairpin gun which function as cathode). The electron beam follows a vertical path through the column of the microscope (always at a vacuum). It makes its way through electromagnetic lenses which focus and direct the beam down towards the sample. Once it hits the sample, backscattered electrons are ejected from the sample. Detectors collect these electrons, and convert them to a signal that is sent to a viewing screen producing an image (figure 38).

Methodology used:

Scanning Electronic Microcopes (SEM), Hitachi 2300 and Hitachi S-4300 are used to investigate surface morphology of the chitosan microspheres. The sample was spread on a conductor adhesive tape previously adhered to SEM aluminium stubs. The sample not adhered is removed by nitrogen flow. Then it is coated (sputtered) with a 40 nm gold layer using a cathodic pulverizer, Jeol JFC-1100 at vacuum. This makes the samples

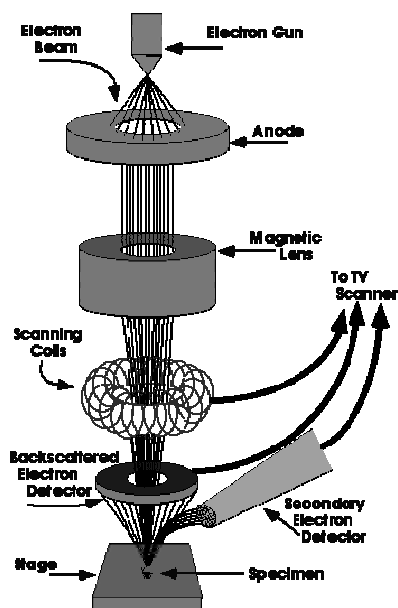


Figure 38: Schematic illustration of how SEM works (Iowa State University, 2007).

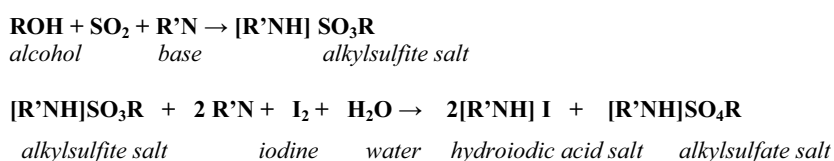
conductive and ready to be viewed by the SEM. The samples were scanned at 15 kV voltages.

B) Particles size distribution

Nano/microspheres were sized using the same Beckman Coulter (model LS 13, 320) than that used for MGA particle size distribution, determining the volume mean diameter (VMD) and polydispersity. In this case, each sample was suspended in acetone.

C) Moisture content by Karl Fischer titration

Karl Fischer titration is a widely used analytical method for quantifying water content in a variety of products. The fundamental principle behind it is based on the Bunsen reaction between iodine and sulfur dioxide in an aqueous medium. Karl Fischer discovered that this reaction could be modified to be used for the determination of water in a non-aqueous system containing an excess of sulfur dioxide. He used a primary alcohol (methanol) as the solvent, and a base (pyridine) as the buffering agent.



The alcohol reacts with sulfur dioxide (SO₂) and base to form an intermediate alkylsulfite salt, which is then oxidized by iodine to an alkylsulfate salt. This oxidation reaction consumes water. Water and iodine are consumed in a 1:1 ratio in the above reaction. Once all of the water present is consumed, the presence of excess iodine is detected voltametrically by the titrator's indicator electrode. That signals the end-point of the titration. The amount of water present in the sample is calculated based on the concentration of iodine in the Karl Fisher titrating reagent (i.e., titer) and the amount of Karl Fisher Reagent consumed in the titration (www.emdchemicals.com).

Methodology used:

The residual moisture content of the spray-dried powders (nano/microspheres) was measured by Karl Fischer titration in dry methanol using a 701 KF Titrino (Metrohm) (figure 39). Samples masses were approximately 100 mg and Aquametric composite 5 RV (Panreac, Spain) was used as the titration reagent. Determinations of moisture content are done with triplicate samples.

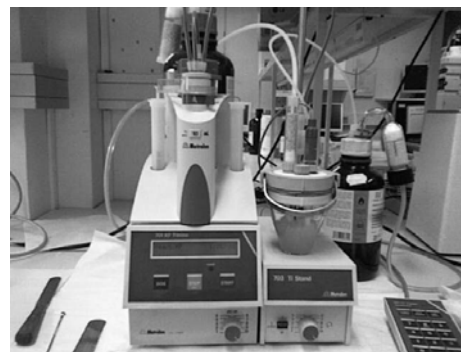


Figure 39: Karl Fischer titration, 701 KF Titrino (Metrohm).

D) Efficiency of encapsulation

To calculate the efficiency of encapsulation (EE) of MGA is necessary to determine the quantity of Sb inside nano/microspheres. Previously, it is necessary to study the possible effect of the excipients of nano/microspheres in Sb quantification by ICP-OES. For this purpose, two different calibration curves were measured:

1. External in only medium (1 % HNO₃ + 0,5 % HF (solution A)).
2. Standard addition in problem HCl aqueous solution diluted 1/5 with solution A.

In case that the excipients of nano/microspheres in HCl aqueous solution affected in the quantification of Sb, different slopes of the calibration curves would be obtained and then, the values of Sb resulted of each equation would be different.

Preparation of the sample: Weight of 10,00 mg of nano/microspheres in balance with sensibility 0,01 mg are taken into a 50 ml volumetric flask and suspended with 0,1 N HCl. The sample is sonicated for minimum 5 minutes until a transparent solution and filtered through 0,45 µm Millipore filter.

Determination: Determination of Sb by ICP-OES in PERKIN ELMER ELAN Optima 3200 RLs apparatus in standard conditions and calibrated with four patrons prepared with solution A. 1/5 sample was diluted with solution A and the lectures were made at emission wavelength of 206,836 nm. The EE (%) is calculated using the following equation:

$$EE (\%) = \frac{X \text{ g Sb / ml}}{(0,010 \text{ g microspheres} \times \text{theoretic MGA \% in microspheres} \times \% \text{ Sb purity}) / 50 \text{ ml}} \times 100$$

E) Z-potential

Z-potential refers to the electrostatic potential generated by the accumulation of ions at the surface of a (colloidal) particle that is organized into an electrical double-layer, consisting of the Stern layer and the diffuse layer. If an electric field is applied in the liquid then these charged particles will move towards either the positive or the negative pole of the applied field. The velocity with which they translate is proportional to the magnitude of the charge. The determination of Z-potential was carried out using Zetasizer Nano S or Zetaplus apparatus by triplicate.

Preparation of the sample: a portion of sample is suspended in a previously prepared 1mM KCl solution. The maximum particle concentration tolerated is 0,01 mg/ml.

F) Determination of yield of spray-drying process

The process yield (% w/w) was calculated using the following equation which consists in dividing the weight of the spray-dried powder by the amount of dry solids fed to the spray dryer.

$$\% \text{ w/w Yield} = \frac{\text{Weight of dry product obtained}}{\text{Theoretic weight of dry product to obtain}}$$

G) In vitro drug release studies

As can be seen in the section 4.6.2, different *in vitro* release methods for microparticulate systems can be used. In this effort, “dialysis bags” has been the method selected.

Preparation dissolution medium

Phosphate buffer solution (pH 7,4) is prepared following 5th edition European Pharmacopeia (5.08).

Preparation dialysis sacs

Dialysis sacs are supplied in rolls and dry. Following the supplier instructions, removal glycerol included as a humectant can be accomplished by washing the tubing in running water for 3-4 hours. Removal of sulfur compounds can be accomplished by treating the tubing with a 0,3 % (w/v) solution of sodium sulfide at 80 °C for 1 minute. Wash with hot water (60 °C) for 2 minutes, followed by acidification with a 0,2 % (v/v) solution of sulphuric acid, then rinse with hot water to remove the acid. The treatment is applied to a piece of dialysis tube and after this is kept in the fridge until its use. Each dialysis bag will be 10 cm of length.

In vitro release testing

In vitro drug release studies of the microspheres were conducted for a period of 24 hours using a six station apparatus II (Turu-Grau DT-6) at 37 °C and 100 rpm. 625 mg of microspheres were taken into the previously treated cellulose dialysis bags (molecular weight cut-off 12,400) and tied to the paddles (figure 40). The dissolution studies were carried out in 250 ml of phosphate buffer of pH 7,4 under sink conditions (table 14). At pre-determined time intervals (0,25, 0,5, 0,75, 1, 3, 6, 10 and 24h) samples of 10 ml were withdrawn through a sampling syringe attached with 0,45 µm membrane filter (Millipore,US) from the dissolution medium and replaced with fresh medium to maintain the volume constant. After filtration, 1/5 diluted samples with 1% HNO₃ + 0,5 % HF were analyzed at two different wavelength for improving the precision, 206,836 nm and 217,582 nm, for antimony by an ICP-OES in PERKIN ELMER ELAN Optima 3200 RLs apparatus in standard conditions and calibrated with four patrons prepared with 1 % HNO₃ + 0,5 % HF. *In vitro* release studies were performed in triplicate (for each microsphere formulation in an identical manner). Drug dissolved at specified periods was plotted as percent release versus time (hours) curve.

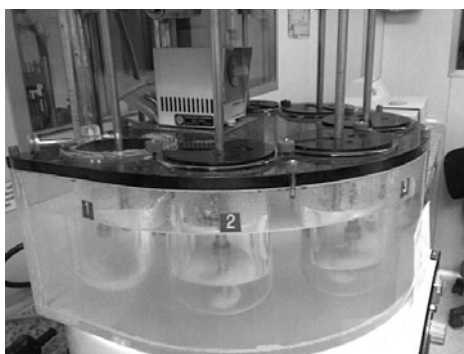


Figure 40: Turu-Grau DT-6 with dialysis bags tied to the paddles.

Solubility of MGA	0,83 g/ml (see section 5.4.2.6)
1/ 3 of MGA solubility	0,27 g/ml = 270 mg/ml
Maximum MGA % into 625 mg microspheres tested	15,38 % = 96,125 mg
MGA concentration at 100 % microspheres dissolved	0,385 mg/ml

Table 14: Calculations of sink conditions to MGA release studies.

Model analysis and statistics

Different kinetic models (zero-order, first-order, Higuchi's equation, Weibull's equation and Korsmeyer's equation) were applied to interpret the drug release kinetics from microspheres with the help of equations 1-5.

1	$Mt/M_{\infty} = K_0t$	Zero-order
2	$Mt = M_{\infty} \cdot (1 - e^{-K_1(t-t_0)})$	First-order
3	$Mt/M_{\infty} = K_H t^{1/2}$	Higuchi's equation
4	$Mt = M_{\infty} \cdot [1 - e^{-(t-t_0/d)\beta}]$	Weibull's equation
5	$Mt/M_{\infty} = K_K t^n$	Korsmeyer's equation

Where, Mt is the cumulative amount of drug released at any specified time point and M_{∞} is the dose of the drug incorporated in the delivery system. K_0 , K_1 , K_H , β and K_k are rate constants for zero-order, first-order, Higuchi, Weibull and Korsmeyer's model respectively. Experimental data were analyzed by a nonlinear least-squares regression using the WinNonlin[®] software (Pharsight, Version 4.1). The estimate values were calculated by linear regression analysis using Microsoft Excel 2003 software.

For the same number of parameters, the coefficient of correlation (R^2) can be used to determine the best of the model equations. However, since a larger number of model parameters could lead to a higher probability of obtaining a higher R^2 value, it was necessary to use a discriminatory criterion that was independent of the number of parameters that each model had. For this reason, the Akaike Information Criterion (AIC) was applied.

The AIC can be defined as:

$$AIC = N (\ln SSR) + 2p$$

where N is number of experimental data points, SSR is the sum of the squared residuals and p is the number of parameters. The model that shows the smallest value for the AIC is the one which, statistically, describes the best the drug release mechanism (Yamoaka K., et al., 1978). Moreover, the amodelistic parameters: Mean Dissolution Time (MDT) and Dissolution Efficiency (DE) were also calculated.

5.3.3.2.2. Chitosan nano/microspheres preparing a novel O/W emulsion technique by spray-drying

A) Pre-formulation

The possibility to achieve a dry formulation with a similar composition that the first formulations mentioned (emulsions, SEDD and suspensions) is interesting on the one hand, in order to maintain the advantages of the likely disruption of PGPA by some of the lipidic components, on the other hand to enhance the oral absorption and target the drug to macrophages by chitosan. Moreover, it would be obtained a more easily phagocytosed product and more stable in a long term. For this reason, different O/W emulsions are prepared to be spray-dried (see table 15). The first parameters studied in the pre-formulation tests to obtain nano/microspheres from emulsions, with an efficient process by spray-drying with a Büchi 290 mini spray-drier, are: (1) the composition of the formulations (dry material and oil phase), (2) the spray conditions: inlet temperature, aspirator flow, feed rate (pump) and the spray air flow.

		Pre-formulated emulsions								
		A1	A2	A3	A4	A5a	A5b	A6	A7	A8
Components (%w/v)	MGA	0	0	0	5	0	0	0	0	0
	MCT2	4	2	2	2	2	2	2	2	2
	Polyoxyl 40 hydrogenated Castor Oil 1	2	1	1	1	1	1	1	1	0
	Deoiled soy lecithin 1	2	1	1	0,5	0,5	0,5	0,5	0,5	0,5
	Glutaraldehyde 1% (ml)	0,5	0,5	2	4	2	2	2	2	2
	Maltodextrin 19D (1)	10	10	10	5	10	10	10	10	10
	Coloidal Silica Dioxide	0	0	0	0,5	0,5	0,5	0	0,5	0,5
	Lactose	0	0	0	0	2	2	0	2	0
	Chitosan	2	1	1	1	1	1	0	1	1
	0,1 M Acetic acid solution	100 ml	100 ml	100 ml	100 ml	100 ml	100 ml	100 ml	100 ml	100 ml
Spray- drying Conditions	% Oil phase	8	4	4	3,5	3,5	3,5	3,5	3,5	2,5
	% surfactants	4	2	2	1,5	1,5	1,5	1,5	1,5	0,5
	% dry material	20	15	15	15	16,5	16,5	14	16,5	14
	Inlet T° (°C)	150	180	130	130	130	130	130	130	130
	% Aspiration flow	100	100	100	100	100	100	100	100	100
	% Pump	30	20	20	20	20	15	15	15	15
	Spray air flow (psi)	30-40	30-40	30-40	30-40	30-40	30-40	30-40	30-40	30-40

Table 15: Composition of the different emulsions (group A) and the spray-drying conditions of pre-formulation studies.

The viability of the spray-drying process has been studied paying attention to the dried sample stuck in the apparatus, the outlet temperature and the morphology of the powders obtained (analysed by SEM).

After the above tests, composition and spray-conditions of the emulsion **A2** are those that produce microspheres with the best morphological characteristics so that these conditions are selected to continue the study. Therefore, emulsion **A2** is modified adding MGA (**A9**) and using maltodextrin 6D (**A10**).

Method of preparation

The method of preparation is shown in the figure 41. Pre-formulations **A7** and **A8** differ to the rest because both phases are heated at 70 °C previous the emulsification step and the other pre-formulations were emulsified at room temperature.

The drug-free and drug loaded microspheres based on chitosan are obtained by spray drying of oil-in-water (O/W) emulsion, using a Büchi mini spray drier B-290 with a standard 0,5 mm nozzle. The liquid is fed to the nozzle with peristaltic pump, atomized by the force of the compressed air and blown together with a hot air to the chamber where the solvent in the droplets is evaporated. The dry product is then collected in a collection receptacle. The drying conditions are as table 15 indicates.

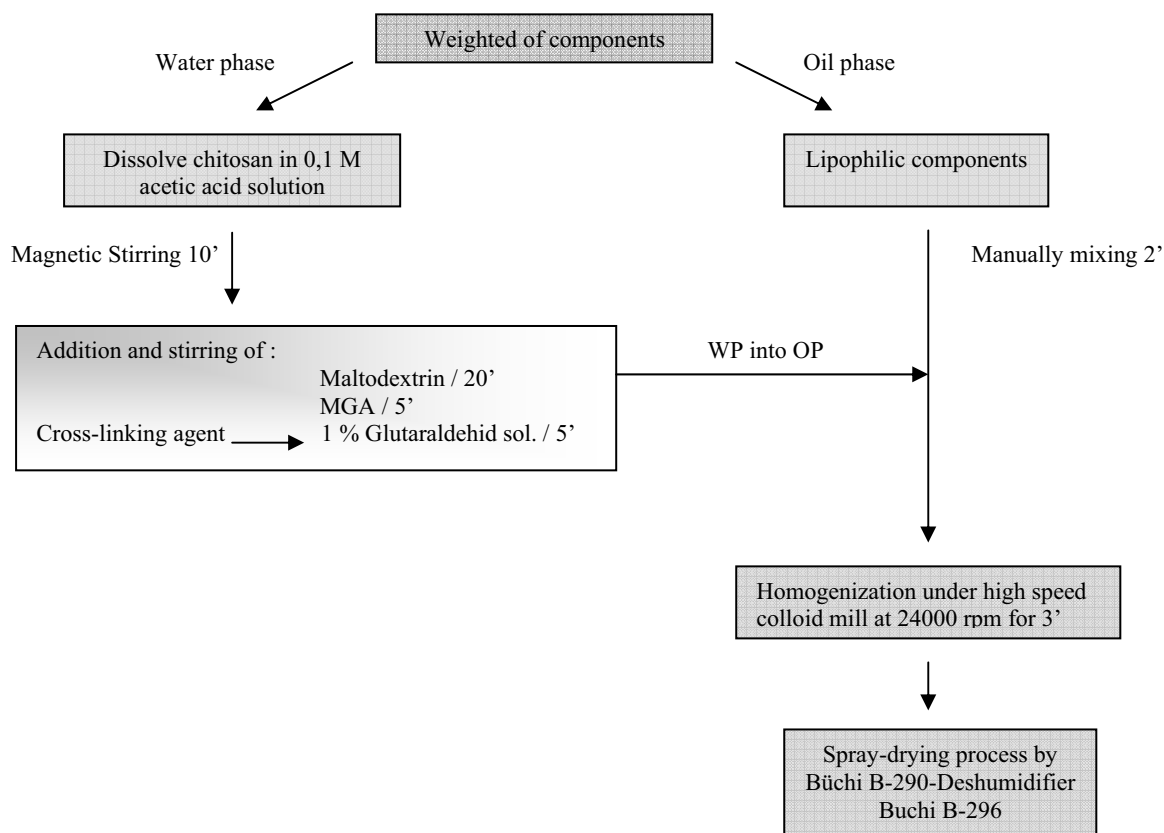


Figure 41: Schematic illustration of the method to obtain chitosan microspheres preparing a O/W emulsion technique by spray-drying.

B) Influence of lipid concentration, inlet temperature and emulsification method

Experimental design 2^3 is used to investigate the effects of both formulation and operational parameters on the process outcomes and the powders characteristics. The independent variables and the two levels are lipid concentration (2 or 4 % w/v) (**A**), inlet temperature (130 or 180 °C) (**B**) and emulsification method under high pressure homogenization (yes (1) or not (-1)) (**C**). The experimental matrix of the design is shown in table 16 and formula compositions and spray drying conditions of the 8 different assays are defined in the table 17 (group B).

N°	A	B	C
1	2	130	-1
2	4	130	-1
3	2	180	-1
4	4	180	-1
5	2	130	1
6	4	130	1
7	2	180	1
8	4	180	1

Table 16: Experimental matrix of design 2^3 .

The responses considered were particles morphology, particle size, polydispersity, process yield, moisture content and efficiency of encapsulation. Statistical analyses were performed using Statgraphics plus 5.1.

Method of preparation

Chitosan O/W emulsions were prepared with the same method shown in the figure 41, 1 % w/v chitosan in 0.1 M acetic acid is used and the percentage of the oil phase was varied from 2 to 4 % w/v and was composed by MCT 2, deoiled soy lecithin 1 and Polyoxyl 40 hydrogenated Castor Oil 1. 0,5 ml of 1 % aqueous solution of glutaraldehyde was added as crosslinking agent. The emulsification methods were: (1) under high speed mixing using a Janke & Kunkel, IKA® Labortechnik at 24000 rpm for 30 min, (2) adding a high pressure homogenization process using a Emulsiflex® -C3 apparatus (Avestin) at 15000 psi recycled two times. Spray drying was conducted using a Büchi Mini Spray Dryer B-290 apparatus with a standard 0,5 mm nozzle. The drying conditions were as follows: feed rate of 4,83 ml/min (20 % pump), spray air flow of 30-40 psi (600-800 l/h) at two different inlet temperatures (180° and 130 °C). The dried particles were recovered, weighted and stored in a dark well closed plastic vessel at 5 °C.

		B1	B2	B3	B4	B5	B6	B7	B8
Components (%w/v)	MGA	2	2	2	2	2	2	2	2
	MCT2	1	2	1	2	1	2	1	2
	Polyoxyl 40 hydrogenated Castor Oil 1	0,5	1	0,5	1	0,5	1	0,5	1
	Deoiled soy lecithin 1	0,5	1	0,5	1	0,5	1	0,5	1
	Glutaraldehyde 1% (ml)	0,5	0,5	0,5	0,5	0,5	0,5	0,5	0,5
	Maltodextrin 19D (1)	10	10	10	10	10	10	10	10
	Chitosan	1	1	1	1	1	1	1	1
	0,1 M Acetic acid solution	100 ml	100 ml	100 ml	100 ml	100 ml	100 ml	100 ml	100 ml
	Spray- drying Conditions	% Oil phase	2	4	2	4	2	4	2
% surfactants		1	2	1	2	1	2	1	2
% dry material		15	17	15	17	15	17	15	17
Inlet T° (°C)		130	130	180	180	130	130	180	180
% Aspiration		100	100	100	100	100	100	100	100
% Pump		20	20	20	20	20	20	20	20
Spray air flow (psi)		30-40	30-40	30-40	30-40	30-40	30-40	30-40	30-40

Table 17: Composition of the different emulsions (group B) and the spray-drying conditions of experimental design 2³.

C) Influence PGPA inhibitors

A new group of microspheres are prepared modifying their lipidic composition in order to study the real influence of the likely disrupters of PGPA (MCT2 and Polyoxyl 40 hydrogenated Castor Oil 1) in front of *Leishmania infantum* (table 18) (group C). At the same time, the efficiency of the formulation process is also studied.

		C1	C2	C3	C4	C5	C6
Components (%w/v)	MGA	2	2	2	2	2	0
	MCT2	0	2	0	2	0	0
	Polyoxyl 40 hydrogenated Castor Oil 1	1	0	0	1	0	0
	Deoiled soy lecithin 1	1	1	0,5	0	0	0
	Glutaraldehyde 1% (ml)	0,5	0,5	0,5	0,5	0,5	0,5
	Maltodextrin 19D (1)	10	10	10	10	10	10
	Chitosan	1	1	1	1	1	1
	0,1 M Acetic acid solution	100 ml	100 ml	100 ml	100 ml	100 ml	100 ml

Table 18: Composition of emulsions (group C) with modified quantities of likely disrupters of PGPA.

5.3.3.2.3. Optimization of chitosan microspheres preparing solutions by spray-drying

A) Pre-formulation

In order to improve morphological aspects, such as the sphericity of chitosan microspheres without lipidic components prepared in the previous section (C5 and C6), some new tests are done. Table 19 shows the compositions of the group of solutions elaborated (named group D). They are prepared increasing the percentage of maltodextrin (D1), glutaraldehyd cross-linking (D2 and D3) and chitosan proportion (D4).

		D1	D2	D3	D4
Components (%w/v)	MGA	2	2	2	2
	Glutaraldehyde 1% (ml)	0,5	1	3	0,5
	Maltodextrin 19D (1)	14	10	10	14
	Chitosan	1	1	1	3
	0,1 M Acetic acid solution	100 ml	100 ml	100 ml	100 ml

Table 19: Composition of the solutions for preparing chitosan microspheres by spray-drying.

The method of preparation is summarised in the figure 42:

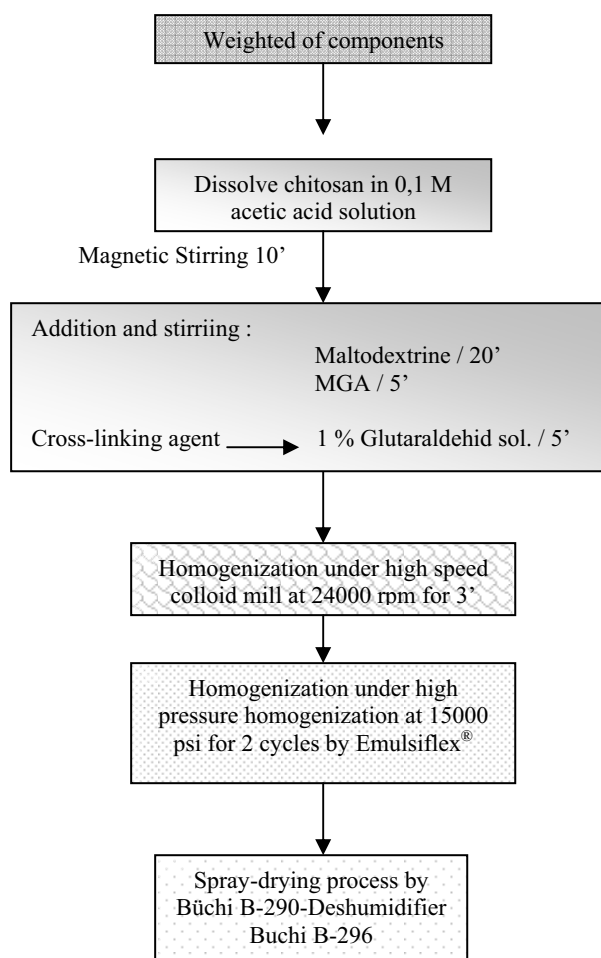


Figure 42: Method of preparation of microspheres by spray-drying from solutions.

B) Fractional experimental design 2^{5-1}

The aim of this fractionated experimental design is to optimize the process of spray-drying described in the figure 42 in order to obtain a definitive formulation of dry chitosan antileishmanial microspheres. The number of experiments is given by $2^{k-p} + C$, where k is the number of variables (k=5), C number of replicates at the centre point (C=1) and p a whole number that indicates how fractionated the experimental design will be (p=1) (Georg E.P. et al., 1989). This design will be useful to estimate the

influence of formulation parameters (glutaraldehyd (A) and chitosan concentration (B)) and process variables (feed rate (pump) (C), spray air flow (D) and inlet temperature (E)) on spray-dried microspheres when using maltodextrin as carrier agent. The interactions among the formulation parameters and process variables are also studied. Responses analyzed for computing these effects and interactions will be outlet temperature, moisture content, operation yield, particles size distribution, Z- potential, efficiency of encapsulation, effectiveness in front of *Leishmania infantum* and dissolution profiles. Additional qualitative responses such as particles morphology will be also considered. Statistical analyses were performed using Statgraphics plus 5.1. The formulation which will be studied with this design is shown in table 20:

Components	
MGA (% w/v)	2
Glutaraldehyde 1% (% v/v)	1 or 3
Maltodextrin 19D (1) (%w/v)	10
Chitosan (% w/v)	1 or 3
0,1 M Acetic acid solution	100 ml

Table 20: Composition of the solutions prepared by experimental design 2^{5-1} (group E).

The constant process variables are 100 % of aspirator flow and nozzle cleaner n° 2. The experimental matrix is shown in the table 21.

Test	A (% v/v)	B (% w/v)	C (%)	D (l/h)	E (°C)
E1	1	1	10	500	180
E2	3	1	10	500	130
E3	1	3	10	500	130
E4	3	3	10	500	180
E5	1	1	20	500	130
E6	3	1	20	500	180
E7	1	3	20	500	180
E8	3	3	20	500	130
E9	2	2	15	600	155
E10	1	1	10	700	130
E11	3	1	10	700	180
E12	1	3	10	700	180
E13	3	3	10	700	130
E14	1	1	20	700	180
E15	3	1	20	700	130
E16	1	3	20	700	130
E17	3	3	20	700	180

Table 21: Experimental matrix of design 2^{5-1} . A: Glutaraldehyd concentration, B: Chitosan concentration, C: Feed rate (pump), D: Spray air flow, E: Inlet temperature.

5.3.4. Investigation of microsphere surface characteristics on macrophage uptake using quantum dots (QD) assisted imaging

The goal is to investigate surface characteristics of drug-free chitosan and poly (lactide-co-glycolide) (PLGA) microspheres and their influence on macrophage uptake, using encapsulated quantum dots (QDs).

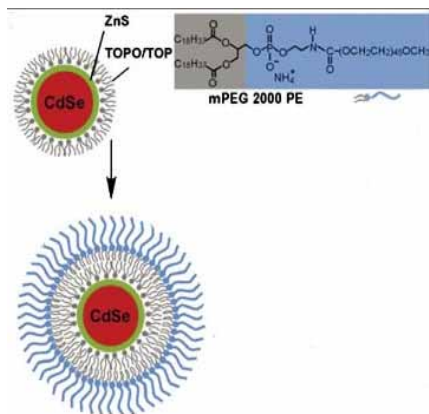


Figure 43: Schematic illustration of water solubilization of CdSe/ZnS core (Srinivasan C., et al.2006)

The kind of QD prepared by Nanomaterials Optoelectronics Laboratory of the Institute of Materials Science of University of Connecticut in Storrs (Connecticut) are CdSe/ZnS (core/shell) hydrophobic QDs, coated with trioctylphosphine oxide (TOPO), conjugated with polyethylene glycol (PEG)-functionalized phospholipids, 1,2-distearoyl-sn-glycero-3-phosphoethanolamine-N-[methoxy(polyethylene glycol)-2000] (ammonium salt) (mPEG 2000 PE) and dissolved in water. The QDs are encapsulated in (PEG)-functionalized

phospholipids to increase stability and entrapment in the microspheres.

5.3.4.1. Synthesis and water solubilization of CdSe/ZnS QDs.

CdSe QDs are synthesized using organometallic precursors according to the method of Murray C.B. and Kagan C.R., 2000. In short, dimethylcadmium and selenium are dissolved in trioctylphosphine and this precursor mixture is injected into hot (300°C) trioctylphosphine oxide solvent. Subsequent ZnS coating is performed by slowly adding diethyl zinc and hexamethyldisilthiane, which are used as Zn and S precursors, respectively. This is followed by annealing at 150 °C for several hours.

5.3.4.2. Encapsulation of CdSe/ZnS QDs in micelles.

CdSe/ZnS QDs are encapsulated in phospholipid/PEG micelles as reported by Dubertret B. et al., 2002. After solvent evaporation, a thin film is formed, to which distilled water or PBS buffer is added followed by vigorous shaking to produce a clear QD micellar dispersion.

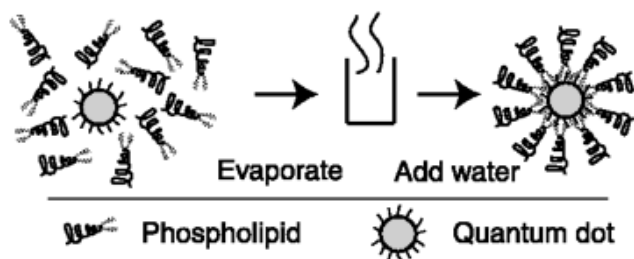


Figure 44: Schematic of single-QD encapsulation in a phospholipid block-copolymer micelle (Dubertret B., et al., 2002).

5.3.4.3. Characterization of QDs solution

5.3.4.3.1. Concentration

It is necessary to calculate the concentration of the solution supplied. In general, the concentration could be determined very easily by optical absorption measurements following Beer-Lambert Law if their molar extinction coefficient was known. In 2001, Schmelz O. et al. report the synthesis of a set of CdSe particles and the determination of the molar extinction coefficient at their first absorption maximum, i.e., at their “excitonic” or “band gap” absorption. Then, in 2003, Yu W.W. et al., confirms that this extinction coefficient per mole of nanocrystals at the first excitonic absorption peak, for high-quality CdTe, CdSe, and CdS nanocrystals was strongly dependent on the size of the nanocrystals, between a square and a cubic dependence. In the present effort, this band gap is determined by UV-vis-near IR spectrophotometer Perkin Elmer Lambda 900 scanning from 800 to 300 nm. Once the first absorption maximum is found, the value is extrapolated to Schmelz O. and Yu W.W. graphs to find the QDs particle size which will let deduce the extinction coefficient indirectly.

The Beer-Lambert law is defined by the equation: $A = \alpha l c$

where,

$$\alpha = \frac{4\pi k}{\lambda}$$

Here, A is absorbance

l is the distance that the light travels through the material (the path length)

c is the concentration of absorbing species in the material

α is the absorption coefficient or the molar absorptivity of the absorber

λ is the wavelength of the light

k is the extinction coefficient

5.3.4.3.2. Fluorescence

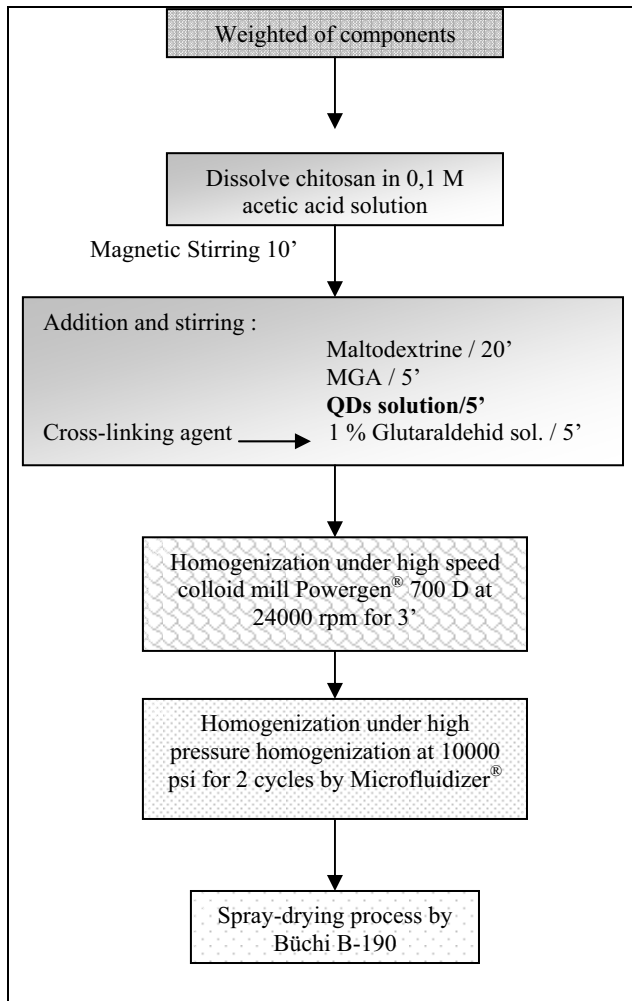
The photoluminescence (PL) emission spectra of QDs solution is obtained by a spectrofluorometer SPEX Fluorolog 3, Horiba. It is equipped with two monochromators (doublegrating, 0:22 m; SPEX 1680, model F2002) and a 450 W Xenon lamp as the excitation source. Xe lamp has a continuous emission spectrum with nearly constant intensity in the range from 300-800 nm and has a sufficient irradiance for measurements down to just above 200 nm. When measuring fluorescence spectra, the wavelength of the excitation light is kept constant (360 nm) and the emission monochromator scans the spectrum (range from 380 to 700 nm).

The excitation spectrum generally is identical to the absorption spectrum as the fluorescence intensity is proportional to the absorption (Sharma A. and Schulman S.G., 1999).

5.3.4.4. Encapsulation of QDs in microspheres

5.3.4.4.1. Encapsulation of QDs in chitosan microspheres by spray-drying

The encapsulation of QDs in chitosan microspheres were produced via spray drying from 1 % w/v chitosan in 0.1M acetic acid solution following the method 1 described in figure 45, and from a novel O/W emulsion of medium chain triglycerides in 1 % w/v chitosan solution using method 2 described in figure 46. QDs-free microspheres are also prepared as blanks in two cases. The composition of the sprayed solutions and emulsions with the process parameters are shown in tables 22 and 23.



Components	
Red CdSe/ZnS quantum dots solution (µl)	200
Glutaraldehyde 1% (% v/v)	0,5
Maltodextrin 19D (2) (%w/v)	10
Chitosan (% w/v)	1
0,1 M Acetic acid solution	100 ml
Spray-drying conditions	
Inlet temperature	180 ° C
% Pump	20
Aspirator	100

Table 22: Composition of 1 % w/v chitosan solutions to encapsulate QDs by spray drying and process parameters.

Figure 45: Schematic illustration of the method 1 of QDs encapsulation in chitosan microspheres by spray drying from solutions.

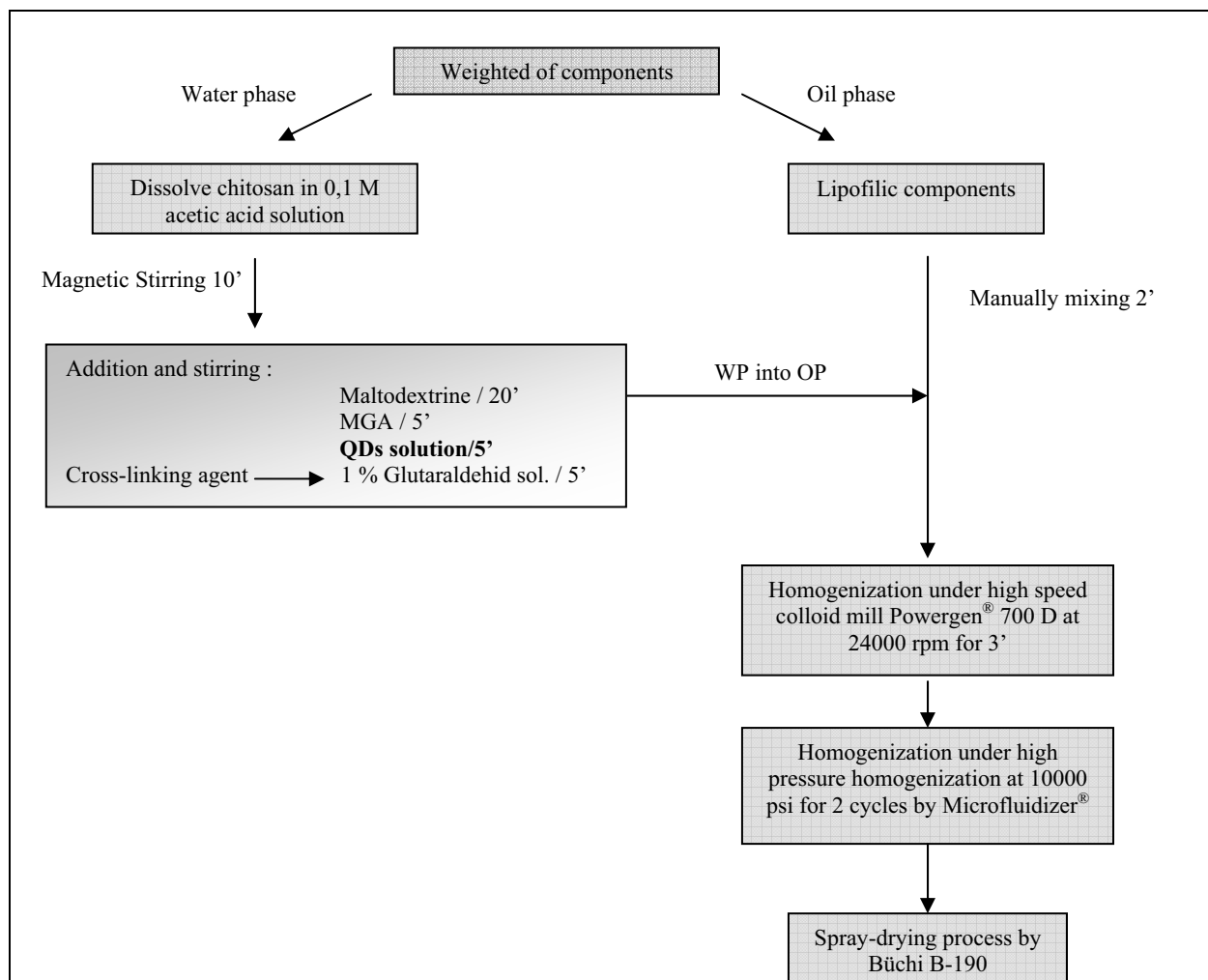


Figure 46: Schematic illustration of method 2 of QDs encapsulation in chitosan microspheres by spray drying from emulsions

Components	
Red CdSe/ZnS quantum dots solution (µl)	200
MCT3	2
Polyoxyl 40 hydrogenated Castor Oil 2	1
Deoiled soy lecithin 2	1
Glutaraldehyde 1% (% v/v)	0,5
Maltodextrin 19D (2) (%w/v)	10
Chitosan 2 (% w/v)	1
0,1 M Acetic acid solution	100 ml
Spray-drying conditions	
Inlet temperature	180° C
% Pump	20
Aspirator	100

Table 23: Composition of O/W chitosan emulsions to encapsulate QDs by spray drying and process parameters.

5.3.4.4.2. Encapsulation of QDs in PLGA microspheres by solvent evaporation technique (double emulsion)

Firstly, it is necessary to prepare a 1 % w/v PVA (30 K) solution, preparing overnight (4/5 h) on magnetic stirrer (500 ml), sonicate for 10 minutes and filter through 0,45 μm membrane filter (stock solution). Secondly, dissolve 2 g of PLGA in 8 ml of methylene chloride in 15/20 ml beaker, homogenize and then add 200 μl of QD solution (1). Afterwards, make 0,1 % PVA 500 ml from 1 % w/v stock in a 1000 ml beaker. Then, take 40 ml of 1 % PVA in a 80/1000 ml beaker (2). Add n° 1 into n° 2 slowly while homogenizing for 2,30 min at 10000 rpm obtaining an emulsion (n° 3). Immediately, add this emulsion into 0,1 % PVA solution in a vacuum chamber and stirred at 600 rpm slowly (4). Stir under vacuum and wait for froth to stop (approximately 15 min). Continue to stir under vacuum for 3-5 h or until there is no methylene chloride left (5). After methylene chloride has gone, let microspheres settle for an hour and then filter through 0,45 μm filter under vacuum (figure 47). Wash for three times with distilled water. Take the cake off filter onto weighting paper and cover with another weighting paper, and then put to dry under vacuum overnight.

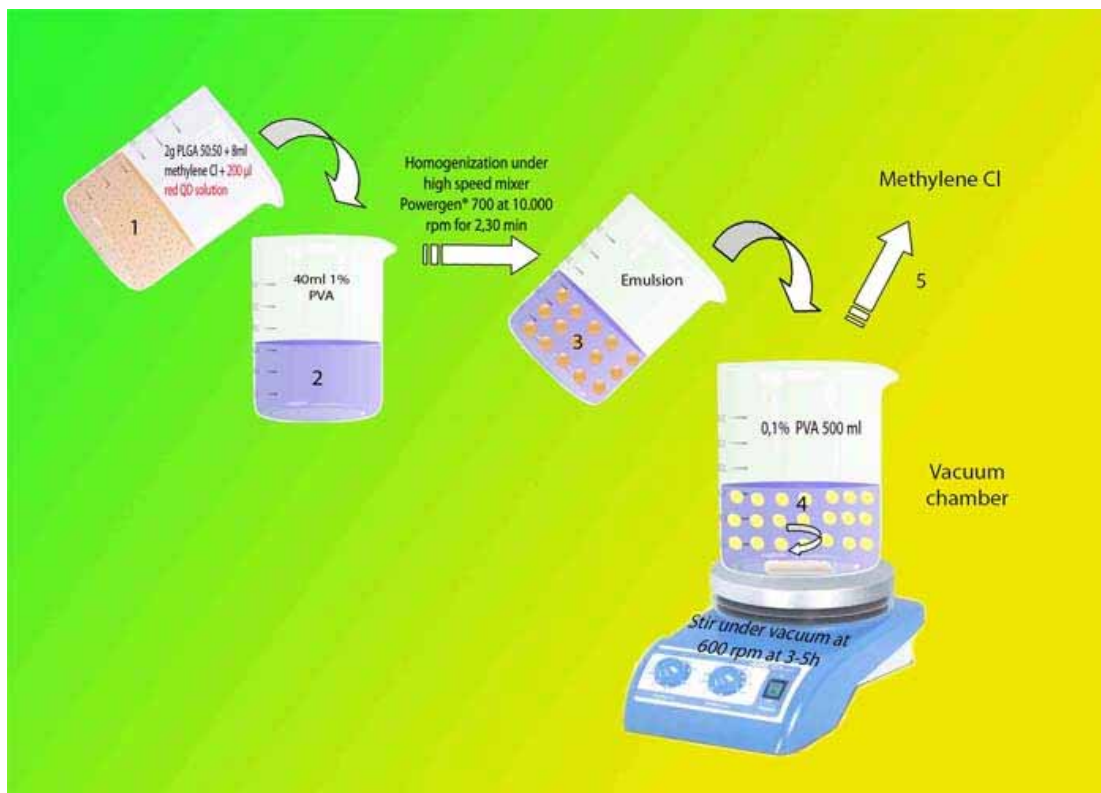


Figure 47: Schematic illustration of the method of QDs encapsulation in PLGA microspheres by solvent-evaporation technique (yellow zone represents the process inside a vacuum chamber under hole).

5.3.4.4.3. Characterization of microspheres

Among the microspheres prepared, table 24 shows the samples characterized (group F).

N°	Chitosan microspheres prepared by method 1 (from solutions)
F1	Blank
F2	With QD
	Chitosan microspheres prepared by method 2 (from O/W emulsion)
F3	Blank
F4	With QD
	PLGA microspheres
F5	Blank
F6	with QD

Table 24: Chitosan and PLGA microspheres characterized for further uptake studies.

A) Particle size distribution

Microspheres are sized using an Accusizer® 780 A Autodiluter, determining the volume mean diameter (VMD) and polydispersity. An amount of sample is suspended in water and measured by triplicate.

B) Z-potential

Z-potential is determined using a Zetaplus® apparatus by triplicate. An amount of sample is suspended in a previously prepared 1 mM KCl solution. The maximum particle concentration tolerated is 0,01 mg/ml.

C) SEM

Microspheres are affixed to double-sided carbon tape, positioned on an aluminum stub, and excess powder removed. The stubs were stored under vacuum overnight. The samples were sputter coated using a Polaron E5100 (Au/Pd, Ar atmosphere, 180 mA, 1 min). SEM images were obtained using a LEO/Zeiss DSM 982 Gemini Field Emission Scanning (2 kV).

D) Confocal microscopy

A confocal laser scanning microscope equipped with Ar/Kr, Kr/Ne, and He/Ne lasers (Leica SP2 spectral confocal microscope, Bannockburn, IL, USA) is used to prove that the CdSe nanoparticles are evenly distributed throughout the microspheres. Microspheres are suspended in water and immediately fixed by evaporation method in

glass slides. The same kind of microscope will be also used to uptake studies of chitosan and PLGA microspheres in macrophages.

A laser scanning confocal microscope (LSCM) works as figure 48 shows. Laser is used to provide the excitation light (in order to get very high intensities). The laser light (blue) reflects off a dichroic mirror and then passes through the microscope objective and excites the fluorescent sample. Dyes or QDs in the sample fluoresces, and the emitted light (green) gets descanned by the same mirrors that are used to scan the excitation light (blue) from the laser. The emitted light passes through the dichroic mirror and is focused onto the pinhole placed in the conjugate focal (hence the term confocal). The light that passes through the pinhole is measured by a detector, ie., a photomultiplier tube. Only one point of the sample is observed. A computer reconstructs the 2D image plane one pixel at a time. A 3D reconstruction of the sample can be performed by combining a series of such slices at different depths (Prasad V. et al., 2007).

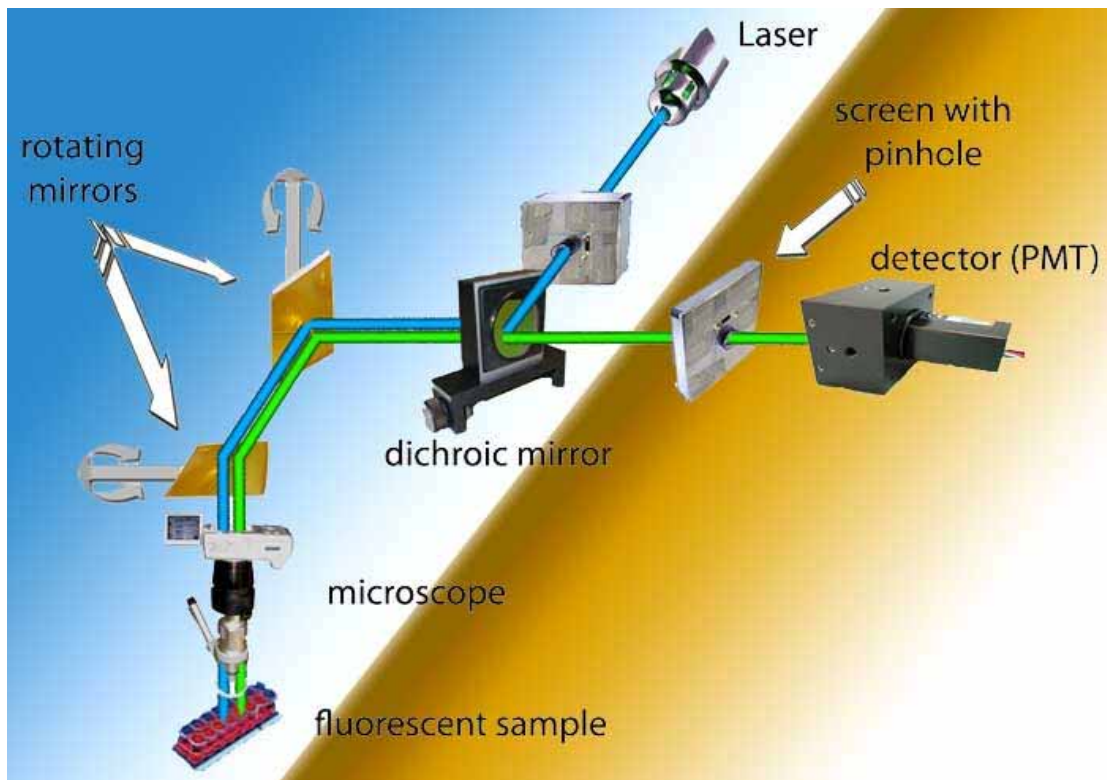


Figure 48: Schematic diagram of a conventional confocal microscope. The screen with the pinhole lies in the back focal plane of the sample with respect to the objective, thus rejecting most out-of-focus light. The rotating mirrors scan the sample pixel by pixel, and are the rate-limiting step for obtaining an image.

5.3.4.3. Uptake studies

CdSe/ZnS QDs will assist the cellular imaging due to be a new class of fluorescent probe. These studies will be carried out with chitosan microspheres, PLGA microspheres and QDs solution.

5.3.4.3.1. Cell cultures

Two different kinds of macrophages cells are used in the uptake studies; MHS and RAW 264.7 cells. Both are supplied in a frozen vial by the Department of Animal Science, Center of Excellence for Vaccine Research of the University of Connecticut and purchased from the ATCC (Manassas, VA; USA). The MHS cell line was derived by SV40 transformation of an adherent cell enriched population of mouse alveolar macrophages and RAW 264.7 was established from a tumor induced by Abelson murine leukemia virus. Both cell subculturing protocols are illustrated in the figure 49.

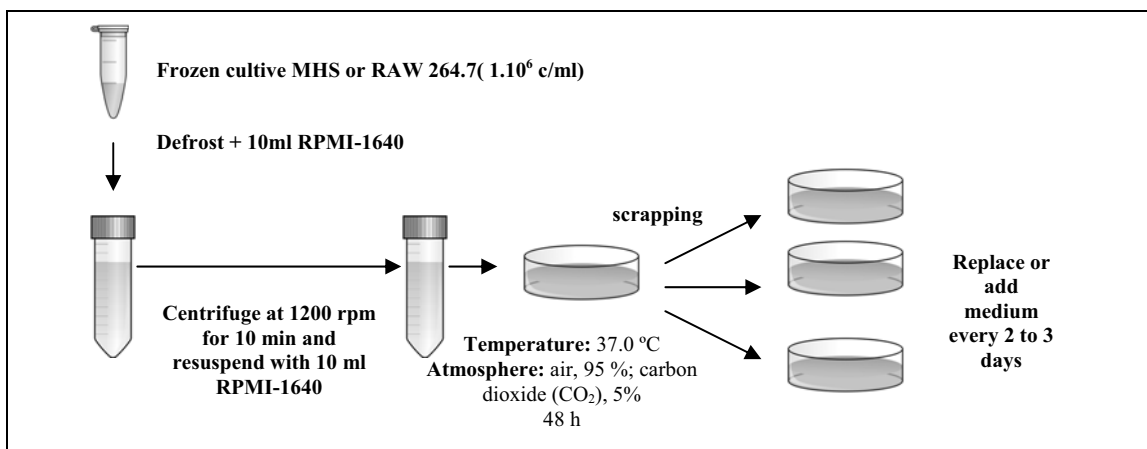


Figure 49: Schematic illustration of subculturing protocol of MHS and RAW 264.7 cells.

5.3.4.3.2. Confocal microscopy

Suspensions of the different microspheres have been prepared using complete RPMI medium just before to transfection studies. The concentrations prepared are 50, 25, 2,5 mg/ml of each sample.

Transfection studies are conducted by plating MHS and RAW 264.7 cells ($0,8 \times 10^5$ cells/well) in 8-well LabTek II chamber glass slides. Once the cultures reached 70-80 %

confluence, the cells are washed with Hank's balanced salt solution (HBSS), and transfections are carried out in complete RPMI medium.

50 µl of sample are taken into the wells of the chamber glass slide. In the case of the QDs solution, 50 µl of Lipofectamine2000 (2,5 µg/µl) which is used as the transfection reagent following the manufacturer's protocol, are added. Wells will be finally filled adding complete RPMI medium until 200 µl. After a 1h incubation period, the transfection mixtures are removed, and the cells are washed with HBSS and covered until further use in the confocal laser scanning microscope. Estimation of the uptake of PLGA and chitosan microspheres is performed watching and measuring the intensity of red fluorescence given by bright orange dots inside the cells.

5.3.5. In vitro parasitological assays

5.3.5.1. *L.infantum* promastigotes culture

L.infantum strain MCAN/ES/92/BCN83 (BCN83) was isolated from bone marrow and lymph node aspirate from an asymptomatic dog, from the Priorat region, a highly endemic area for canine leishmaniasis in Iberian Peninsula (Fisa R. et al., 1999). Parasite isolation and *in vitro* maintenance is done through passages in NNN medium. Promastigotes from NNN are cultured at 26 °C in Schneider's insect medium, pH 7, containing 20 % previously tested heat-inactivated fetal calf serum, 25 µg/ml gentamycin solution and 1 % penicillin (100 U/ml)-streptomycin (100 µg/ml) solution.

5.3.5.2. *L.infantum* amastigotes culture

5.3.5.2.1. Obtain peritoneal macrophage cells

Peritoneal murine macrophage cells are obtained after the stimulation of female Swiss mice with 3 ml of 3 % sodium thioglycolate. After 48 h, 4 ml of physiological serum at 4 °C were injected intraperitoneally, and after 15 min peritoneal liquid was collected and centrifuged. 5×10^4 cells/ml suspensions were prepared and 0,3 ml were seeded in an LabTek 8 chamber slide system and incubated at 37 °C for 24 h in a 5 % CO₂ atmosphere in Heater Heraeus 6000.

5.3.5.2.2. Obtain *L.infantum* amastigotes

As a condition to take the infection of macrophages it is used a ratio of 10 promastigotes for one macrophage. Previously, $1,5 \times 10^3$ cells/well in an LabTek 8

chamber slide system have been seeded, then, the medium is removed and 0,3 ml of late stationary phase promastigote culture in Schneider's medium (pH 7.0) is added at a concentration of 5×10^5 cells/ml ($1,5 \times 10^4$ promastigotes/well). The culture is incubated at 37 °C in a 5 % CO₂ atmosphere for 24 h and then washed to eliminate free promastigotes. After 24 hours we get the amastigote stage inside the macrophage.

5.3.5.3. Preparation of samples for testing

Lecithin 1 is solubilised with MCT 2, Polyoxyl 40 hydrogenated Castor Oil 1 with ethanol, 1 % w/v of chitosan in 0.1 M acetic acid and the rest of the components in water. The microspheres are suspended in water and mixed by OVAN vibra mixer. All these samples are diluted in DMSO. Further working dilutions are performed in culture medium under hole. Only the dilutions with 2 % w/v DMSO or less are assayed. All the components are weighted in balance with sensibility 0,01 mg.

5.3.5.4. Assay on promastigotes

5.3.5.4.1. Counting of *Leishmania infantum* promastigotes

It is necessary to prepare a suspension of promastigotes in Schneider's medium with a concentration of 10^6 cells/ml. First, the concentration of available promastigotes suspension has to be calculated. The count of cells is performed with a 1/10 dilution of culture with formol in a Neubauer[®] counting chamber. Formol immobilizes the parasite and facilitates the count. Z ml will be necessary to dilute up to X ml to have the desired concentration (figure 50).

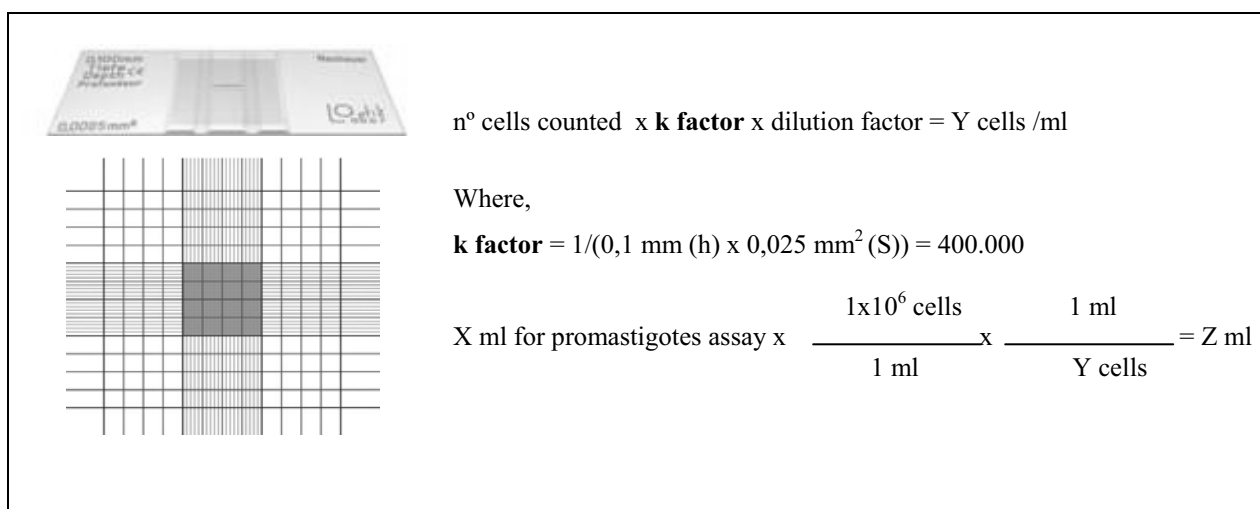


Figure 50: Neubauer[®] counting chamber and mathematics method to calculate initial suspension of promastigotes.

5.3.5.4.2. Preparation of reagents

The reagents necessary to prepare in this assay are the sodium citrate lysis buffer and the p-nitrophenyl phosphate (p-NPP) solution to measure the acid phosphatase activity. The components and quantities of each one are shown in table 25. Solutions are heated at 37 °C in thermostatic bath SBS and P-Selecta precisterm.

Reagents	Components	Quantities
Sodium citrate lysis buffer	Sodium citrate	290 mg
	Triton X-100 (Dow chemical)	100 µl
	dH ₂ O	qsp 10 ml
	pH adjustment to 4,8 with 1N HCl	
p-nitrophenyl phosphate (p-NPP) solution	p-NPP (Sigma N-6260) (4°C)	46 mg
	H ₂ O	qsp 10 ml

Table 25: Composition of reagents necessary for promastigotes assay.

5.3.5.4.3. Phosphatases assay

The promastigote drug susceptibility is assessed using the method described by Carrió J. et al., 2000a,b. Serial dilutions of samples to test in promastigote culture (100 µl) are performed on 96-well microtiter plates (Costar 3595) (figure 51); then 100 µl of culture medium with 10⁵ promastigotes in their logarithmic growth phase are added to each well and incubated at 26 °C for 48 h.

Following this, 40 µl of culture from each well are transferred to a new microtiter plate and cells are lysed by the addition of 100 µl/well of sodium citrate lysis buffer, 90 mM 1% Triton X-100, pH 4,8, at 37 °C. Growth of parasite is measured through acid phosphatase (AP) activity by the addition of 100 µl/well of 10 mM p-nitrophenyl phosphate (p-NPP). After 2 h, the enzymatic reaction is stopped with 60 µl/well of 1 N NaOH and the optical density is determined at 405 nm with a Tittertek multiscan. The concentration that produced a 50 % reduction in growth (IC₅₀) is determined using a least-squares linear regression of growth rate versus log component concentration.

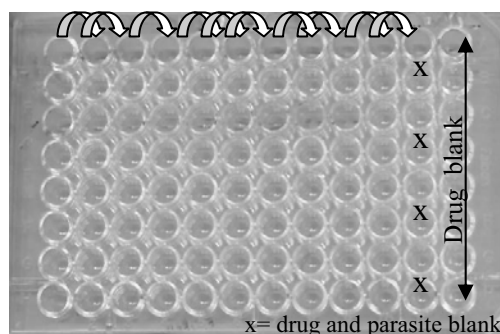


Figure 51: Schematic illustration of preparation of 96-well microtiter plate.

5.3.5.5. Assay on intracellular amastigotes (IA)

Once intracellular amastigotes have been obtained following the process described above, 0,3 ml of RPMI medium with serial double dilutions of each component are added to each well and incubated at 37 °C in a 5 % CO₂ atmosphere for 48 h. Infected cells are subsequently washed and slides are stained with Giemsa dye. Drug activity was evaluated by counting the number of IA and the number of infected cells by examining 300 macrophages at three different places in the reaction area (100 macrophages in each). All experiments are performed in duplicate.

5.3.5.6. Assay of cytotoxicity

The cytotoxicity of excipients, microspheres and solvents is assessed using a modified version of the method described above. Peritoneal macrophage cells (0,3 ml at a concentration of 5×10^4 cells / ml) are cultured in a LabTek 8 chamber slide system (Nunc 177402) and incubated at 37 °C for 24 h in a 5 % CO₂ atmosphere. Then, 0,3 ml of RPMI medium with serial double dilutions of each component are added to each well and incubated at 37 °C in a 5 % CO₂ atmosphere for 48 h. The cells are subsequently washed and slides are stained with Trypan blue dye. Drug cytotoxicity is evaluated by counting the number of macrophages at three different places in the reaction area and comparing with the blank. All experiments were performed in duplicate. The selectivity index (SI) ratios (CC₅₀ for murine macrophages /IC₅₀ for protozoans) are calculated.

5.3.5.7. Statistical analysis

Statistical analysis is performed by using Fischer's test post hoc following ANOVA in which we compare the IC₅₀ values for different kind of microspheres and the t-student test for comparing the technologies used (SPSS 12.0 software for Windows (Chicago, USA). The results are expressed as IC₅₀ mean values ± standard deviation (SD). P-values <0.05 are considered significant.

5.4. RESULTS AND DISCUSSION

5.4.1. Obtention of meglumine antimoniate by lyophilization

In lyophilization is important to freeze the material at a temperature below the eutectic point of the material. Since the eutectic point occurs at the lowest temperature where the solid and liquid phase of the material can coexist, freezing the material at a temperature below this point ensures that sublimation rather than melting will occur in the following steps. Due to MGA is an amorphous (glassy) material it does not has eutectic point, but does has a critical temperature, below which the product must be maintained to prevent melt-back or collapse during primary and secondary drying. Freeze-dryer Telstar machine has lead to deduce the critical temperature of the drug, which is between -14 and -15 °C, from the graphic of the process obtained (figure 52). It is noteworthy, that the weight of the freeze-dried products is below the value of solid material declared (table 26), taking into account the similar Sb purity obtained compared to the declared value (see section 5.4.2.1) it can be deduced that not loading materials exist in the commercial product without be declared.

Product	MGA (g)	Potassium metabisulfite (g)	Anhydrous sodium sulfite (g)	Theoretical weight (g)	Real weight (g)	Loss (%)
Glucantime® 1 (150 ml)	45,000	0,240	0,027	45,27	40,92	9,60
Glucantime® 2 (50 ml)	15,000	0,009	0,080	15,09	14,32	5,10

Table 26: Solid composition of Glucantime® 1 and 2 and percentages of loss by freeze-drying.

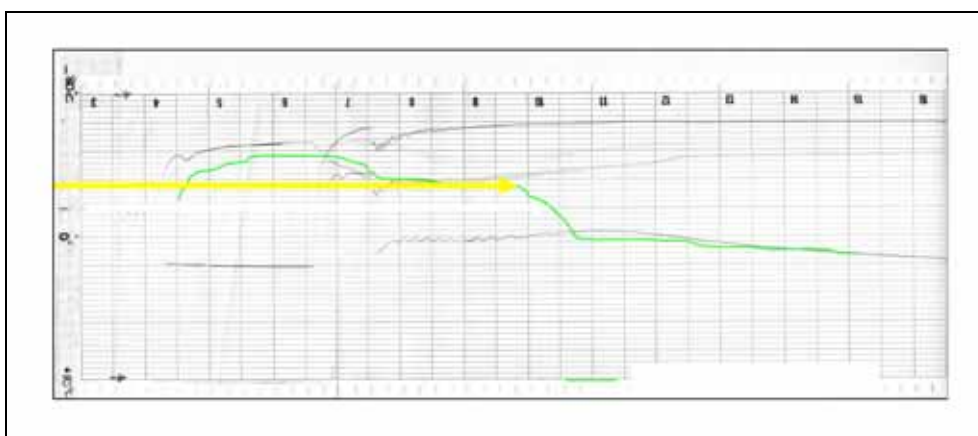


Figure 52: Graphic of the freeze-drying process, green line indicates the temperature of the product. Yellow arrow indicates critical temperature of Glucantime®.

5.4.2. Characterization of meglumine antimoniate

5.4.2.1. Antimony purity

Sb percentages of lyophilized Glucantime[®] and pure MGA obtained by ICP-OES are shown in table 27. In the last case, calibration curves indicate that there are not significant differences between the slopes, and then their results are considered equivalents. The intensities of light at 206,836 nm (highlighted in table 28) are fitted in the equations resulted of calibrations curves obtaining concentration values.

Obtained Sb purity (%)				Reference Sb purity (%)		
Lyophilized product						
Glucantime [®] 1				28,30		
Glucantime [®] 2				na		
Pure MGA				27,10		
External calibration curve $y = 69,4 x + 1,4$ $R^2 = 0,99996$				Standard addition calibration In HCl solution: $y = 70,0 x + 4,3$ $R^2 = 0,99999$ In aqueous solution: $y = 70,2 x + 7,8$ $R^2 = 0,99997$		
	[ppm Sb] 1/5 dilution	[ppm Sb] sample	%	[ppm Sb] 1/5 dilution	[ppm Sb] sample	%
0,1 M HCl solution	10,8	53,8	26,66	10,7	53,3	26,14
Aqueous solution	11,3	56,3	26,19	11,1	55,6	25,86

[intensities] 1/5 dilutions		
	Sb	Sb
	206,836	
S 0	5,51	-1,29
S 1	142,84	131,72
S 2	279,95	265,81
S 3	687,75	645,52
S 4	1393,70	1300,30
HCl 0	746,37	692,35
HCl 1	886,44	824,23
HCl 2	1021,34	946,67
HCl 3	1448,16	1350,56
HCl 4	2144,09	1996,06
H ₂ O 0	780,98	725,39
H ₂ O 1	917,72	855,77
H ₂ O 2	1060,50	986,47
H ₂ O 3	1490,90	1388,94
H ₂ O 4	2181,58	2040,42

Table 27: Sb purities of lyophilized products and pure MGA by ICP-OES

Table 28: Intensities of Sb emission obtained by ICP-OES

As can be seen in the table 27 either commercial ampules or pure MGA has Sb in similar quantities that those declared by the supplier.

5.4.2.2. IR Assay

Lyophilized Glucantime[®] and pure MGA produce the same IR spectrum than that obtained from MGA used as reference in the bibliography (see section 5.3.2.2) (Demicheli C. et al., 1999). IR spectrum of each sample are shown in figures 54 and 55.

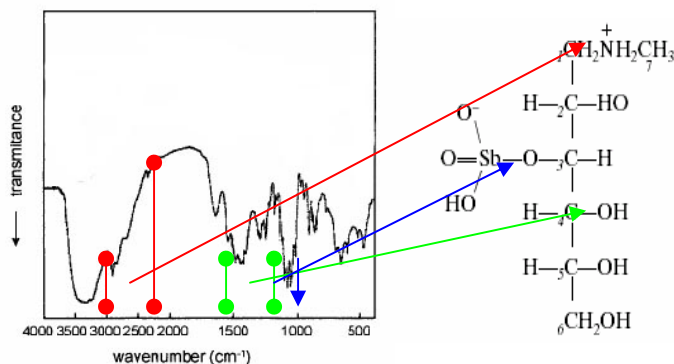


Figure 53: IR Spectrum of MGA related with molecular structure (Demichelli C. et al., 1999).

The absorption bands around 3000 cm^{-1} extending to 2300 cm^{-1} can be attributed to stretching vibrations in the -NH_2^+ -group. Bands around ($1500\text{-}1200\text{ cm}^{-1}$) and ($1100\text{-}1000\text{ cm}^{-1}$) are due to the angular deformation in the plane of O-H groups and C-O stretching vibrations, respectively (see figure 53).

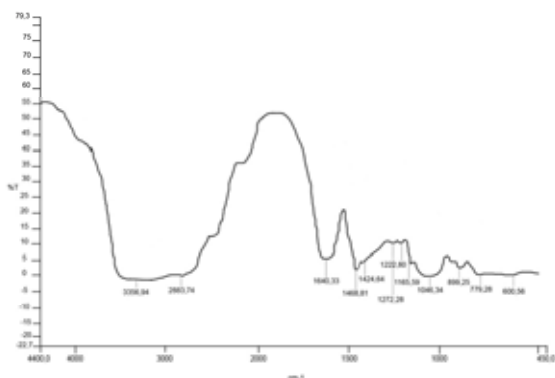


Figure 54: IR spectrum of pure MGA

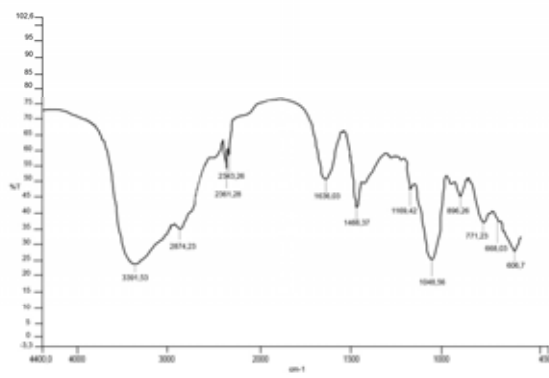


Figure 55: IR spectrum of lyophilized Glucantime 2[®]

5.4.2.3. X-rays diffraction assay

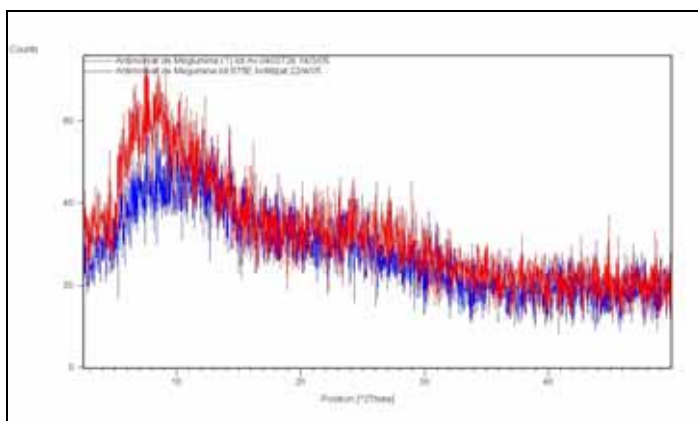


Figure 56: X-rays diffraction patterns of MGA (red) and lyophilized Glucantime 2[®] (blue).

X-rays diffraction patterns of both samples analyzed, pure MGA (red) and lyophilized Glucantime 2[®] (blue), are similar and confirm an amorphous structure of the drug (figure 56).

5.4.2.4. Particle size distribution

The particle size of MGA is 89,7 % lower than lyophilized Glucantime[®] powder.

	Mean (μm)	C.V (%)	d10 (μm)	d50 (μm)	d90 (μm)
Lyophilized Glucantime [®] 1	50,20 \pm 36,07	36,07	7,343	44,25	101,9
Lyophilized Glucantime [®] 2	53,01 \pm 37,42	70,60	8,148	47,22	106,3
MGA	5,11 \pm 7,21	141	0,906	2,564	12,39

Table 29: Particles size distribution of lyophilized Glucantime[®] and pure MGA.

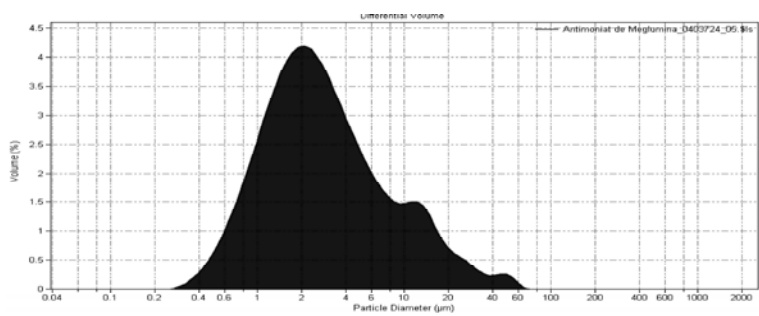


Figure 57: Particle size distribution of MGA.

Pictures of samples are taken by optical microscope (figures 58 and 59); they show differences in aspect because lyophilized powders contain potassium metabisulfite and anhydrous sodium sulfite. The last one has crystalline aspect and the pure drug is amorphous. The pictures confirm the particle size differences.

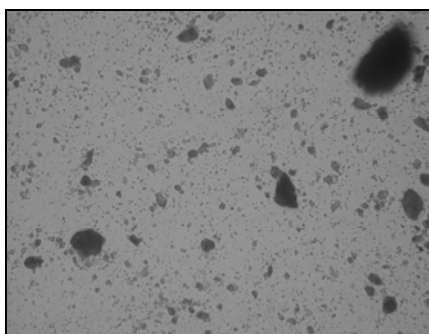


Figure 58: Picture of MGA obtained by optical microscope.

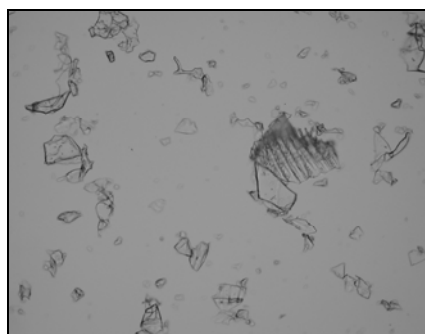


Figure 59: Picture of lyophilized Glucantime[®] 2 obtained by optical microscope.

5.4.2.5. Scanning Differential Calorimetry

The fusion temperature of MGA is 106 °C. The excipients analyzed do not interact to the drug in any case due not to appear different signs than their own fusion temperatures signs. The DSC charts of MGA, chitosan and their combination in proportions 1:1 (2 g/1 g) are shown in the figures 60, 61 and 62 as examples.

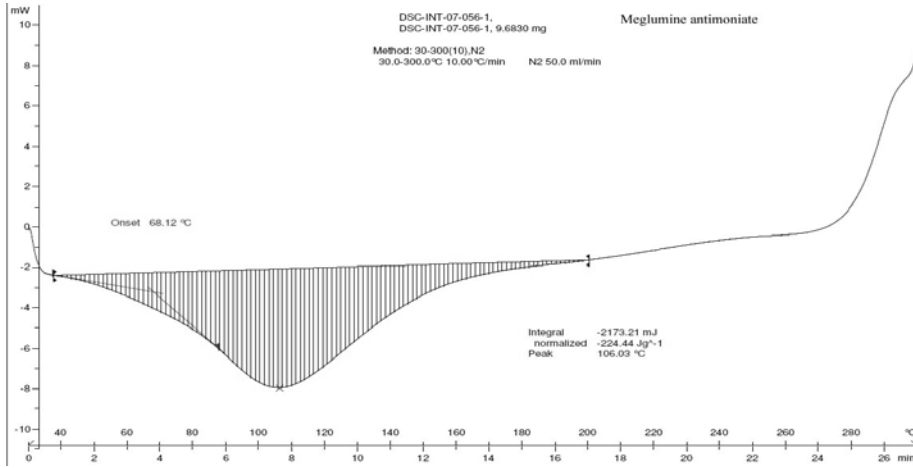


Figure 60: Chart of Differential Scanning Calorimetry of MGA

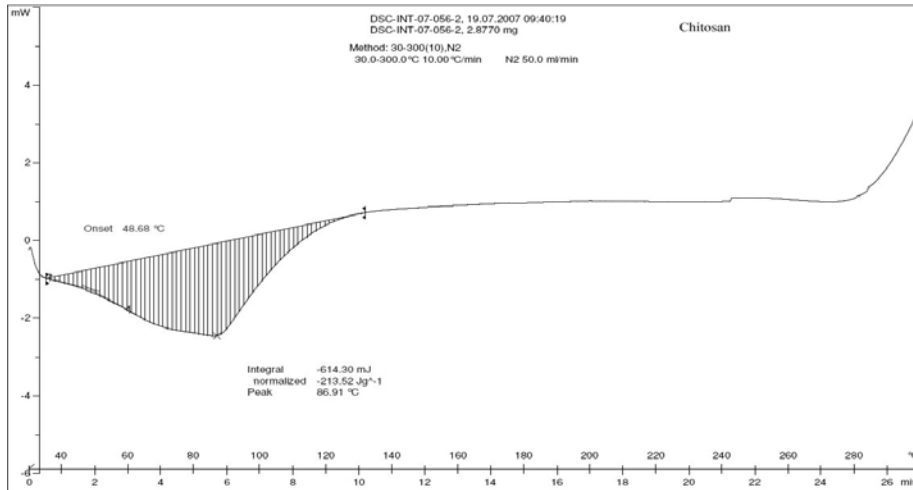


Figure 61: Chart of Differential Scanning Calorimetry of MGA

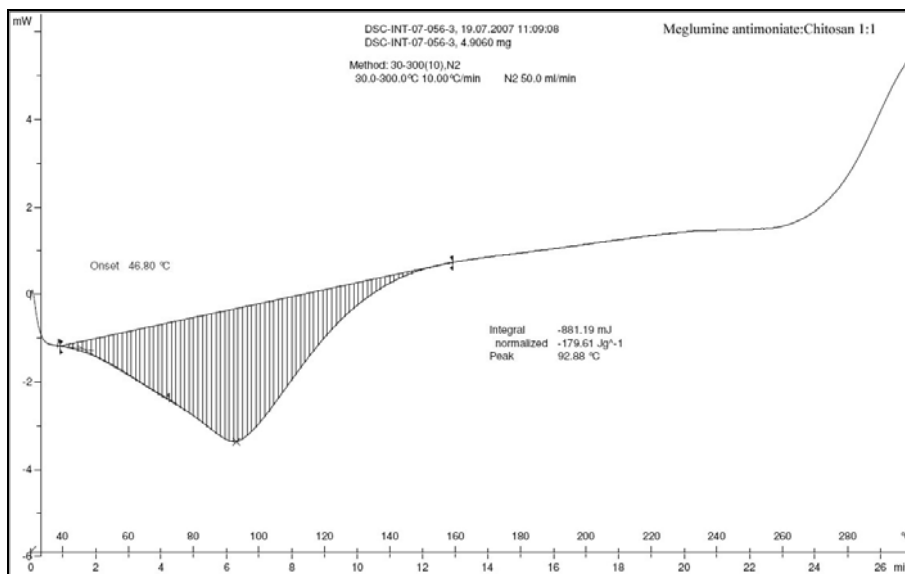


Figure 62: Chart of Differential Scanning Calorimetry of MGA and chitosan 1:1

5.4.2.6. Solubility

Both lyophilized Glucantime[®] and MGA are considered easily soluble in water due to 1g of product is soluble in 1,2 ml of water (833,3 mg/ml). Other studies where solubility of MGA have been described indicates a solubility of > 300 mg/ml (Martins P.S. et al., 2006).

5.4.2.7. pH in aqueous solution

All the solutions carry out the Brazilian Pharmacopea specifications (F.Bras.IV,2002) (pH between 5,5 and 7,5) as can be shown in the table 30.

Solutions	pH
5% w/v MGA solution	7.43
5% w/v Glucantime [®] lyophilized powder solution	7.06
30% w/v MGA solution with 0,16% w/v sodium metabisulfite	6.68
Glucantime [®] vials	6.71

Table 30: pH's of the different MGA solutions prepared.

5.4.3. Development of a new dosage form for meglumine antimoniate

5.4.3.1. Emulsions, self-emulsifying drug delivery systems and nanosuspensions

Three different MGA **emulsions** were designed to be developed (see section 5.3.3.1). Either formulations n° 1 or 2 lead to obtain fluid and amber emulsions and separation of phases does not appear in 48 hours. However, it is not possible to obtain an emulsion from formulation n° 3; the aspect of pure MGA changes in the moment when water phase is added into the baker which contain the oil phase and then the formula becomes a thick mass which is impossible to mix. Different reasons could be the cause of this behaviour such as: (1) particle size difference between lyophilised Glucantime[®] (used in formulations n° 1 and 2) and pure MGA (used in formulation n° 3) (particle size decreases 89,78 % respectively, see section 5.4.2.4). Consequently, if particle size is smaller, there is more specific surface which can be surrounded by water. Then, solvated pure MGA in solution is not be able to be dispersed in oil phase. (2) Some incompatibility between excipients. This last possible cause is sorted out by DSC.

The behaviour of the emulsions n° 1 and n° 2 in front of different pH, HCl pH 1,5 and phosphate buffer solution, is as follow: once drops of emulsion are taken into both bakers, they go down and become more white of colour. The oil phase disperses and moves upward slowly, and then the powder dissolves. However, some difference between samples can be appreciated. Dispersion of both formulations is faster in higher pH. Nevertheless, in low pH emulsion n° 1 disperses slower than n° 2 and in high pH disperses faster. It is believed that emulsion n° 2 could be an adequate candidate for an intestinal delivery of MGA, however it is necessary to study other options after finding undesirable behaviour of pure MGA during the emulsification process.

Both **SEDDS** prepared emulsify correctly after be mixed with aqueous and acidic solution under shaking manually. pH values at 10 % w/v in water of O/W and W/O SEDDS are 6,61 and 6,70, respectively. These lipophilic formulations could minimise problems derived of water presence such as microbiological contamination or product instability.

The results of the controls of the ‘macro’-**suspensions** elaborated are summarised in the next table:

Suspensions	Aspect	Viscosity (mPa)	Density	Particle size distribution
N°1	Cream colour, easy resuspension	876,6	1,05 g/ml	n.a
N°1 (drug-free)	Amber colour, easy resuspension	140	1,00 g/ml	n.a
N°2	Cream-white colour, resuspension easy	190	1,05 g/ml	93,4 % : 1-10 µm 6,6 %: 10-50 µm
N°2 (drug-free)	Cream-white colour, easy resuspension	116,6	1,00 g/ml	79.73 % : 10-1 µm 12.96 %: 50-10 µm 2.33 %: 100-50 µm 2.99 %: 200-100 µm 1.66 %: 300-200 µ m 0.33% >300 µm

Table 31: Controls of MGA and drug-free suspensions

Viscosity is lower in formulation n° 2 due to be homogenized by high speed mixer. Moreover, the nanosuspensions obtained from Emulsiflex C-3 are satisfactory in aspect but not characterized because the process is not possible to scale up using a high pressure homogenizer (Liquids Stansted fluid power LTD).

According to the results above it is thought to give up the three different strategies studied at the beginning and continue with the development of a solid dosage form

produced by a scalable technique, spray-drying, where MGA was encapsulated. The excipients used previously will be taken into account in the new formulations.

5.4.3.2. Nano/microspheres by spray-drying

5.4.3.2.1. Chitosan microspheres preparing a novel O/W emulsion technique by spray-drying

A) Pre-formulation

The viability of spray-drying process has been studied with 8 formulations. Sample **A1** remains totally stuck in apparatus after be processed, hence not powder is recollected. However, all the rest of samples remain only partially stuck along the cylinder and the cyclone. Sample **A8**, without polyoxyl 40 hydrogenated castor oil 1, is stuck in less magnitude than others; therefore this excipient is the main cause of the problem.

Watching the pictures by SEM (numerated by letters) it is possible to confirm the possibility to obtain microspheres from samples **A2** to **A8**. Microspheres **A2** are more spherical and smaller, have less porosity and particle size dispersity than the others (figure 63).

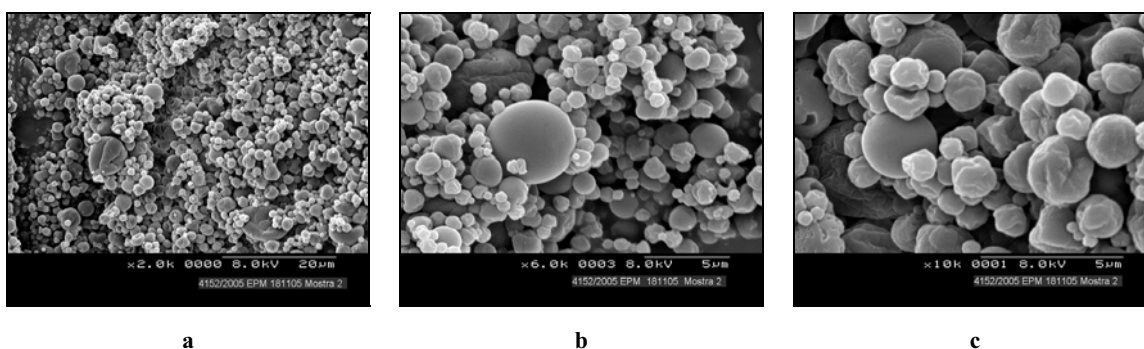


Figure 63: Chitosan microspheres A2 under SEM.

Microspheres **A3** (d) and **A4** (e and f) show a porous surface and the last one a higher particle dispersity (figure 64).

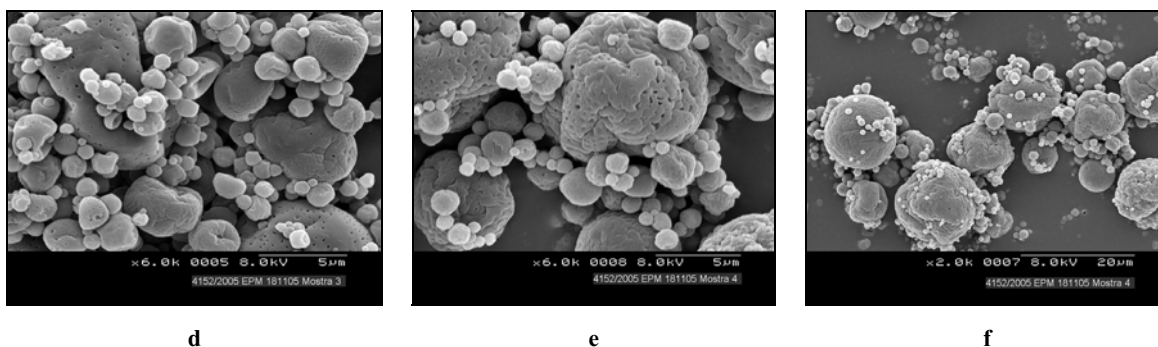


Figure 64: Chitosan microspheres A3 (d) and A4 (e and f) under SEM.

Few differences exist between microspheres where lactose has been used as excipient (figure 65): **A5a** (g and h), **A5b** (i and j) and **A7** (k and l), having in all cases wrinkly surface and high particle size dispersity. However, can be appreciated a loss of sphericity in **A7** which can be attributed to the different step in the elaboration process (emulsion phases are heated before emulsification). The difference between **A5a** and **A5b** is the percentage of pump, 20 % and 15 % respectively, which does not seem influence on morphology.

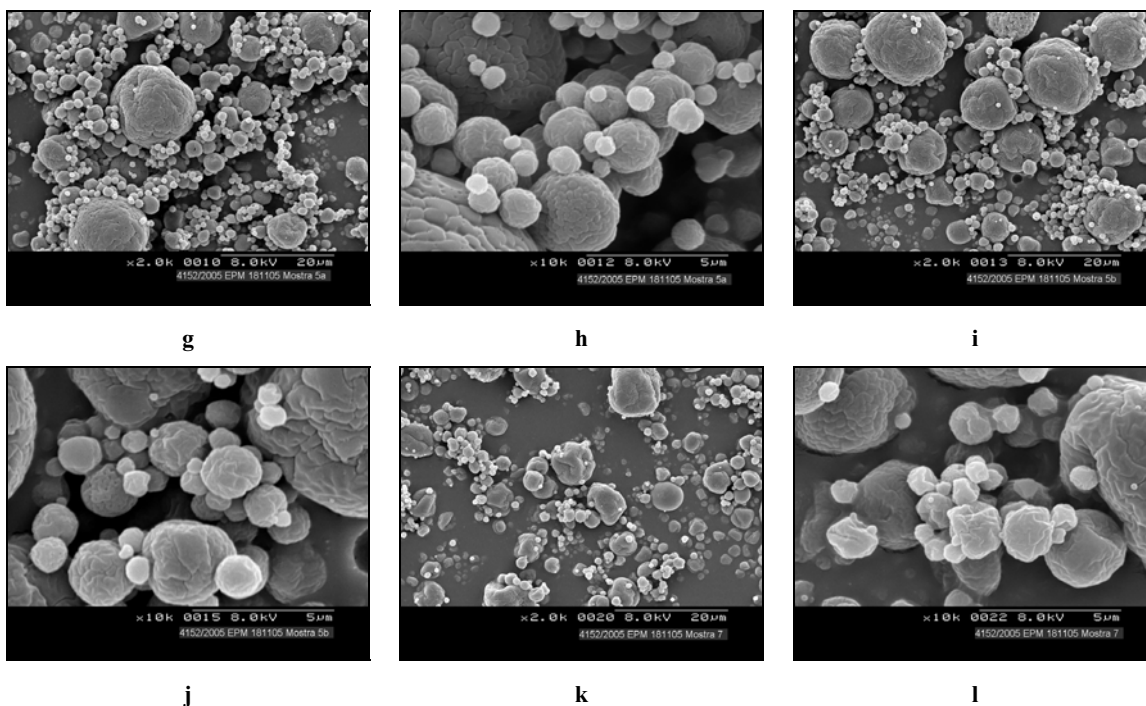


Figure 65: Chitosan microspheres with lactose : A5a (g and h), A5b (i and j) and A7 (k and l) under SEM.

Microspheres **A6** do not contain chitosan and they are irregular and not spherical (figure 66). Maltodextrin is being used as carrier in this effort but this polymer is also considered a wall material (Watanabe Y. et al., 2002) which is the responsible of the microspheres obtained in this case. The white agglomerate which can be seen in picture **m** (figure 66) could be a contamination of MGA if it is compared to the picture of pure MGA under SEM (figure 68).

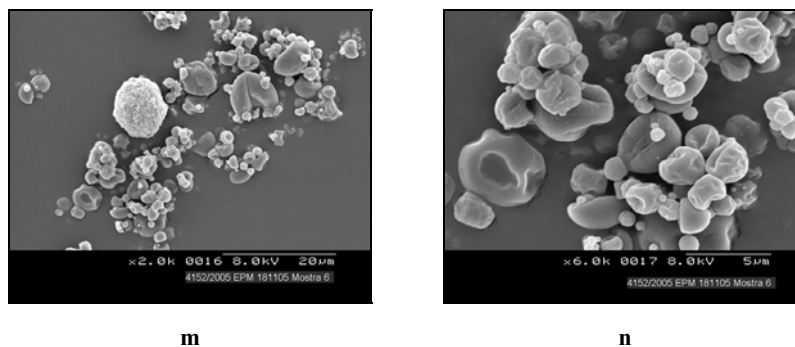


Figure 66: Pictures of particles A6 which do not contain chitosan under SEM.

Microspheres **A8** which do not contain polyoxyl 40 hydrogenated castor oil, a non-ionic surfactant, present a curious morphology. They are irregular and folded inward, probably due to an increment of surface tension. Moreover, there is high particle size dispersity (figure 67).

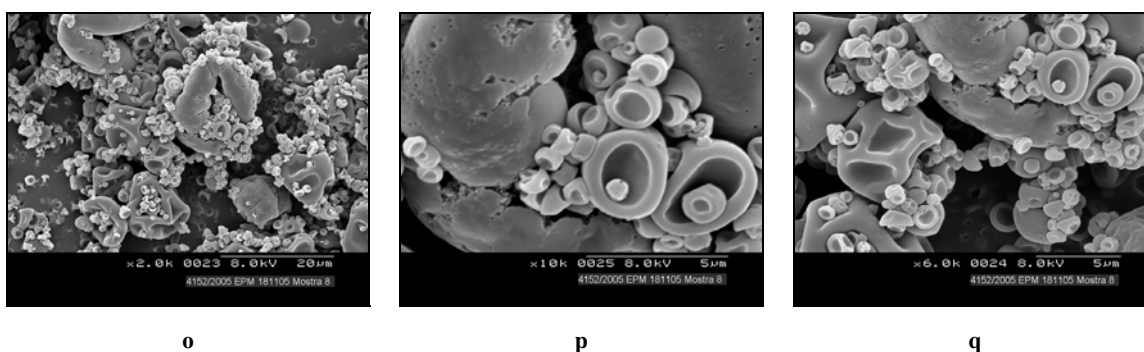


Figure 67: chitosan microspheres A8 without polyoxyl 40 hydrogenated castor oil 1 under SEM.

After these results, morphological characteristics of microspheres **A2** are considered better than the others, for this reason its formulation is selected to continue the studies. Straight afterwards, 2 % w/v MGA is incorporated in the formulation **A2** in order to be encapsulated into microspheres **A9** (formula A9).

One simple preliminary test to know if the drug is being encapsulated is to compare the pictures by SEM of MGA alone to the pictures of the powders of formulation **A9**. Figure 68 shows the appearance of the drug without any excipient, in which it is possible to see a not spherical and irregular mass.

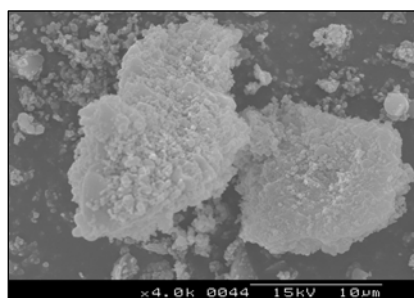


Figure 68: Pure MGA under SEM.

The figure 69 shows the microspheres **A9** that are recollected in the vessel located in the final part of spray-drier apparatus and the powder recovered from the cyclone. In these pictures, it is possible to see how MGA has been encapsulated into microspheres because its amorphous structure does not appear. It is worth highlight that microspheres recovered from the cyclone appear more irregular, put out of shape and bigger than those from the vessel. The particle sizes are $5,221 \mu\text{m} \pm 5,635 \mu\text{m}$ and $4,666 \pm 5,132 \mu\text{m}$, respectively.

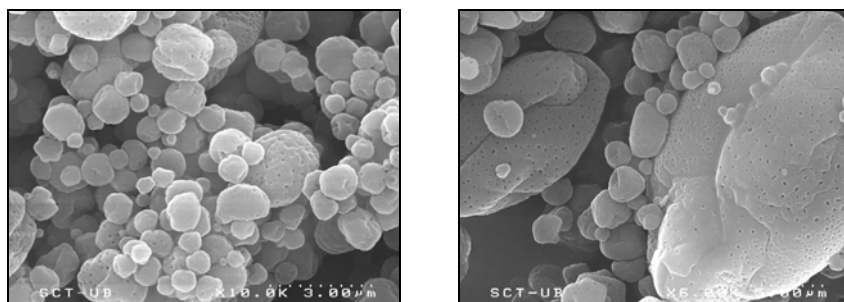


Figure 69: SEM pictures of microspheres **A9** recollected in final bottle (left) and cyclone (right).

The possibility to change the kind of maltodextrin excipient to a lower grade of dextrose equivalent (from 19 D to 6D, therefore less hygroscopic) could imply lower final residual moisture. A new formulation (**A10**) is prepared to study it. Figure 70 shows the microspheres obtained. Although microspheres **A9** and **A10** are morphologically similar, the fact to change the maltodextrin 19 D to 6D, produce an increase of loss because more powder remains stuck in the apparatus (cylinder) in form of crunchy amber layer. In this case, the morphology of the powder stuck in the cyclone has been also studied and it presents more porosity and irregular shapes. The mean particle size of formulation **A10** (from cyclone and vessel together) is $5,099 \mu\text{m} \pm 3,561$.

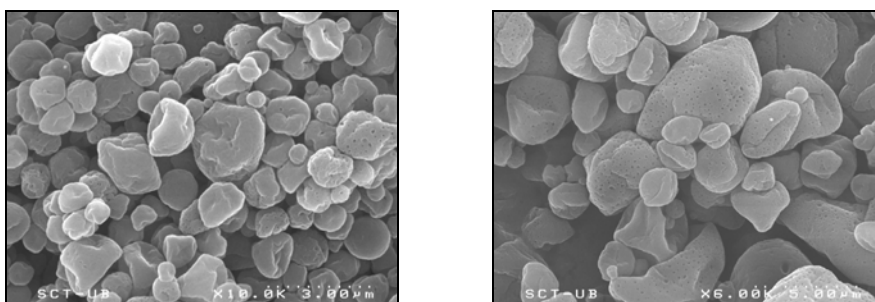


Figure 70: SEM pictures of microspheres **A10** recollected in final bottle (left) and in cyclone (right).

The formulation **A9** is selected as the best formulation technological developed in the pre-formulation studies because MGA has been efficiently encapsulated in chitosan

microspheres atomizing an O/W emulsion. These microspheres are rather regular and spherical having an interesting size range under SEM.

B) Influence of lipid concentration, inlet temperature and emulsification method

Taking pre-formulation studies as reference, new microspheres are prepared by spray-drying using an experimental design 2³ to study in depth the effects of both formulation and operational parameters on the process outcome and powder properties. The characteristics of MGA microspheres prepared by spray dried are summarized in the table 32.

N°	% oil phase (A)	Inlet t° (B)	HPH (C)	Yield (%)	Moisture content (%)	Drug contents (%)			Particle size (µm)	Polidispersity (CV%)
						Added [ppm Sb]	Found [ppm Sb]	Efficiency		
B1	2	130	-1	22,59	3,58	71,69	68,46	108,70	3,62	80,00
B2	4	130	-1	33,98	3,14	63,03	60,17	95,87	5,90	93,10
B3	2	180	-1	34,45	3,37	71,65	70,20	97,97	4,94	74,80
B4	4	180	-1	40,21	3,32	62,98	57,25	79,99	4,37	91,10
B5	2	130	1	33,37	3,34	71,58	68,47	108,63	4,10	80,10
B6	4	130	1	42,34	3,42	62,77	60,51	84,54	5,22	109,00
B7	2	180	1	36,22	2,92	71,57	71,21	99,33	4,39	83,00
B8	4	180	1	44,63	3,29	63,24	60,92	96,33	4,07	72,40

Table 32: The influence of lipid concentration, inlet temperature and emulsification method in meglumine antimoniate microspheres prepared by spray dried method.

It is worth pointing out that formulation **A9**, selected in pre-formulation studies, would be equivalent to **B4** in this factorial design.

Factorial ANOVA test has been used to analyze the results comparing the variances to the F-ratio values.

B.1. Influence of parameters on morphological properties

The mean particle size of O/W chitosan microspheres of this design is $4,576 \mu\text{m} \pm 0,734 \mu\text{m}$ with a mean polidispersity of $85,438 \% \pm 11,911 \%$. All cases have a normal particle size distribution. It is noteworthy that the particle size range includes nanoparticles (table 33), however, in order to facilitate the lecture, microspheres will be the term used from now on.

Microspheres	Mean (μm)	Median (μm)	Mode (μm)	S.D. (μm)	C.V. (%)	d10 (μm)	d25 (μm)	d50 (μm)	d90 (μm)
B1	3,616	2,654	2,539	2,894	80,00	0,879	1,441	2,654	7,982
B2	5,895	4,099	4,877	5,487	93,10	1,037	1,933	4,099	13,22
B3	4,940	4,181	5,878	3,694	74,80	0,945	1,812	4,181	10,52
B4	4,374	3,080	4,047	3,983	91,10	0,956	1,595	3,080	9,641
B5	4,103	3,033	4,877	3,287	80,10	0,864	1,490	3,033	9,460
B6	5,223	3,298	3,059	5,680	109,00	0,935	0,621	3,298	5,680
B7	4,390	3,242	5,354	3,642	83,00	0,875	3,242	3,242	10,19
B8	4,070	3,230	5,354	2,947	72,40	0,982	3,230	3,230	8,602

Table 33: Particle size distribution of O/W chitosan microspheres prepared by spray-drying.

Lipid concentration, inlet temperature, emulsification method factors and their interactions do not influence significantly in the morphological parameters studied ($P>0,05$). However, high inlet temperature results in smaller sized and spherical microspheres (a) whereas; lower inlet temperature results in larger microspheres with irregular shape and a wrinkled appearance (b, c, d) (figure 71).

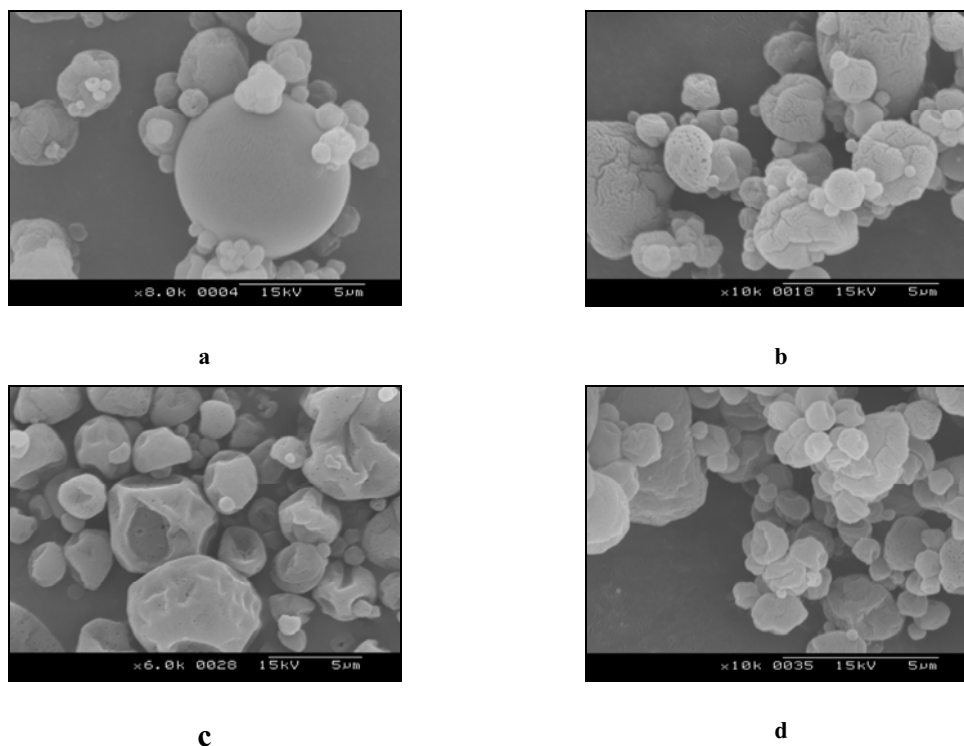


Figure 71: SEM pictures of B7 microspheres (a) produced at 180 °C and B5 (b), B6 (c) and B2 (d) microspheres produced at 130 °C.

Moreover, the interaction between inlet temperature and lipid concentration tends to reduce the particle size and dispersity although it is not significant. Furthermore, high pressure homogenization, high inlet temperature and their interaction also reduce the particle size (figure 72).

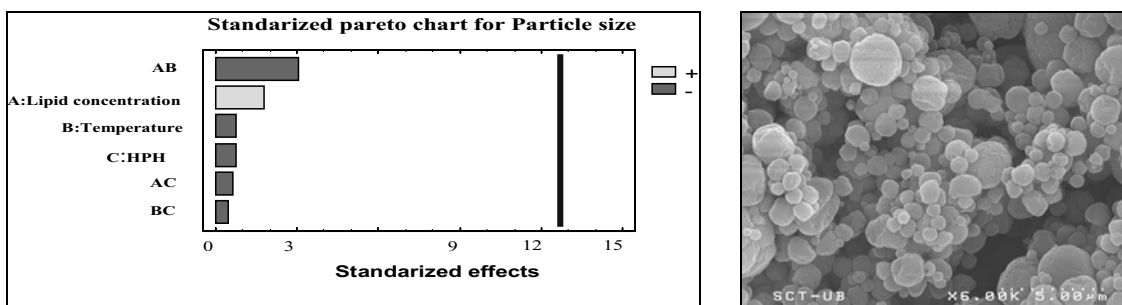


Figure 72: Standardized pareto chart for particle size (left) and chitosan microspheres B8 under SEM obtained from high pressure homogenised emulsion (right).

Summarizing, the processing parameters investigated have a greater influence on the morphological characteristics compared to the formulation parameters investigated. To obtain spherical O/W emulsion chitosan microspheres with low polydispersity and relatively smooth surfaces, high pressure homogenization and a high inlet spray drier temperature appeared to be important processing parameters.

B.2. Influence of parameters on residual moisture

The mean moisture value obtained from chitosan microspheres is 3,298 % ± 0,196 %. ANOVA test reflects how the factors and their interactions do not influence significantly on the residual moisture ($P > 0,05$) but high level of each factor decrease the residual moisture. In the figure 73, main effects plot for moisture is shown:

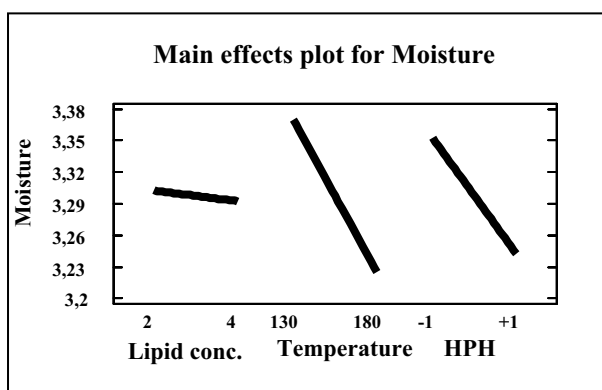


Figure 73: Main effects plot for moisture

B.3. Influence of parameters on the yield of the process

The mean yield of obtaining chitosan microspheres from O/W emulsions is 35,973 % ± 6,820 %. Studying the influence of the factors on the yield of the process by ANOVA test the following results are obtained (table 34):

Analysis of variance for Yield					
Source	Sum of Squares	Df	Mean square	F-Ratio	P-Value
A:Lipid concentration	149,04	1	149,04	46,38	0,0928
B:Temperature	67,4541	1	67,4541	20,99	0,1368
C:HPH	80,2011	1	80,2011	24,96	0,1258
AB	4,78951	1	4,78951	1,49	0,4369
AC	0,0066125	1	0,0066125	0,00	0,9711
BC	20,9628	1	20,9628	6,52	0,2376
Total error	3,21311	1	3,21311		

Total (corr.)	325,667	7			

R-squared = 99,0134 percent
R-squared (adjusted for d.f.) = 93,0936 percent
Standard error of Est. = 1,79252
Mean absolut error = 0,63375
Durbin-Watson statistic= 2,5
Residual autocorrelation Lag 1 = -0,375

Table 34: ANOVA test for yield

The sum of squares of the interaction between lipid concentration and high pressure homogenization (AC) is lower than total error and F-ratio is 0. It means that this parameter does not have a significant influence in the yield so that it can be included in the total error. The results are shown in the table 35:

Analysis of variance for Yield					
Source	Sum of Squares	Df	Mean square	F-Ratio	P-Value
A:Lipid concentration	149,04	1	149,04	92,58	0,0106
B:Temperature	67,4541	1	67,4541	41,90	0,0230
C:HPH	80,2011	1	80,2011	49,82	0,0195
AB	4,78951	1	4,78951	2,98	0,2267
BC	20,9628	1	20,9628	13,02	0,0689
Total error	3,21972	2	1,60986		

Total (corr.)	325,667	7			

R-squared = 99,0113 percent
R-squared (adjusted for d.f.) = 96,5397 percent
Standard error of Est. = 1,2688
Mean absolut error = 0,63375
Durbin-Watson statistic = 2,50103 (P=0,0000)
Residual autocorrelation Lag 1 = -0,375513

Table 35: ANOVA test for yield

Taking into account P-values (table 35) in a 95% confidence interval it can be deduced that the probability of the differences in the factors lipid concentration, temperature and high pressure homogenization were by chance is 1,6 %, 2,3 % and 1,95 % respectively and they influence significantly in the yield because P-values are lower than 0,05. These significant influences also can be seen in the standardized pareto chart for yield in the figure 74. Moreover, there is also described the optimised answer for yield obtained by the statistical program. In order to obtain the optimum yield value, 43,99 % , all factors should have to be applied at high levels: 4 % of lipid concentration, 180 °C of inlet temperature and use high pressure homogenization (figure 74).

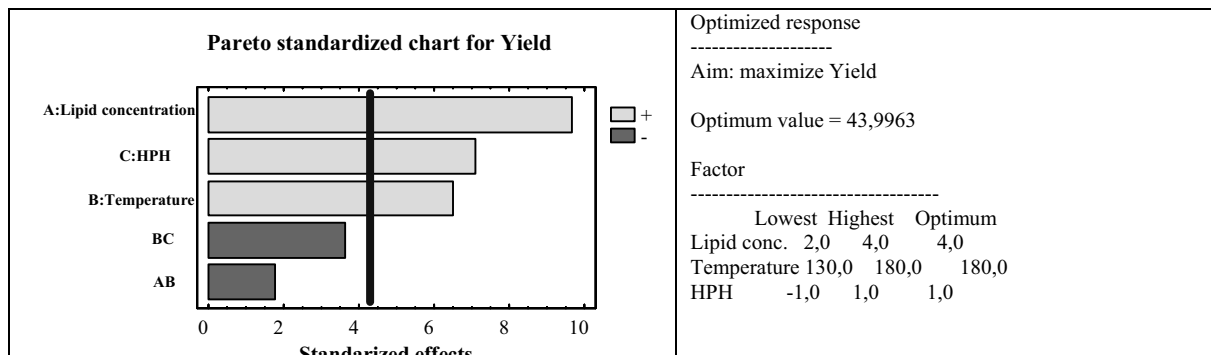


Figure 74: Pareto standardized chart (left) and optimized response for yield (right)

B.4. Influence of parameters on efficiency of encapsulation

Efficiency of encapsulation has been calculated considering the two different w/w percentage of MGA in the samples (13,33 % in low level of lipid concentration and 11,76 % in high level) and the drug purity. The only possibility to quantify MGA included into the drug device is detecting its antimony content; for this reason, the antimony purity of the MGA added in the formulations has been considered to calculate efficiency encapsulation (26,6 % w/w by ICP-OES at 206,836 nm). The results of the efficiency of drug encapsulation into microspheres are shown in the table 36, where ICP-OES intensities signals are also present.

N°	Sb 206,836 nm		[ppm Sb] 1/5 dilution	[ppm] 1/5 found	[ppm Sb] found	% encapsulation
	intensity	[ppm Sb] added				
B1	661,32	62,98	12,60	13,69	68,46	108,70
B2	581,26	62,77	12,55	12,03	60,17	95,87
B3	678,06	71,65	14,33	14,04	70,20	97,97
B4	553,02	71,57	14,31	11,45	57,25	79,99
B5	661,41	63,03	12,61	13,69	68,47	108,63
B6	584,50	71,58	14,32	12,10	60,51	84,54
B7	687,85	71,69	14,34	14,24	71,21	99,33
B8	588,44	63,24	12,65	12,18	60,92	96,33
$y = 48,32x - 0,4081$ $R^2 = 1$						

Table 36: Efficiency of encapsulation of meglumine antimoniate into chitosan microspheres.

The mean efficiency encapsulation percentage is 96,42 % +/- 3,28. The results of ANOVA test are shown in the table 37.

Analysis of variance for efficiency of encapsulation					
Source	Sum of Squares	Df	Mean square	F-Ratio	P-Value
A:Lipid concentration	419,051	1	419,051	4,87	0,2709
B:Temperature	72,7218	1	72,7218	0,84	0,5268
C:HPH	4,96125	1	4,96125	0,06	0,8500
AB	31,7604	1	31,7604	0,37	0,6525
AC	1,7298	1	1,7298	0,02	0,9103
BC	105,851	1	105,851	1,23	0,4671
Total error	86,0672	1	86,0672		

Total (corr.)	722,143	7			
R-squared = 88,0817 percent					
R-squared (adjusted for d.f.) = 16,5719 percent					
Standard Error of Est. = 9,27724					
Mean absolut error= 3,28					
Durbin-Watson Statistic= 2,5					
Residual Autocorrelation Lag 1 = -0,375					

Table 37: ANOVA for efficiency of encapsulation

Highlighted F-ratios in the table 37 which are almost 0, are included in the total error. The results are shown in the table 38:

Analysis of variance for efficiency of encapsulation					
Source	Sum of Squares	Df	Mean square	F-Ratio	P-Value
A:Lipid concentration	419,051	1	419,051	9,55	0,0907
B:Temperature	72,7218	1	72,7218	1,66	0,3269
C:HPH	4,96125	1	4,96125	0,11	0,7687
AB	31,7604	1	31,7604	0,72	0,4846
BC	105,851	1	105,851	2,41	0,2607
Error Total	87,797	2	43,8985		

Total (corr.)	722,143	7			
R-squared = 87,8422 percent					
R-squared (adjusted for d.f.) = 57,4476 percent					
Standard error of Est. = 6,62559					
Mean absoluto error= 3,28					
Durbin-Watson statistic= 2,50985 (P=0,0000)					
Residual autocorrelation Lag 1 = -0,379926					

Table 38: ANOVA for efficiency of encapsulation

Taking into account P-values (table 38) in a 95% confidence interval it can be deduced that the factors and interactions do not influence significantly in the efficiency of encapsulation of the process because P-values are higher than 0,05. However, slightly differences can be appreciated; high percentage of lipids and high temperatures reduce efficiency of encapsulation and high pressure homogenization tends to increase it (figure 75).

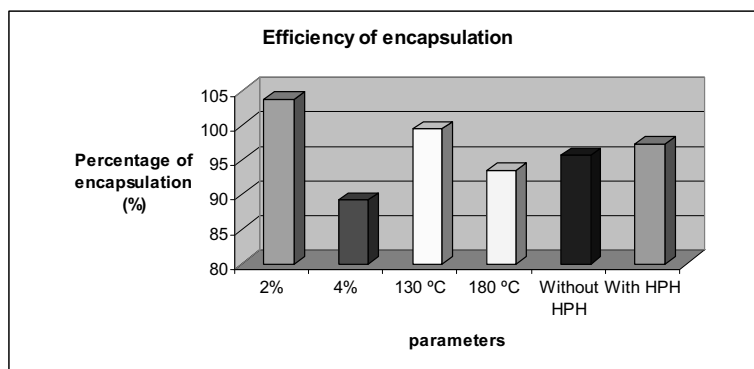


Figure 75: Efficiencies of encapsulation by groups of experiments.

From this factorial design, **B8** conditions (4 % lipid concentration, 180 °C and high pressure homogenization) are selected as the most appropriated to produce spherical O/W emulsion chitosan microspheres with low polydispersity, relatively smooth surface and with the lowest residual moisture. These conditions lead to maximize the yield of the process and to obtain a high efficiency of encapsulation. The only different parameter compared to **A9** pre-formulation is the high pressure homogenization which will be included in the formulations of the next studies.

C) Influence of PGPA inhibitors

The likely disrupters of PGPA, MCT and Polyoxyl 40 hydrogenated Castor Oil, had been the reason to formulate an emulsion of MGA due to their lipophilic characteristics. They have been deleted individually or both at the same time in the new formulations prepared in order to study how they affect in the effectiveness *in vitro* against *L.infantum* and in the technological process. The spray-drying conditions and compositions are established following the previous results. **B8** microspheres are used as reference. Formula composition can be seen in the table 18 in section C of 5.3.3.2.2.

During the process is observed that formulations without Polyoxyl 40 hydrogenated Castor Oil (**C2** and **C3**) tends to stick less in the cyclone, even formulation **C3** does not stick anything there. **C1**, **C2** and **C3** formulations have been studied morphologically by SEM and it is possible to appreciate that **C3** microspheres have smoother surfaces than **C1** and **C2**. Curiously, the absence of Polyoxyl 40 hydrogenated Castor Oil in pre-formulation studies (inside different compositions and under other conditions) produced totally collapsed and irregular microspheres but it does not occur in the present cases. Some broken microparticles appear in the sample **C2**. Their SEM pictures and mean particle size values are shown in table 39:

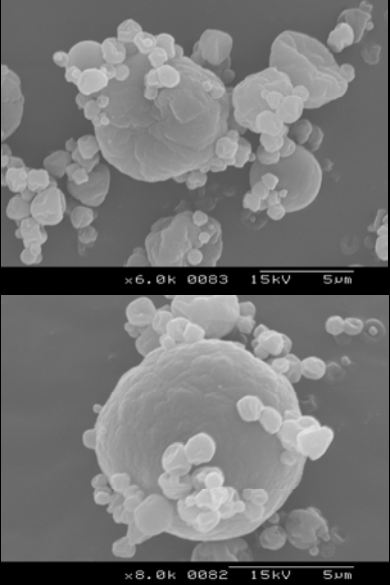
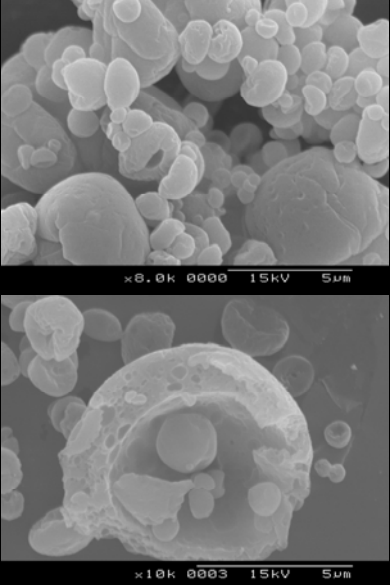
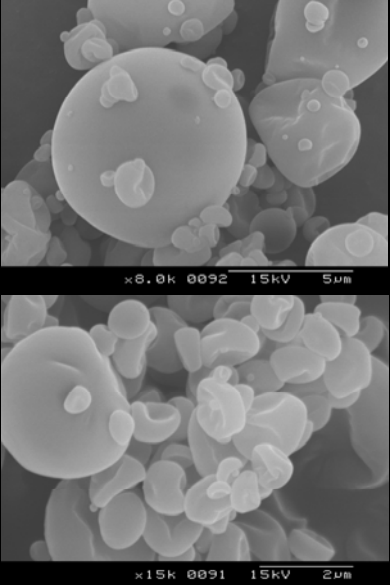
	Formulations		
	C1	C2	C3
SEM			
Particle size	4,988 ± 4,559	3,613 ± 3,300	4,628 ± 3,827

Table 39: SEM pictures of microspheres C1 (without MCT), C2 (without Polyoxyl Hydrogenated 40 Castor oil) and C3 (without both PGPA inhibitors) and their mean particle size values.

It has been tested the possibility to eliminate only the third lipidic component, lecithin, without any relation with PGPA in order to complete the study of the disrupters in the *in vitro* assays in front *Leishmania*. Lecithin is used to stabilize the emulsion due to act as surfactant, consequently the emulsion **C4** (without lecithin but with MCT and Polyoxyl Hydrogenated 40 Castor oil) is not stable and tends to separate in two phases. This sample requires to be homogenized twice by high speed mixer, then once it is passed through the spray-drier it is highly stuck in cyclone and the yield of the process is only of 23,57 % compared to 43,99 % established as the optimum.

Microspheres without lipidic components should be also tested *in vitro* so that microspheres which are obtained from a solution (**C5** and **C6**) are prepared. The stuck powder in the spray-drier decrease considerably obtaining a yield process of 58,16 % . The morphology studied by SEM of these last microspheres is similar to **C3**, they have smooth surfaces and some particles are fold inward (figures 76 and 77). Afterwards, these new kind of microspheres from simple solutions will be studied in depth.

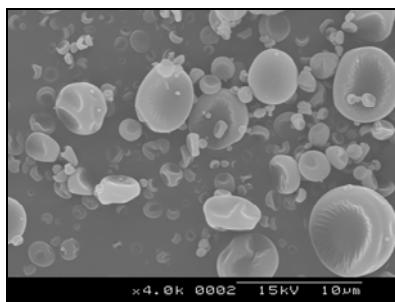


Figure 76: SEM picture of C5 microspheres

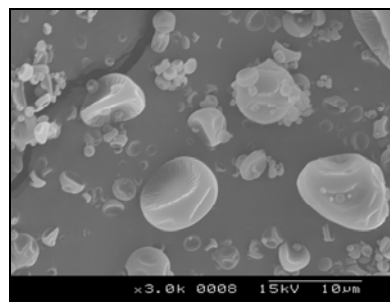


Figure 77: SEM pictures of C6 microspheres

5.4.3.2.3. Optimization chitosan microspheres preparing solutions by spray-drying

A) Pre-formulation

The fact to eliminate all the lipidic components of the formulation **B8**, obtaining microspheres **C5** and **C6**, simplifies the method because it is only necessary to prepare a solution to be spray dried. The preparation is faster and the loss of material during the process is lower, then the yield is higher.

The previous chitosan microspheres from a solution (**C5** and **C6**) should be morphologically improved; hence some changes in formulation are done (figure 78).

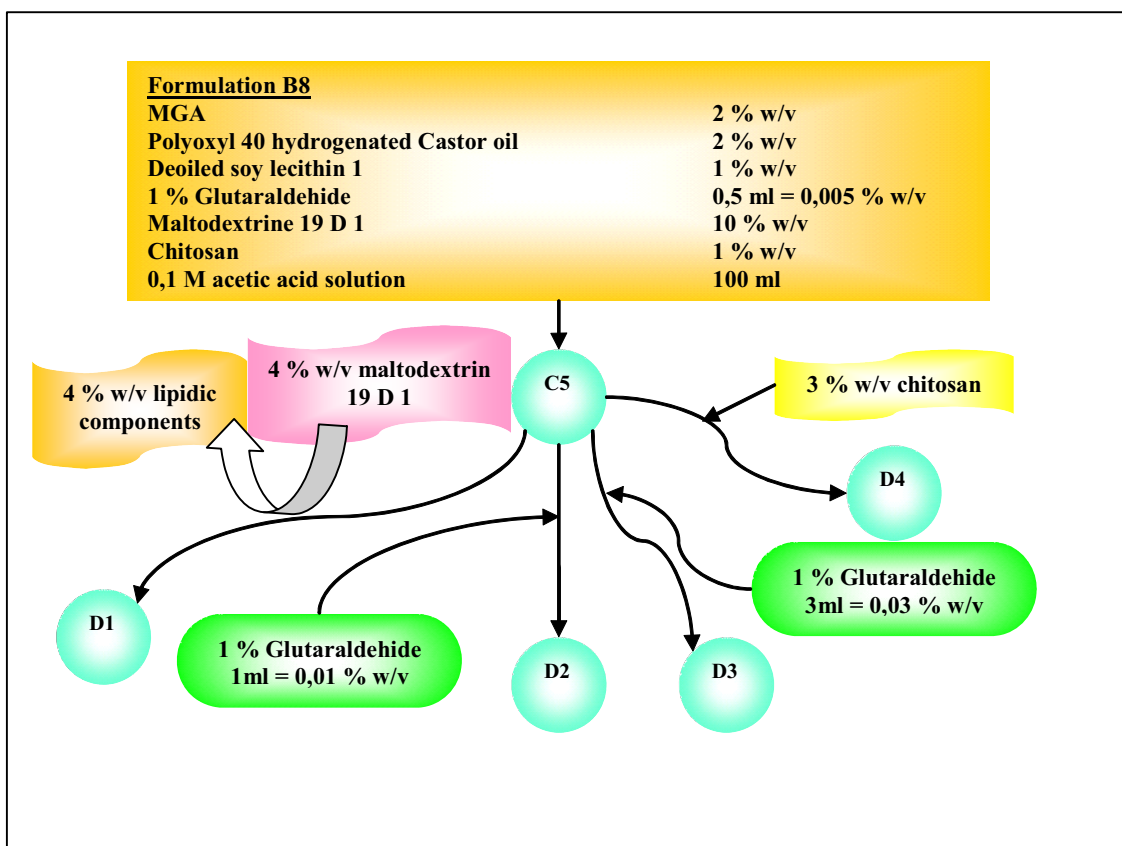


Figure 78: Schematic illustration of pre-formulation studies in the optimization of chitosan microspheres preparing solutions by spray-drying.

The deleted percentage of weight of oil phase in the formula (4 %) is replaced by more maltodextrin 1 (**D1**). Most of the particles continue appearing fold inward (**a**), some of them are too big and broken (**b**) and even there is some irregular and not defined particle (**c**) (figure 79).

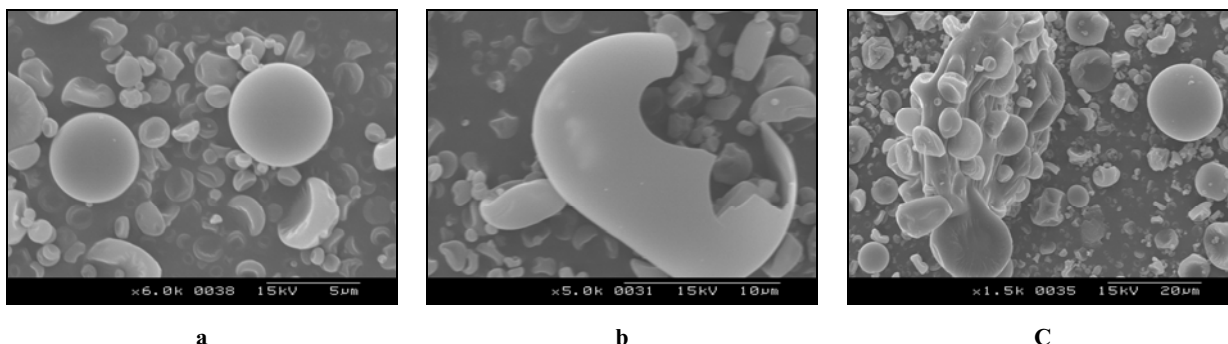


Figure 79: Chitosan microspheres D1 prepared with 14 % w/v of maltodextrin 1.

In order to harden the surfaces trying to avoid the invaginated appearance, the percentage of glutaraldehyd is increased. Until now, only 0,005 % w/v was added in the solutions (0,5 % weight glutaraldehyd / weight chitosan). This quantity is replaced by 0,01 % (w/v) (1 % weight glutaraldehyd / weight chitosan) to form microspheres **D2**, and 0,03 % (w/v) (3% weight glutaraldehyd /weight chitosan) forming **D3**. In figure 80 can be seen that in the lower percentage tested, some microspheres continue appearing folded inward although those smaller seem more spherical (**d**). Using 3 % w/w of glutaraldehyd the microspheres obtained are bigger (**e**) and some of them appear broken (**f**). In the last picture is possible to appreciate how the wall is wider than microspheres done with 0,5 % w/w of glutaraldehyd and high level of maltodextrin (**b**) but thinner compared to that microspheres prepared from an emulsion (table 39).

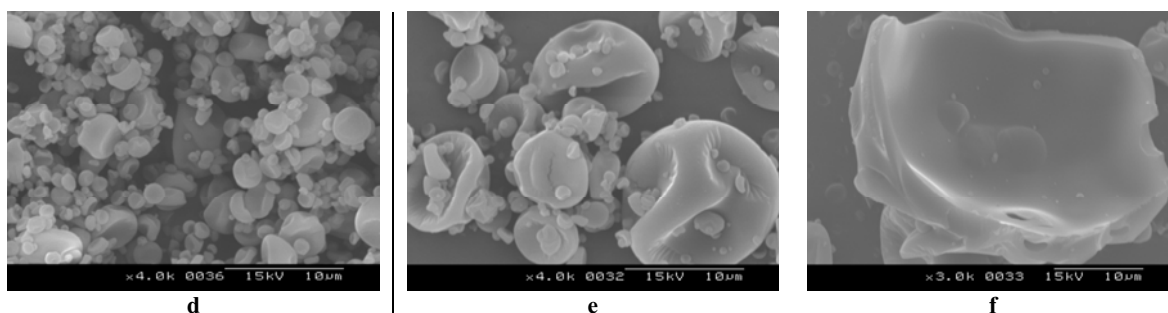


Figure 80: Chitosan microspheres obtained by spray-drying at different percentages w/w of glutaraldehyd/chitosan. D2: at 1% w/w (d) and D3: 3% w/w (e and f)

Besides to search the maximum sphericity in the microspheres, the viability of the process using a higher percentage of chitosan is studied. If it was viable it would be

interesting in order to study its influence in the effectiveness *in vitro*. A new formulation is performed with 3 % w/v of chitosan maintaining the original percentage of 0,5 % w/w of glutaraldehyd (**D4**). The viscosity of the solution prepared is higher however, it is not a problem for spray-drying it. The process is viable with a yield of 52,79 %. SEM pictures (**g**, **h** and **i**) show how most of the 3 % chitosan microspheres have wrinkled appearance and others a really smooth surface.

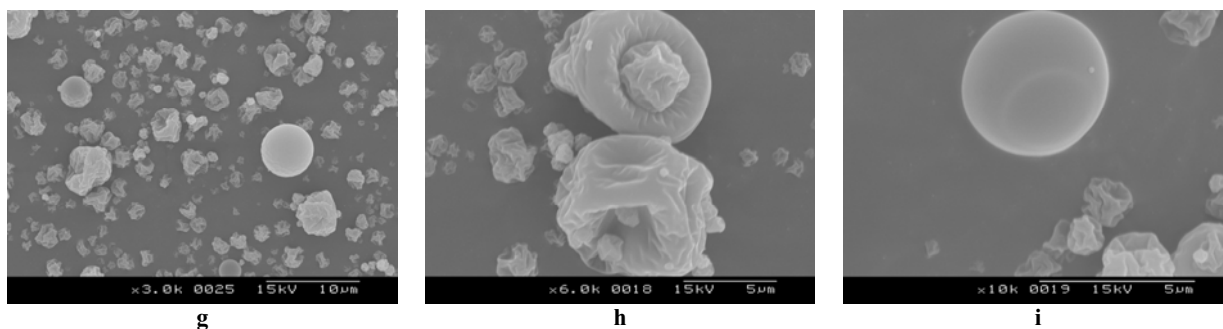


Figure 81: 3 % w/v chitosan microspheres obtained by spray drying.

B) Fractional experimental design

Chitosan microspheres produced from a solution considering the previous formulation parameters are studied in depth by a fractional experimental design. The results obtained from the morphological characterization of the seventeen different microspheres, the residual moistures and operational parameters are summarized in the table 40.

Parameters ¹										Responses						
microspheres	A	B	C	D	E	Outlet temperature (°C)	Moisture (%)	Yield (%)	Efficiency of encapsulation		Particle size distribution		Z potential (mV)	Morphology by SEM		
									Added	Found	%	Mean (µm)			CV (%)	Surface ²
E1	1	1	10	500	180	125	4,620 ± 1,272	67,208	81,903	80,174	97,890	6,781 ± 6,657	98,200	50,133 ± 0,404	9	6
E2	3	1	10	500	130	87	5,443 ± 1,050	67,685	81,879	75,644	92,380	9,348 ± 13,130	140,000	52,633 ± 1,007	9	4
E3	1	3	10	500	130	90	6,293 ± 0,541	58,300	70,983	76,311	94,580	10,970 ± 18,610	170,000	46,500 ± 1,900	1	6
E4	3	3	10	500	180	124	5,150 ± 0,560	32,200	70,948	74,243	99,170	11,360 ± 19,810	174,000	46,667 ± 1,644	2	5
E5	1	1	20	500	130	83	6,437 ± 0,609	63,646	81,887	73,794	93,190	6,435 ± 5,176	80,400	49,267 ± 0,451	10	5
E6	3	1	20	500	180	113	5,177 ± 0,093	71,692	81,887	67,932	90,670	6,771 ± 6,379	94,200	59,933 ± 3,664	10	7
E7	1	3	20	500	180	112	5,583 ± 0,576	55,530	70,955	74,132	99,320	9,505 ± 5,848	61,500	47,567 ± 1,222	4	7
E8	3	3	20	500	130	85	7,003 ± 0,748	57,533	70,962	76,849	92,810	6,709 ± 7,036	105,000	51,900 ± 0,854	3	6
E9	2	2	15	600	155	95	5,893 ± 0,795	56,860	76,038	67,134	91,100	5,641 ± 5,606	99,400	56,067 ± 1,848	5	6
E10	1	1	10	700	130	83	6,277 ± 0,335	72,154	81,903	70,356	90,100	5,132 ± 4,937	96,200	54,133 ± 1,650	10	7
E11	3	1	10	700	180	116	5,273 ± 0,339	67,380	81,895	70,474	82,950	5,657 ± 5,174	91,500	57,967 ± 3,553	10	8
E12	1	3	10	700	180	112	6,123 ± 0,355	59,933	70,940	65,858	87,430	6,232 ± 6,825	110,000	57,367 ± 2,485	5	8
E13	3	3	10	700	130	89	6,113 ± 0,890	61,067	70,990	69,273	95,790	6,525 ± 9,832	151,000	51,000 ± 0,900	4	6
E14	1	1	20	700	180	104	5,973 ± 0,339	70,385	81,895	62,026	90,520	5,372 ± 5,059	94,200	50,333 ± 2,303	10	7
E15	3	1	20	700	130	82	6,823 ± 0,501	66,230	81,887	67,998	93,850	6,137 ± 10,480	171,000	51,833 ± 0,839	9	6
E16	1	3	20	700	130	84	5,980 ± 0,877	48,060	70,976	72,957	102,790	5,379 ± 5,534	103,000	51,567 ± 3,525	4	7
E17	3	3	20	700	180	113	5,693 ± 0,725	60,730	70,969	68,874	97,050	7,163 ± 7,948	111,000	49,867 ± 0,451	4	7

Table 40: Characteristics of chitosan microspheres of experimental design 2⁵⁻¹. A: % v/v glutaraldehyd, B: % w/v chitosan, C: % pump, D: flow rate (l/h), E: inlet temperature (°C).

² Values from 1 to 10 represent a range of wrinkled and smooth surfaces respectively. ³ Values from 1 to 10 represent low to high sphericity respectively.

B.1. Influence of parameters on outlet temperature

The mean values of outlet temperature divided by groups of inlet temperatures (130 °C and 180 °C) are as follow: $85,375 \pm 6,854$ °C and $114,875 \pm 2,973$ °C respectively. The outlet temperatures are analysed by ANOVA test and table 41 shows the results:

Analysis of variante for outlet temperature					
Source	Sum of Squares	Df	Mean square	F-Ratio	P-Value
A:Glutaraldehyd conc.	16,0	1	16,0	0,65	0,5687
B:Chitosan conc.	16,0	1	16,0	0,65	0,5687
C:Pump	156,25	1	156,25	6,32	0,2410
D:Flow rate	81,0	1	81,0	3,28	0,3213
E:Inlet temperature	3481,0	1	3481,0	140,81	0,0535
AB	6,25	1	6,25	0,25	0,7034
AC	1,0	1	1,0	0,04	0,8736
AD	20,25	1	20,25	0,82	0,5317
AE	6,25	1	6,25	0,25	0,7034
BC	4,0	1	4,0	0,16	0,7565
BD	6,25	1	6,25	0,25	0,7034
BE	6,25	1	6,25	0,25	0,7034
CD	16,0	1	16,0	0,65	0,5687
CE	25,0	1	25,0	1,01	0,4982
DE	30,25	1	30,25	1,22	0,4679
Total error	24,7206	1	24,7206		

Total (corr.)	3896,47	16			
R-squared = 99,3656 percent					
R-squared (adjusted for d.f.) = 89,849 percent					
Standard error of Est. = 4,97198					
Mean absolut error = 0,567474					
Durbin-Watson statistic = 2,125					
Residual autocorrelation Lag 1 = -0,0661765					

Table 41: ANOVA for outlet temperature

F-ratios of the interactions highlighted in the table 41 are near to 0 and the sum of squares lower than total error. It means that they do not have a significant influence on the outlet temperature and then their sum of squares can be included in the total error. The results are shown in the table 42. Taking into account P-values (table 42) in a 95 % confidence interval it can be deduced that the probability of the differences in the factors pump, flow rate and inlet temperature were by chance is 0,29 %, 1,47 % and 0 % respectively so that they influence significantly in the outlet temperature of the process because P-values are lower than 0,05.

Analysis of variante for outlet temperature					
Source	Sum of Squares	Df	Mean square	F-Ratio	P-Value
A:Glutaraldehyd conc	16,0	1	16,0	2,05	0,1956
B:Chitosan concentra	16,0	1	16,0	2,05	0,1956
C:Pump	156,25	1	156,25	19,99	0,0029
D:Flow rate	81,0	1	81,0	10,36	0,0147
E:Inlet temperature	3481,0	1	3481,0	445,30	0,0000
AD	20,25	1	20,25	2,59	0,1515
CD	16,0	1	16,0	2,05	0,1956
CE	25,0	1	25,0	3,20	0,1169
DE	30,25	1	30,25	3,87	0,0899
Total error	54,7206	7	7,81723		
Total (corr.)	3896,47	16			

R-squared = 98,5956 percent
R-squared (adjusted for d.f.) = 96,79 percent
Standard error of Est. = 2,79593
Mean absolut error = 1,41349
Durbin-Watson statistic = 2,4014 (P=0,2147)
Residual autocorrelation Lag 1 = -0,297499

Table 42: ANOVA for outlet temperature

The figure 82 illustrates the above results:

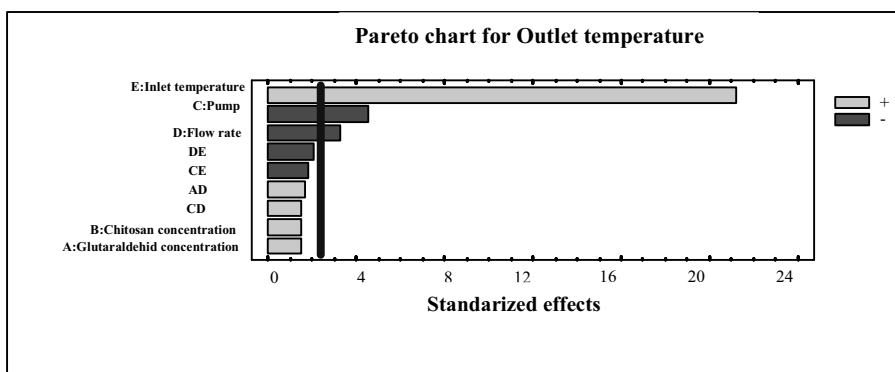


Figure 82: Pareto chart for outlet temperature

The process parameters influence as expected. Firstly, as higher is the inlet temperature higher is the outlet temperature. Secondly, if pump rate increase more quantity of material have to be dried, then the temperature decrease. Finally, as higher is the flow rate, smaller are the drops sprayed, then more specific surface to be dried. It will decrease the temperature due to a higher exchange of heat.

B.2. Influence of parameters on moisture

The mean value of the final humidity of product is 5,874 % +/- 0,005 % which is 2,576 % higher than that humidity of microspheres with lipids. ANOVA test reflects that most of the factors and interactions influence significantly. Results are shown in table 43.

Analysis of variance for moisture					
Source	Sum of Squares	Df	Mean square	F-Ratio	P-Value
A:Glutaraldehyd conc	0,0232563	1	0,0232563	58,09	0,0831
B:Chitosan concentra	0,229601	1	0,229601	573,47	0,0266
C:Pump	0,712617	1	0,712617	1779,91	0,0151
D:Flow rate	0,406406	1	0,406406	1015,08	0,0200
E:Inlet temperature	2,8702	1	2,8702	7168,91	0,0075
AB	0,0203063	1	0,0203063	50,72	0,0888
AC	0,264367	1	0,264367	660,31	0,0248
AD	0,00525625	1	0,00525625	13,13	0,1714
AE	0,123084	1	0,123084	307,43	0,0363
BC	0,307101	1	0,307101	767,05	0,0230
BD	0,486506	1	0,486506	1215,15	0,0183
BE	0,0751674	1	0,0751674	187,75	0,0464
CD	0,252506	1	0,252506	630,69	0,0253
CE	0,0458674	1	0,0458674	114,56	0,0593
DE	0,395851	1	0,395851	988,72	0,0202
Total error	0,000400368	1	0,000400368		

Total (corr.)	6,21849	16			
R-squared = 99,9936 percent					
R-squared (adjusted for d.f.) = 99,897 percent					
Standard error of Est. = 0,0200092					
Mean absolut error = 0,00228374					
Durbin-Watson Statistic= 2,125					
Residul autocorrelation Lag 1 = -0,0661765					

Table 43: ANOVA test

When temperature is 180 °C, the final humidity of product is lower due to a lower relative humidity in air. As can be seen in the figure 83, although pump, flow rate and chitosan lead to increase the moisture significantly, their interactions influence on reducing it.

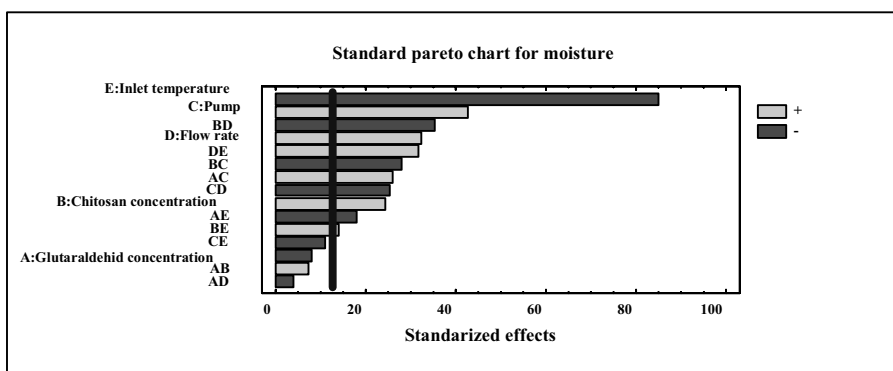


Figure 83: Standard pareto chart for moisture

It has been reported that cross-linking agent can reduce the humidity of the final product (Desai K.G.H. and Park H.J., 2005). In this design, the influence of this parameter is not significant although the estimated effect with 1 d.f is negative (-0,076 +/- 0,010).

B.3. Influence of parameters on yield

The mean yield value is $62,979 \% \pm 6,524 \%$ which has been improved with respect to the pre-formulation studies ($52,79 \%$). It is considered a high percentage if it is compared to 50% as the maximum reported in a spray drying process (Vila Jato J. L., 1997). The influence of factors and their interactions on yield have been analysed by ANOVA test. The results are shown in table 44:

Analysis of variance for yield						
Source	Sum of Squares	Df	Mean square	F-Ratio	P-Value	
A:Glutaraldehyd conc	34,0793	1	34,0793	0,86	0,5246	
B:Chitosan concentra	389,828	1	389,828	9,80	0,1968	
C:Pump	42,805	1	42,805	1,08	0,4883	
D:Flow rate	0,226624	1	0,226624	0,01	0,9520	
E:Inlet temperature	37,3107	1	37,3107	0,94	0,5102	
AB	36,4907	1	36,4907	0,92	0,5137	
AC	11,8629	1	11,8629	0,30	0,6818	
AD	11,5617	1	11,5617	0,29	0,6852	
AE	0,436194	1	0,436194	0,01	0,9336	
BC	28,1531	1	28,1531	0,71	0,5548	
BD	11,8023	1	11,8023	0,30	0,6825	
BE	6,93401	1	6,93401	0,17	0,7482	
CD	1,04438	1	1,04438	0,03	0,8977	
CE	28,3636	1	28,3636	0,71	0,5536	
DE	0,422175	1	0,422175	0,01	0,9346	
Total Error	39,7817	1	39,7817			

Total (corr.)	681,102	16				
R-squared = 94,1592 percent						
R-squared (adjusted for d.f.) = 6,54746 percent						
Standard Error of Est. = 6,30727						
Mean absolute error = 0,719877						
Durbin-Watson Statistic= 2,125						
Residual autocorrelation Lag 1 = -0,0661765						

Table 44: ANOVA test for yield

Sum of squares of that factors and the interactions which have F-ratios near to 0 value have been included in the total error due not to influence significantly. The results are shown in the table 45.

Chitosan concentration influence significantly reducing the yield of the process because the probability of its differences was by chance is $0,10 \%$ (table 45) in a 95% confidence interval. As in pre-formulation studies, 3% chitosan solutions are more viscous then there is more loss during the process of elaboration, homogenization and spray-drying.

Analysis of variance for yield					
Source	Sum of Squares	Df	Mean square	F-Ratio	P-Value
A:Glutaraldehyd conc	34,0793	1	34,0793	4,07	0,0998
B:Chitosan concentra	389,828	1	389,828	46,51	0,0010
C:Pump	42,805	1	42,805	5,11	0,0734
E:Inlet temperature	37,3107	1	37,3107	4,45	0,0886
AB	36,4907	1	36,4907	4,35	0,0913
AC	11,8629	1	11,8629	1,42	0,2876
AD	11,5617	1	11,5617	1,38	0,2931
BC	28,1531	1	28,1531	3,36	0,1263
BD	11,8023	1	11,8023	1,41	0,2887
BE	6,93401	1	6,93401	0,83	0,4048
CE	28,3636	1	28,3636	3,38	0,1252
Total Error	41,9111	5	8,38221		
Total (corr.)	681,102	16			

R-squared = 93,8466 percent
R-squared (adjusted for d.f.) = 80,3091 percent
Standard Error of Est. = 2,8952
Mean absoluto error = 0,767078
Durbin-Watson Statistic= 2,2288 (P=0,2037)
Residual autocorrelation Lag 1 = -0,115109

Table 45: ANOVA test for yield

The main effects of this ANOVA test are represented in the figure 84:

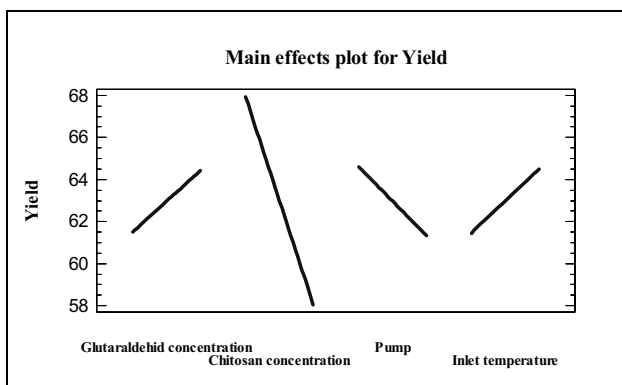


Figure 84: Main effects plot for yield

It is worth to point out that pump tends to decrease the yield; probably it could be related to the residual moisture of the product which was significantly higher when pump was high. Consequently, it could be more stuck product in the apparatus. On the contrary, temperature tends to

increase the yield due to dryer product prevent sticking. These results have been reported before by Desai K.G.H. and Park H.J., 2006.

B.4. Influence of parameters on efficiency of encapsulation

To calculate the efficiency of encapsulation of the process in this design, three different calibration curves have been prepared: 1) an external curve in only medium (1 % HNO₃ + 0,5% HF (solution A)), 2) a standard addition curve in problem HCl aqueous solution diluted 1/5 with solution A for the group of microspheres with 1 % of chitosan and 3) a standard addition curve in problem HCl aqueous solution diluted 1/5 with solution A for 3 % chitosan group. The three different equations obtained are: $y_1 = 58,9x (R^2 = 1,0)$,

$y_2 = 58,355x + 939,46$ ($R^2 = 0,9999$), $y_3 = 58,496x + 814,17$ ($R^2 = 0,9994$). The different composition does not affect the measure due to the slopes are very similar. The results obtained are shown in the table 46 using the external calibration curve to calculate the concentrations.

Test	Sb 206,836 nm intensity	[ppm Sb] added	[ppm Sb] 1/5 dilution	[ppm Sb] 1/5 dilution found	[ppm Sb] found	%
E1	941,209	81,903	16,381	16,035	80,174	97,89
E2	888,024	81,879	16,376	15,129	75,644	92,38
E3	788,125	70,983	14,197	13,427	67,134	94,58
E4	825,947	70,948	14,190	14,071	70,356	99,17
E5	895,862	81,887	16,377	15,262	76,311	93,19
E6	871,583	81,887	16,377	14,849	74,243	90,67
E7	827,334	70,955	14,191	14,095	70,474	99,32
E8	773,148	70,962	14,192	13,172	65,858	92,81
E9	813,239	76,038	15,208	13,855	69,273	91,1
E10	866,304	81,903	16,381	14,759	73,794	90,1
E11	797,488	81,895	16,379	13,586	67,932	82,95
E12	728,157	70,940	14,188	12,405	62,026	87,43
E13	798,270	70,990	14,198	13,600	67,998	95,79
E14	870,282	81,895	16,379	14,826	74,132	90,52
E15	902,177	81,887	16,377	15,370	76,849	93,85
E16	856,486	70,976	14,195	14,591	72,957	102,79
E17	808,546	70,969	14,194	13,775	68,874	97,05

Table 46: Efficiencies of encapsulation of chitosan microspheres by ICP-OES.

The mean value of efficiency of encapsulation is 93,623 % +/- 0,344 %, it is considered a high result if it is compared to the encapsulation of MGA percentage reported in liposomes, 38 % (Schettini D.A. et al., 2003).

Analysis of variance for efficiency of encapsulation					
Source	Sum of Squares	Df	Mean square	F-Ratio	P-Value
A:Glutaraldehyd conc	7,77016	1	7,77016	1,15	0,4779
B:Chitosan concentra	87,3758	1	87,3758	12,92	0,1727
C:Pump	24,7755	1	24,7755	3,66	0,3065
D:Flow rate	23,8388	1	23,8388	3,52	0,3116
E:Inlet temperature	6,87751	1	6,87751	1,02	0,4973
AB	9,84391	1	9,84391	1,46	0,4406
AC	8,59956	1	8,59956	1,27	0,4619
AD	4,78516	1	4,78516	0,71	0,5548
AE	0,0162563	1	0,0162563	0,00	0,9688
BC	6,36301	1	6,36301	0,94	0,5097
BD	12,0583	1	12,0583	1,78	0,4092
BE	1,26001	1	1,26001	0,19	0,7406
CD	80,8651	1	80,8651	11,96	0,1792
CE	0,00680625	1	0,00680625	0,00	0,9798
DE	93,4606	1	93,4606	13,82	0,1673
Total error	6,76306	1	6,76306		
Total (corr.)	374,659	16			

R-squared = 98,1949 percent
R-squared (adjusted for d.f.) = 71,118 percent
Estandar Error of Est. = 2,60059
Mean absolut error = 0,296817
Durbin-Watson statistic = 2,125
Residual autocorrelation Lag 1 = -0,0661765

Table 47: ANOVA results for efficiency of encapsulation

The ANOVA results are shown in the table 47. Once the interactions with F-ratios near to 0 values are included in the total error, the results obtained are as follow (table 48):

Analysis of variance for efficiency of encapsulation					
Source	Sum of Squares	Df	Mean square	F-Ratio	P-Value
A:Glutaraldehyd conc	7,77016	1	7,77016	3,86	0,1208
B:Chitosan conc.	87,3758	1	87,3758	43,44	0,0027
C:Pump	24,7755	1	24,7755	12,32	0,0247
D:Flow rate	23,8388	1	23,8388	11,85	0,0262
E:Inlet temperature	6,87751	1	6,87751	3,42	0,1381
AB	9,84391	1	9,84391	4,89	0,0914
AC	8,59956	1	8,59956	4,28	0,1075
AD	4,78516	1	4,78516	2,38	0,1979
BC	6,36301	1	6,36301	3,16	0,1499
BD	12,0583	1	12,0583	5,99	0,0706
CD	80,8651	1	80,8651	40,20	0,0032
DE	93,4606	1	93,4606	46,46	0,0024
Total error	8,04613	4	2,01153		
Total (corr.)	374,659	16			

R-squared = 97,8524 percent
R-squared (adjusted for d.f.) = 91,4097 percent
Estandar Error of Est. = 1,41828
Mean absolut error = 0,412526
Durbin-Watson statistic = 2,25165 (P=0,2542)
Residual autocorrelation Lag 1 = -0,142709

Table 48: ANOVA results for efficiency of encapsulation

Taking into account P-values (table 48) in a 95 % confidence interval it can be deduced that the probability of the differences in the factors chitosan concentration, pump and flow rate were by chance is 0,27 %, 2,47 % and 2,62 % respectively and they influence significantly on the efficiency of encapsulation of the process because P-values are lower than 0,05.

Usually, polymer concentration leads to increase the encapsulation of drugs during spray-drying (Martinac A. et al., 2005) and percentage of cross-linking agent decrease it lightly (Desai K.G.H. and Park H.J., 2005). It is confirmed in this design where chitosan increases significantly the percentage of encapsulation and glutaraldehyd has a lightly negative estimated effect (decrease) as show the figure 85:

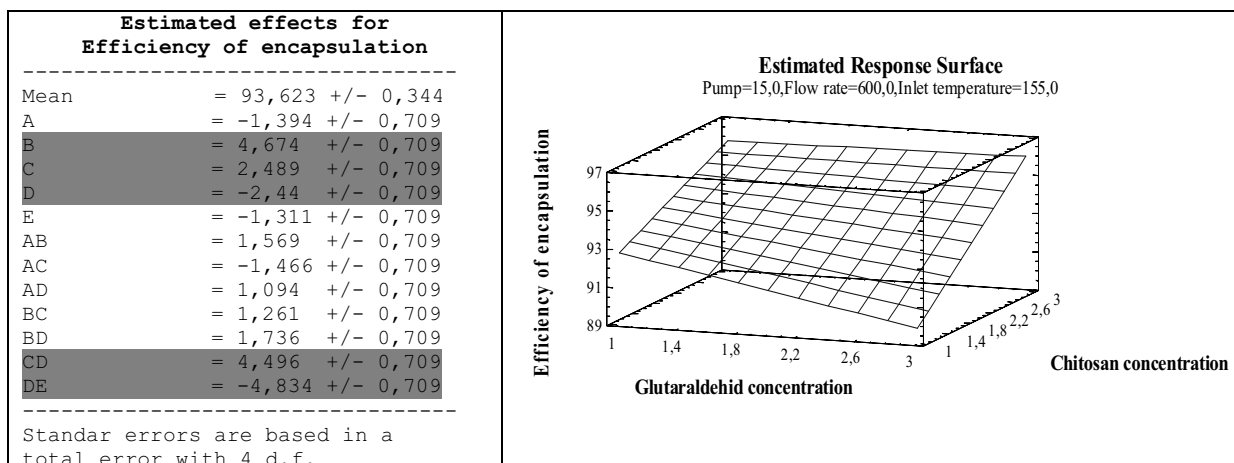


Figure 85: Estimated effects (left) and estimated response surface (right) for efficiency of encapsulation.

B.5. Influence of parameters on particle size distribution

Particle size distribution is in all cases normal and the mean particle size of the chitosan microspheres in this design is 7,125 μm +/- 0,371 μm . A particle size distribution plot of microspheres **E7** is shown in the figure 86 as example. Moreover, the results of particle size analysis are shown in table 49.

Microspheres	Mean	Median	Mode	S.D.	C.V.	d10	d25	d50	d90
E1	6,781	4,790	8,536	6,657	98,2	0,711	1,830	4,790	15,43
E2	9,348	5,853	9,370	13,13	140	0,870	2,336	5,853	18,54
E3	10,97	5,302	11,29	18,61	170	0,776	1,706	5,302	23,31
E4	11,36	5,638	10,29	19,81	174	0,835	1,950	5,638	23,73
E5	6,435	5,211	7,775	5,176	80,4	0,766	2,239	5,211	14,11
E6	6,771	4,747	9,370	6,379	94,2	0,741	1,758	4,747	15,90
E7	9,505	8,475	10,29	5,848	61,5	2,828	5,059	8,475	17,95
E8	6,709	4,053	10,29	7,036	105	0,795	1,555	4,053	16,36
E9	5,641	3,517	7,083	5,606	99,4	0,748	1,459	3,517	13,85
E10	5,132	3,614	4,047	4,937	96,2	0,640	1,685	3,614	11,63
E11	5,657	4,117	7,083	5,174	91,5	0,762	1,629	4,117	12,79
E12	6,232	3,575	1,919	6,825	110	0,777	1,474	3,575	15,44
E13	6,525	3,381	1,919	9,832	151	0,745	1,423	3,381	14,88
E14	5,372	3,831	6,452	5,059	94,2	0,747	1,557	3,831	12,15
E15	6,137	3,489	4,877	10,48	171	0,699	1,500	3,489	11,90
E16	5,379	3,325	3,059	5,534	103	0,769	1,479	3,325	13,02
E17	7,163	4,135	8,536	7,948	111	0,768	1,575	4,135	18,02

Table 49: Particle size distribution of chitosan microspheres.

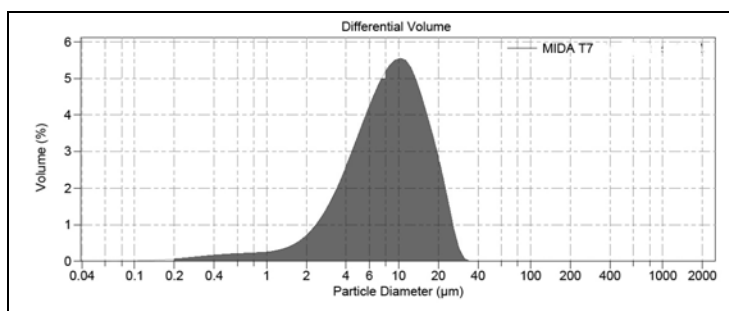


Figure 86: Particle size distribution plot of microspheres n° E7

The influence of the factors and their interactions on particle size is studied by ANOVA (table 50):

Analysis of variance for particle size					
Source	Sum of Squares	Df	Mean square	F-Ratio	P-Value
A:Glutaraldehyd conc.	0,933156	1	0,933156	0,40	0,6413
B:Chitosan conc.	9,31776	1	9,31776	3,98	0,2957
C:Pump	4,55182	1	4,55182	1,95	0,3959
D:Flow rate	25,71	1	25,71	10,99	0,1865
E:Inlet temperature	0,304152	1	0,304152	0,13	0,7796
AB	1,27803	1	1,27803	0,55	0,5947
AC	0,849162	1	0,849162	0,36	0,6547
AD	0,514806	1	0,514806	0,22	0,7207
AE	0,31866	1	0,31866	0,14	0,7749
BC	1,06502	1	1,06502	0,46	0,6221
BD	2,4087	1	2,4087	1,03	0,4953
BE	3,19337	1	3,19337	1,37	0,4506
CD	5,693	1	5,693	2,43	0,3628
CE	2,32258	1	2,32258	0,99	0,5011
DE	0,005476	1	0,005476	0,00	0,9692
Total error	2,33841	1	2,33841		

Total (corr.)	60,8041	16			
R-squared = 96,1542 percent					
R-squared (adjusted for d.f.) = 38,4669 percent					
Standard Error of Est. = 1,52919					
Mean absolut error= 0,174533					
Durbin-Watson Statistic = 2,125					
Residual autocorrelation Lag 1 = -0,0661765					

Table 50: ANOVA results for particle size.

The results obtained after include interaction DE in total error are:

Analysis of variance for particle size					
Source	Sum of Squares	Df	Mean square	F-Ratio	P-Value
A:Glutaraldehyd conc.	0,933156	1	0,933156	0,80	0,4664
B:Chitosan conc.	9,31776	1	9,31776	7,95	0,1061
C:Pump	4,55182	1	4,55182	3,88	0,1875
D:Flow rate	25,71	1	25,71	21,94	0,0427
E:Inlet temperature	0,304152	1	0,304152	0,26	0,6611
AB	1,27803	1	1,27803	1,09	0,4060
AC	0,849162	1	0,849162	0,72	0,4843
AD	0,514806	1	0,514806	0,44	0,5756
AE	0,31866	1	0,31866	0,27	0,6540
BC	1,06502	1	1,06502	0,91	0,4411
BD	2,4087	1	2,4087	2,06	0,2881
BE	3,19337	1	3,19337	2,72	0,2406
CD	5,693	1	5,693	4,86	0,1584
CE	2,32258	1	2,32258	1,98	0,2945
Total error	2,34389	2	1,17194		

Total (corr.)	60,8041	16			
R-squared = 96,1452 percent					
R-squared (adjusted for d.f.) = 69,1614 percent					
Standard error of Est. = 1,08256					
Mean absolute error= 0,174533					
Durbin-Watson Statistic = 2,12617 (P=0,0027)					
Residual autocorrelation Lag 1 = -0,066898					

Table 51: ANOVA results for particle size

Considering P-values (table 51) in a 95 % confidence interval, flow rate influences in the particle size significantly. The probability of the differences was by chance is only 4,27 % and the estimated effects are represented in the figure 87.

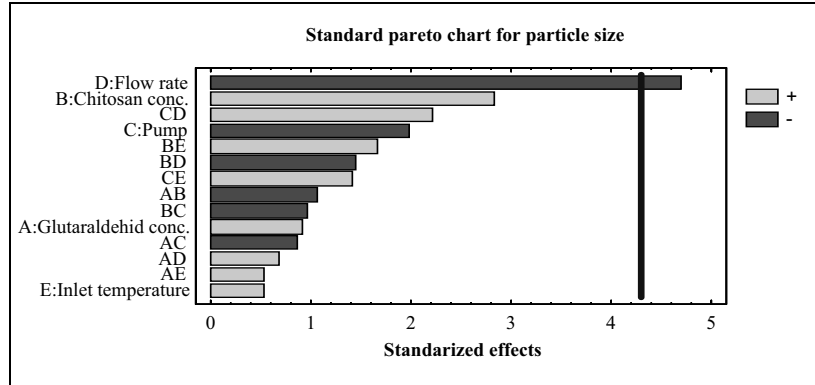


Figure 87: Standard Pareto chart for particle size

There is an apparent reduction of particle size from 8,485 to 5,950 μm when the air flow rate is increased from 500 l/h to 700 l/h. At greater air flow rate, liquid was disrupted into smaller droplets. Therefore, microspheres with a smaller particle size are produced at greater air flow rate (Desai K.G.H. and Park H.J., 2006).

Larger microspheres with greater size dispersion are formed from the more concentrated chitosan solution. This is probably due to the effect of solution viscosity on the size of the droplets formed during the atomization step. In general, the mean size of droplets formed by atomization is proportional to liquid viscosity and surface tension and indirectly affects the size of the spray-dried powder, which is an important processing variable (Oliveira B.F. et al., 2005).

The results of ANOVA test of the influence of factors on the % C.V of particle size are shown in tables 52 and 53.

Analysis of variance for CV					
Source	Sum of Squares	Df	Mean square	F-Ratio	P-Value
A:Glutaraldehyd conc.	3141,6	1	3141,6	12,56	0,1751
B:Chitosan conc.	897,003	1	897,003	3,59	0,3093
C:Pump	2772,02	1	2772,02	11,09	0,1858
D:Flow rate	1,3225	1	1,3225	0,01	0,9538
E:Inlet temperature	2070,25	1	2070,25	8,28	0,2129
AB	60,84	1	60,84	0,24	0,7083
AC	225,0	1	225,0	0,90	0,5168
AD	20,25	1	20,25	0,08	0,8235
AE	7,0225	1	7,0225	0,03	0,8943
BC	3552,16	1	3552,16	14,21	0,1651
BD	357,21	1	357,21	1,43	0,4435
BE	85,5625	1	85,5625	0,34	0,6631
CD	4610,41	1	4610,41	18,44	0,1457
CE	14,0625	1	14,0625	0,06	0,8518
DE	138,063	1	138,063	0,55	0,5932
Total error	250,061	1	250,061		

Total (corr.)	18202,8	16			
R-squared = 98,6263 percent					
R-squared (adjusted for d.f.) = 78,02 percent					
Standard error of Est. = 15,8133					
Mean absolute error = 1,80484					
Durbin-Watson Statistic= 2,125					
Residual autocorrelation Lag 1 = -0,0661765					

Table 52: ANOVA results for CV

Analysis of variance for CV					
Source	Sum of Squares	Df	Mean square	F-Ratio	P-Value
A:Glutaraldehyd conc.	3141,6	1	3141,6	31,58	0,0025
B:Chitosan conc.	897,003	1	897,003	9,02	0,0300
C:Pump	2772,02	1	2772,02	27,86	0,0032
E:Inlet temperature	2070,25	1	2070,25	20,81	0,0060
AB	60,84	1	60,84	0,61	0,4696
AD	20,25	1	20,25	0,20	0,6708
BC	3552,16	1	3552,16	35,70	0,0019
BD	357,21	1	357,21	3,59	0,1166
BE	85,5625	1	85,5625	0,86	0,3963
CD	4610,41	1	4610,41	46,34	0,0010
DE	138,063	1	138,063	1,39	0,2918
Total error	497,469	5	99,4937		

Total (corr.)	18202,8	16			
R-squared = 97,2671 percent					
R-squared (adjusted for d.f.) = 91,2547 percent					
Standard error of Est. = 9,97465					
Mean absolute error = 4,43183					
Durbin-Watson statistic= 3,05064 (P=0,0903)					
Residual autocorrelation Lag 1 = -0,573355					

Table 53: ANOVA results for CV

It is worth pointing out that cross-linking agent increases particle size lightly and moreover, it influences significantly ($P < 0,05$) in the CV percentage, increasing it. Contrary, pump rate reduces particle size and the CV percentage. These results do not fit in with other studies previously reported where particle size decreases lightly when

cross-linking is high and increases when pump rate is also high (He P. et al., 1999a and Desai K.G. H. and Park H.J., 2005).

Furthermore, when the sample is atomized in high inlet temperatures, CV percentage is significantly lower (figure 88). High inlet temperatures also decreased particle size dispersity when chitosan microspheres were produced from emulsions.

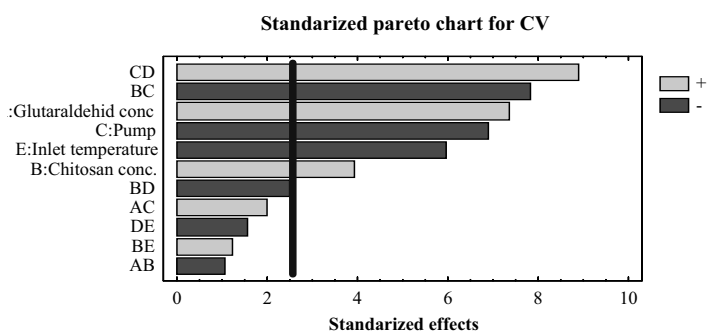


Figure 88: Standardized Pareto chart for CV

B.6. Influence of parameters on Z-potential

As can be seen in the summary table of results (table 40) the surface charge (zeta potential) of all chitosan microspheres prepared in this experimental design, are charged positively. The mean value is 52,043 +/- 0,458. An example of Z-potential distribution of microspheres E2 is shown in the figure 89.

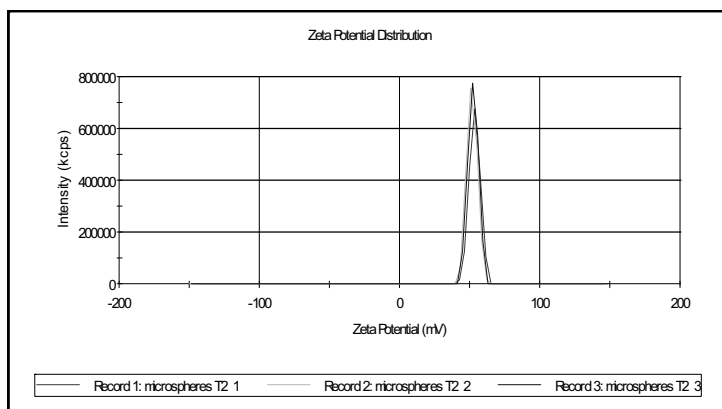


Figure 89 : Z-potential distribution of chitosan microspheres E2.

The influence of factors and interactions on Z-potential is studied by ANOVA test. After include that parameters with F-values near 0 inside total error, the results obtained are as follow:

Analysis of variance for Z-potential					
Source	Sum of Squares	Df	Mean square	F-Ratio	P-Value
A:Glutaraldehyd conc.	13,9378	1	13,9378	3,92	0,0952
B:Chitosan conc.	35,4025	1	35,4025	9,95	0,0197
D:Flow rate	23,6844	1	23,6844	6,65	0,0418
E:Inlet temperature	7,5625	1	7,5625	2,12	0,1952
AB	30,4336	1	30,4336	8,55	0,0265
AC	13,4444	1	13,4444	3,78	0,1000
AD	26,01	1	26,01	7,31	0,0354
BD	13,8136	1	13,8136	3,88	0,0964
BE	6,25	1	6,25	1,76	0,2334
CD	54,76	1	54,76	15,38	0,0078
Total Error	21,3584	6	3,55973		

Total (corr.)	246,657	16			

R-squared = 91,3409 percent
R-squared (adjusted for d.f.) = 76,909 percent
Standard Error of Est. = 1,88672
Mean absolute error = 0,615802
Durbin-Watson Statistic= 1,80942 (P=0,3312)
Residual autocorrelation Lag 1 = 0,0936773

Table 54: ANOVA results for Z-potential

Manufacturing parameters should not influence significantly in Z-potential, however flow rate seems to increase it (figure 90). Furthermore, many studies have reported the influence of cross-linking on the Z-potential. Usually, higher concentrations of cross-linking agent form less charged positively chitosan microspheres (He P. et al., 1999a). The results show that glutaraldehyd concentration does not affect on Z-potential in the studied conditions significantly ($P > 0,05$) but, unexpectedly, high concentrations of cross-linking agent increase Z-potential slightly. However, the interaction between glutaraldehyd and chitosan (AB) reduces Z-potential values and the probability that influences significantly by chance is only 2,65 % in a 95% confidence interval (table 54).

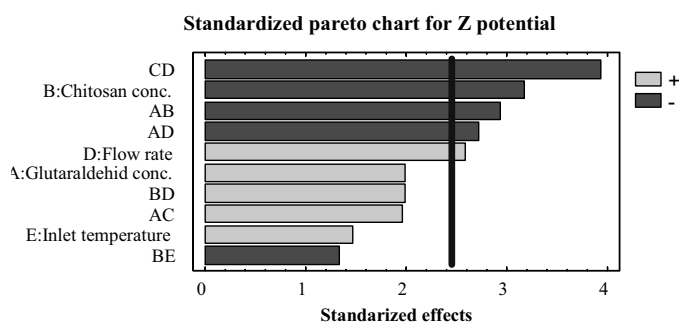


Figure 90: Standardized pareto chart for Z-potential

B.7. Influence of parameters on morphology

As expected, all the chitosan solutions atomized produce nano and microspheres which have been studied by SEM. Optical differences on surfaces morphology and sphericity in shape have been defined using a numerical range. Values from 1 to 10 represent a range of wrinkled and smooth surfaces or low to high sphericity respectively. These values are shown in the summary table 40 and they have been used to evaluate statistically the influence of the parameters on morphology by ANOVA test. The only factor that influence significantly on the surface morphology is chitosan concentration which tends to form wrinkled microspheres when is used in high concentrations (P=0,001).

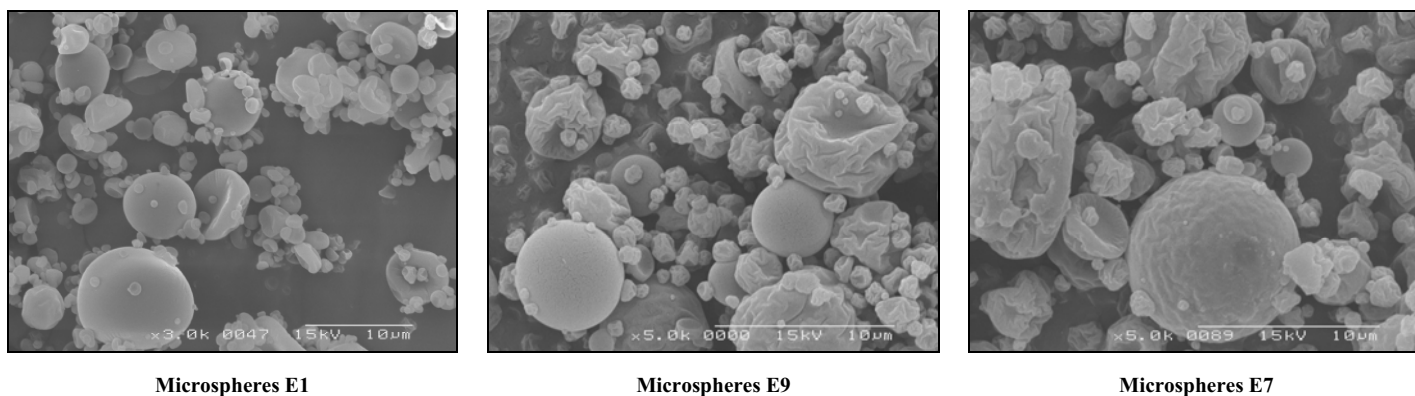


Figure 91: Scanning electron microscopic pictures of chitosan microspheres produced with 1 % (left), 2 % (middle) and 3 % chitosan solution (right).

The table 55 shows the combination of levels of factors which maximize the formation of smooth surfaces above the indicated region. The main effects plot located next to this table indicates how all the manufacturing parameters reduce slightly the wrinkled appearance of the microspheres when they are used in high levels in exception of chitosan and glutaraldehyd that reduce smooth appearance when they are used at high levels.

Optimized answer			

Aim: maximum surface value			
Optimum value = 10,4118			
Factor	Lower	Higher	Optimum
-----	-----	-----	-----
Glutaraldehyd conc.	1,0	3,0	1,0
Chitosan conc.	1,0	3,0	1,0
Pump	10,0	20,0	20,0
Flow rate	500,0	700,0	500,0
Inlet temperature	130,0	180,0	180,0

Main effects plot for surface morphology

The main effects plot shows the relationship between surface morphology and four factors. The y-axis is labeled 'surface' and ranges from 3,2 to 11,2. The x-axis lists the factors: Glutar. conc., Chitosan conc., Pump, Flow rate, and Inlet temperature. The plot shows that 'Chitosan conc.' has the most significant negative effect, with a steep downward slope. 'Glutar. conc.' also shows a slight downward trend. 'Pump', 'Flow rate', and 'Inlet temperature' all show slight upward trends, indicating that higher levels of these factors lead to smoother surfaces.

Table 55: Optimized answer and main effects plot for surface morphology.

As can be seen in the standardized pareto chart for sphericity (figure 92) more than one factor influence significantly on the formation of spherical microspheres. High flow rates and inlet temperatures produce more spherical forms. The probability that this influence was by chance is 0,02 % and 0,04 % respectively in a 95 % of confidence interval. In this design glutaraldehyd concentration affects microspheres shapes significantly reducing the sphericity. Other studies have reported how high percentages of cross-linking can lead to reduce the sphericity of the microspheres (Desai K.G.H. and Park H.J., 2006). Moreover, it has been shown that spherical forms are independent of chitosan concentration, previously described (Oliveira B.F. et al., 2005).

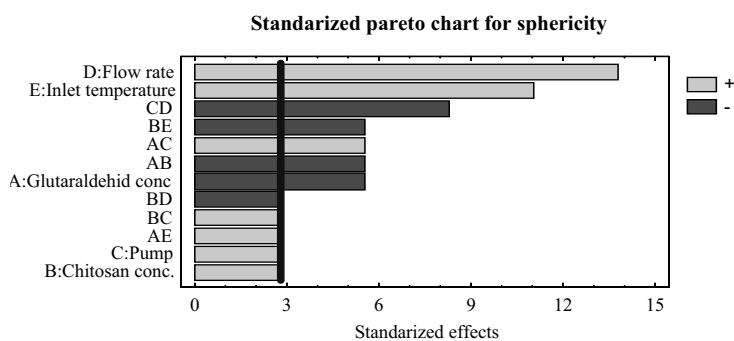
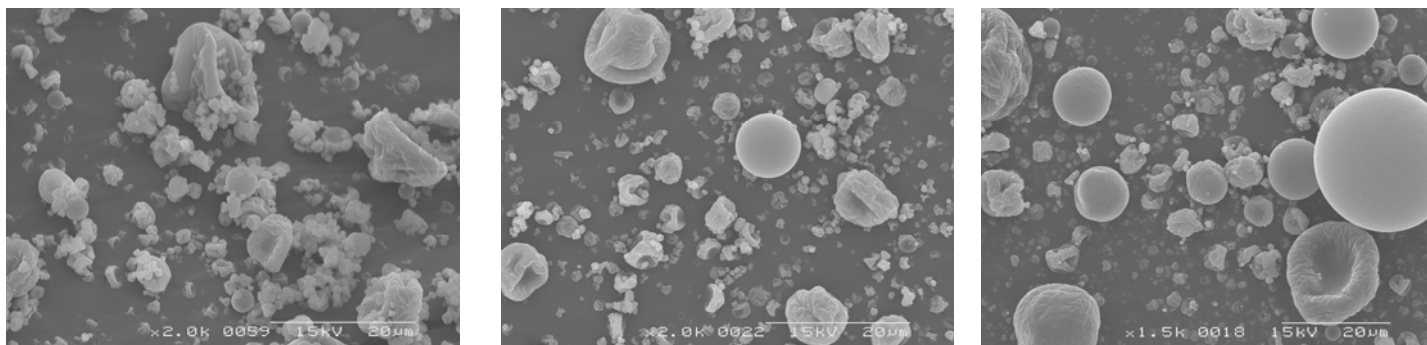


Figure 92: Optimized answer and standardized pareto chart for sphericity.

The next pictures (figure 93) show microspheres produced with 3 % w/v of chitosan. Both microspheres **E4** and **E17** are cross-linked with 3 % v/v of glutaraldehyd and sprayed at 180 ° C and flow rate of 500 l/h and 700 l/h respectively. When flow rate is higher microspheres appear more spherical. Furthermore, if microspheres **E12** (produced at 180 ° C and 700 l/h of flow rate but with 1 % v/v of glutaraldehyd) are also compared, it can be seen as the number of microspheres perfectly spherical is higher and it is even possible to reduce the wrinkled appearance.



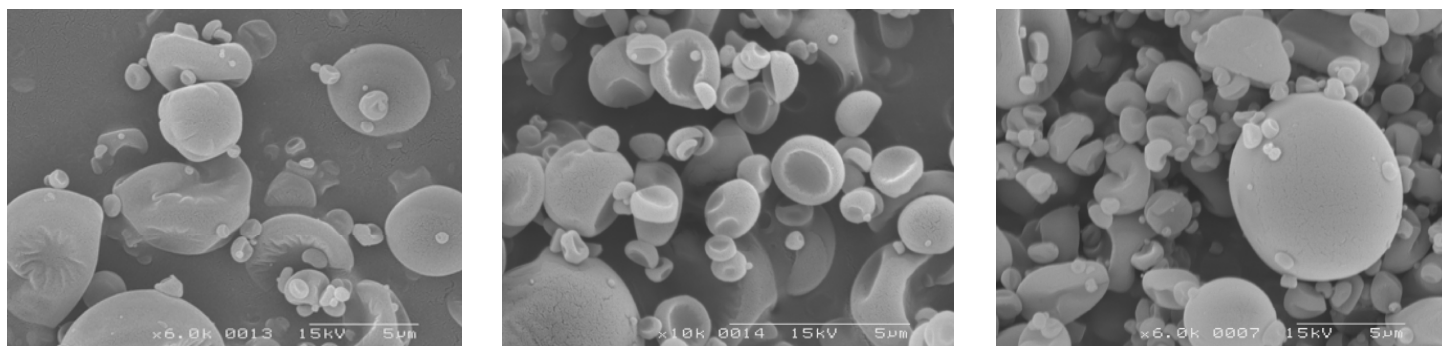
Microspheres E4

Microspheres E17

Microspheres E12

Figure 93: Scanning electron microscopic pictures of chitosan microspheres produced with 3 % chitosan solution.

As can be seen in the figure 94, the influence of inlet temperature in the form of microspheres is important. Low inlet temperatures produce more microspheres folded inward. Microspheres **E11** and **E15** are prepared with 1 % w/v of chitosan and 3 % v/v of glutaraldehyd at 700 l/h of flow rate and 180 ° C and 130 ° respectively. The picture on the right shows the microspheres **E14** produced at high level of flow rate, high inlet temperature and low proportion of cross-linking. They seem to be more spherical. As pump rate is not a significant factor, differences of this parameter have not been considered.



Microspheres E11

Microspheres E15

Microspheres E14

Figure 94: Scanning electron microscopic pictures of chitosan microspheres produced with 1% chitosan solution.

B.8. Dissolution studies

B.8.1. Percentages of drug dissolved

Percentage of drug dissolved in each interval of time has been calculated considering the real weight of microspheres taken into the dialysis bag and the efficiency of encapsulation obtained for each one. The mean values and the standard deviations are shown in the tables 55 and 56. Figure 95 shows the *in vitro* release behaviour of

chitosan microspheres. The standard deviation at each point, measured in triplicate, was less than 11,57 %.

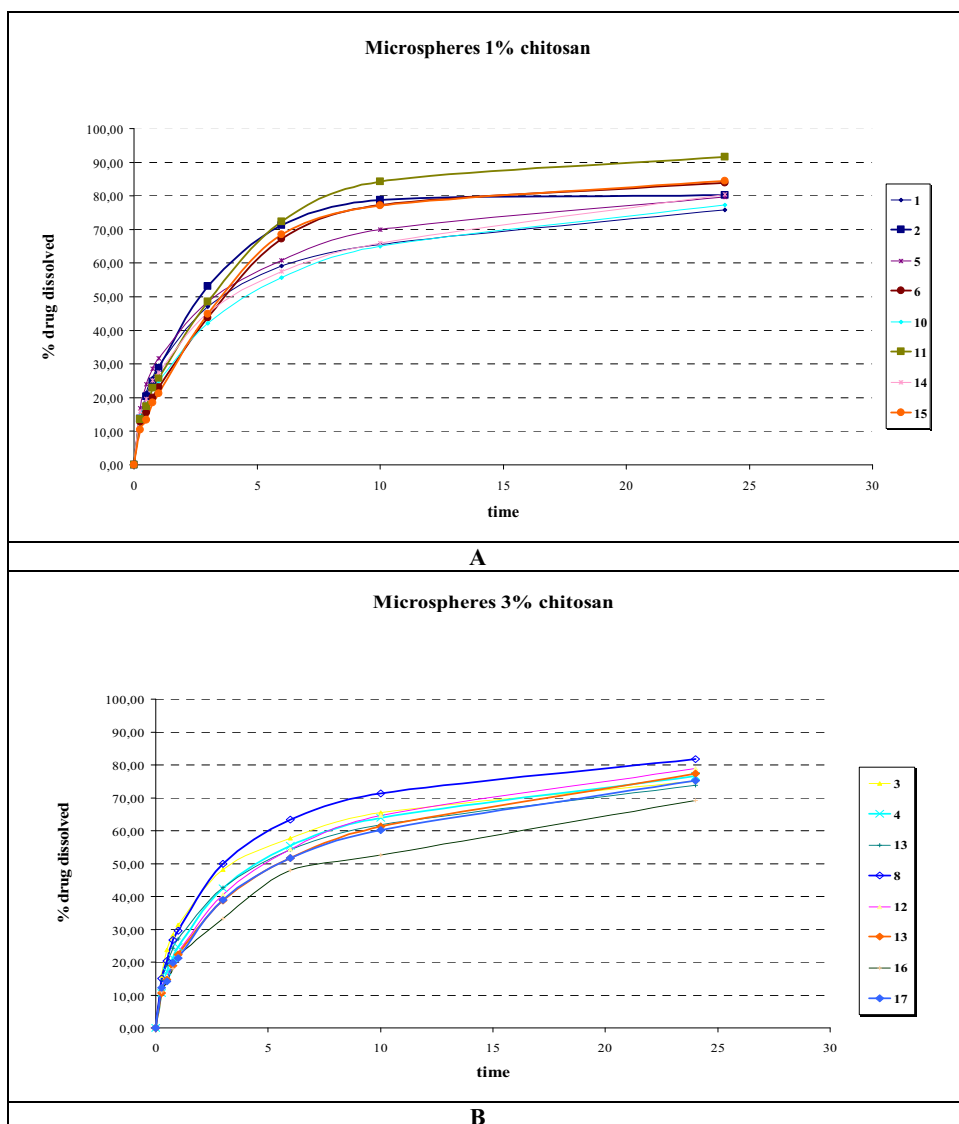


Figure 95: *In vitro* release behaviour of chitosan microspheres prepared from a A: 1 % chitosan solution, B: 3 % chitosan solution.

Microspheres								
Time (h)	E1	E2	E3	E4	E5	E6	E7	E8
0	0 ± 0	0 ± 0	0 ± 0	0 ± 0	0 ± 0	0 ± 0	0 ± 0	0 ± 0
0,25	13,223 ± 2,913	13,739 ± 2,726	15,863 ± 2,139	10,647 ± 0,625	16,864 ± 1,349	12,853 ± 3,400	14,255 ± 1,456	15,035 ± 6,304
0,5	21,388 ± 7,396	20,299 ± 1,725	23,685 ± 2,187	17,129 ± 3,061	24,029 ± 2,745	15,567 ± 2,222	19,060 ± 3,314	20,357 ± 4,747
0,75	25,862 ± 7,046	24,680 ± 3,001	28,214 ± 2,083	21,225 ± 3,513	28,616 ± 2,377	20,042 ± 3,944	24,256 ± 4,183	26,786 ± 8,018
1	29,482 ± 7,987	28,712 ± 2,921	31,274 ± 0,376	24,642 ± 3,875	31,773 ± 3,154	23,091 ± 4,385	27,165 ± 5,142	29,646 ± 8,008
3	47,047 ± 1,057	53,093 ± 4,059	48,102 ± 1,208	42,539 ± 7,065	48,519 ± 5,110	43,824 ± 6,247	42,643 ± 8,114	49,852 ± 11,573
6	59,198 ± 9,201	71,288 ± 2,644	57,691 ± 0,565	55,352 ± 7,748	60,832 ± 5,288	67,232 ± 2,907	54,078 ± 9,667	63,385 ± 10,716
10	65,624 ± 6,735	78,821 ± 2,869	65,522 ± 0,078	63,922 ± 7,037	69,938 ± 4,820	77,257 ± 1,086	61,795 ± 8,845	71,281 ± 8,572
24	75,806 ± 2,013	80,294 ± 2,277	74,993 ± 2,680	76,636 ± 1,022	79,602 ± 2,290	83,904 ± 1,919	73,828 ± 7,693	81,776 ± 4,788

Table 55: Percentage of drug released from microspheres 1 to 8 at different times.

Microspheres									
Time (h)	E9	E10	E11	E12	E13	E14	E15	E16	E17
0	0 ± 0	0 ± 0	0 ± 0	0 ± 0	0 ± 0	0 ± 0	0 ± 0	0 ± 0	0 ± 0
0,25	13,737 ± 3,669	14,398 ± 1,105	13,499 ± 2,409	12,141 ± 3,535	10,611 ± 2,374	15,927 ± 1,656	10,357 ± 1,431	10,966 ± 1,068	12,193 ± 2,344
0,5	17,393 ± 3,481	17,879 ± 3,196	17,419 ± 1,127	15,555 ± 2,197	14,720 ± 1,865	19,672 ± 3,075	13,290 ± 2,586	13,802 ± 3,641	14,198 ± 2,543
0,75	22,558 ± 4,384	22,691 ± 1,467	22,981 ± 1,739	19,806 ± 3,895	18,960 ± 2,558	25,103 ± 4,642	18,465 ± 1,744	18,034 ± 3,051	19,884 ± 3,227
1	25,560 ± 3,241	24,915 ± 2,894	25,812 ± 2,867	22,770 ± 2,309	22,251 ± 2,491	27,388 ± 4,225	21,197 ± 3,060	21,810 ± 2,011	21,166 ± 3,570
3	43,861 ± 2,825	42,133 ± 4,497	48,573 ± 4,595	40,590 ± 1,579	38,822 ± 4,707	45,164 ± 7,354	44,831 ± 4,895	33,214 ± 5,007	38,894 ± 4,114
6	58,399 ± 3,995	55,676 ± 5,599	72,346 ± 6,199	54,423 ± 1,918	51,604 ± 6,339	57,553 ± 6,375	68,544 ± 2,229	47,901 ± 0,508	51,722 ± 5,051
10	69,781 ± 3,725	65,025 ± 6,296	84,174 ± 4,154	64,518 ± 1,790	61,190 ± 5,938	65,984 ± 6,645	77,138 ± 3,587	52,601 ± 5,735	60,189 ± 5,987
24	84,514 ± 1,391	77,307 ± 5,455	91,622 ± 3,005	78,864 ± 2,122	77,341 ± 6,593	80,399 ± 5,468	84,513 ± 0,824	69,270 ± 1,875	75,155 ± 4,787

Table 56: Percentage of drug released from microspheres 9 to 17 at different times.

All selected microspheres exhibited a prolonged release for 24 hours. Microspheres **E11** released 91,62 % drug in 24 h, the maximum value obtained. The minimum quantity released in 24 h was 69,27 % by the microspheres **E16**. The release pattern observed was a biphasic, characterized by an initial burst effect followed by slow release. Chitosan proportion has a remarkable influence on the drug release in all the intervals studied; higher polymer ratios reduces the drug release in all the study but it is significant from 10 to 24 h ($P < 0,05$). Curiously, the influence of glutaraldehyd in the percentage of drug release seems to change during the studied time. At the beginning, higher cross-linking agent ratios reduces the drug release but it changes in the 3 h interval when microspheres with same proportion of chitosan and more quantity of glutaraldehyd, start to release more quantity of drug (figure 96). This difference appears significant at 24 h ($P < 0,05$). It will be necessary to analyze in depth the influence of glutaraldehyd percentage on the drug release mechanism and kinetics elucidated in this study.

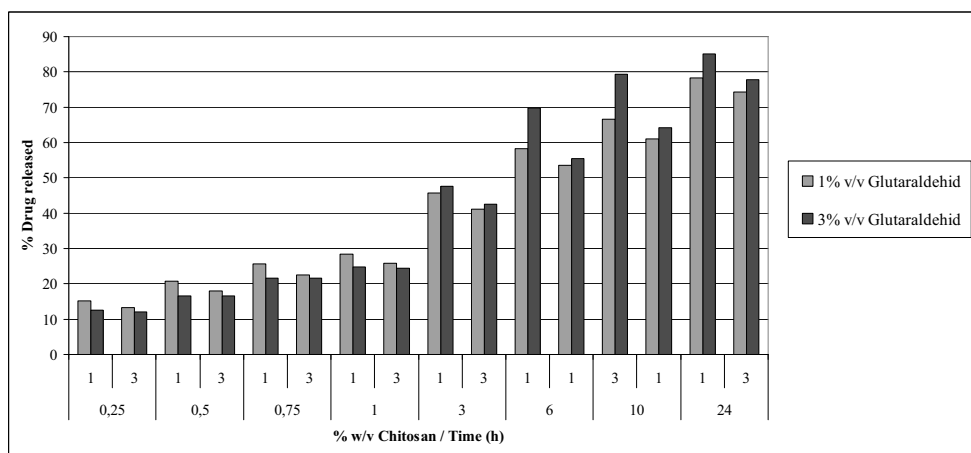


Figure 96: Mean values of % drug released in different times depending on % w/v chitosan and % v/v of glutaraldehyd.

B.8.2. Drug release mechanism

Microspheres	Zero-order			First-order			Higuchi			Weibull			Kormeyer-Peppas		
	R ²	AIC	R ²	AIC	R ²	AIC	R ²	AIC	R ²	AIC	R ²	AIC	R ²	AIC	
E1	0,8182	53,6806 ± 4,7003	0,9850	26,0413 ± 5,2125	0,9437	37,2598 ± 9,5042	0,9995	-6,8626 ± 8,9238	0,9956	-39,3861 ± 0,7362					
E2	0,7834	55,6507 ± 1,1289	0,9952	18,1551 ± 4,5446	0,9261	41,6966 ± 1,7118	0,9986	7,3912 ± 1,0012	0,9989	-48,1785 ± 4,2413					
E3	0,8151	51,5291 ± 0,6597	0,9748	26,4717 ± 0,5968	0,9452	37,2260 ± 1,8139	0,9993	-5,0570 ± 4,2056	0,9971	-49,0320 ± 10,8080					
E4	0,8581	48,8637 ± 3,7136	0,9868	23,7229 ± 2,9983	0,9666	29,6257 ± 9,0125	0,9996	-12,2712 ± 12,0982	0,9971	-32,4186 ± 9,3978					
E5	0,8265	54,2597 ± 2,0261	0,9735	30,4997 ± 2,2990	0,9518	39,1608 ± 3,6163	0,9997	-10,4533 ± 2,6569	0,9979	-42,8950 ± 10,3298					
E6	0,8386	52,4933 ± 1,6747	0,9948	19,9172 ± 3,7383	0,9543	36,1821 ± 2,1733	0,9972	13,6981 ± 3,4180	0,9956	-48,4879 ± 7,3144					
E7	0,8493	49,7749 ± 3,4427	0,9745	27,3295 ± 2,2957	0,9631	32,9444 ± 5,8767	0,9996	-15,2662 ± 11,8235	0,9953	-30,0107 ± 5,4291					
E8	0,8183	51,2634 ± 4,1310	0,9800	26,5561 ± 4,9685	0,9412	35,6593 ± 7,4345	0,9925	16,7978 ± 7,9500	0,9972	-52,5277 ± 14,2063					
E9	0,8750	49,6310 ± 2,2516	0,9833	27,2208 ± 3,3524	0,9756	29,8217 ± 5,6314	0,9993	-4,3917 ± 7,7994	0,9893	-47,5666 ± 10,3131					
E10	0,8625	50,4312 ± 2,0371	0,9810	28,2565 ± 1,7968	0,9704	32,4372 ± 3,1676	0,9990	-4,6399 ± 12,6373	0,9949	-47,9839 ± 13,4136					
E11	0,8404	52,4775 ± 1,5411	0,9946	19,9279 ± 5,6104	0,9560	35,6341 ± 3,2802	0,9978	9,9225 ± 6,3190	0,9951	-43,3909 ± 3,0718					
E12	0,8777	46,0640 ± 1,2601	0,9851	22,4592 ± 4,9193	0,9767	26,0699 ± 3,7977	0,9995	-10,9984 ± 9,1440	0,9966	-48,1246 ± 5,7154					
E13	0,8879	46,4404 ± 2,3353	0,9847	25,0258 ± 1,3578	0,9812	24,8738 ± 5,1891	0,9994	-7,1393 ± 6,3139	0,9976	-49,0946 ± 3,5611					
E14	0,8539	51,8019 ± 0,9342	0,9688	32,0622 ± 3,2564	0,9622	35,4531 ± 0,2799	0,9921	15,9557 ± 12,7942	0,9981	-45,5390 ± 5,8706					
E15	0,8371	52,9060 ± 1,6080	0,9978	13,3982 ± 1,7004	0,9525	36,7928 ± 2,0810	0,9984	9,1565 ± 4,9222	0,9963	-46,8830 ± 6,5354					
E16	0,8877	46,0438 ± 2,2098	0,9761	27,5646 ± 0,7545	0,9796	25,9959 ± 3,3345	0,9965	-2,1450 ± 19,6812	0,9984	-44,2629 ± 1,1119					
E17	0,8810	46,8555 ± 2,5349	0,9844	25,1912 ± 1,6403	0,9781	26,5367 ± 4,6204	0,9986	-1,0964 ± 10,2526	0,9983	-48,0234 ± 5,6068					

Table 57: Coefficients of correlation and AIC values for the kinetic models: Zero-order, First-order, Higuchi, Weibull and Kormeyer- Peppas fitted in the experimental data of microspheres 1-17.

The model of Korsmeyer-Peppas shows the smallest value for the AIC then it is the one which, statistically, describes the best drug release mechanism (see table 57). Consequently, N values will be considered to define it. It leads to differentiate two different kinds of mechanisms among the microspheres prepared. On one side, most of the mass transfers in the microspheres follow the Fick's law because N values are less than 0,5. On the other side, another group (**E11, E2, E6 and E15**) follows an anomalous transport because N values are > 0,5. Curiously, the last group shows the same characteristic in their composition, 3 % v/v of glutaraldehyd has been used in the formulation and the relation of weights between glutaraldehyd and chitosan is 3 % w/w. ANOVA has been used to study the influence of the experimental design factors on N values (table 58). The significant influence of glutaraldehyd and chitosan concentration is shown in the table below (P<0,05). The possibility that the influence of glutaraldehyd concentration was by chance is only 1,49 % then it could be deduced that high proportions of glutaraldehyd are inducing the anomalous release mechanism in chitosan microspheres. Flow rate and the interaction between flow rate and inlet temperature are also influent parameters in N values. The first one influences increasing N value and the interaction reducing it.

Analysis of variance for N Korsmeyer					
Source	Sum of squares	Df	Mean square	F-Ratio	P-Value
A:Glutaraldehyd conc	0,0383588	1	0,0383588	1830,36	0,0149
B:Chitosan concentra	0,00655364	1	0,00655364	312,72	0,0360
C:Pump	0,000226876	1	0,000226876	10,83	0,1878
D:Flow rate	0,00958743	1	0,00958743	457,48	0,0297
E:Inlet temperature	0,000495088	1	0,000495088	23,62	0,1292
AB	0,0140998	1	0,0140998	672,80	0,0245
AC	0,00201074	1	0,00201074	95,95	0,0648
AD	0,00040651	1	0,00040651	19,40	0,1421
AE	0,000221134	1	0,000221134	10,55	0,1901
BC	0,000505182	1	0,000505182	24,11	0,1279
BD	0,00057391	1	0,00057391	27,39	0,1202
BE	0,000235477	1	0,000235477	11,24	0,1846
CD	0,00000842209	1	0,00000842209	0,40	0,6403
CE	0,00252042	1	0,00252042	120,27	0,0579
DE	0,00503032	1	0,00503032	240,03	0,0410
Total Error	0,000020957	1	0,000020957		

Total (corr.)	0,0808546	16			
R-squared = 99,9741 percent					
R-squared (adjusted for d.f.) = 99,5853 percent					
Standard Error of Est. = 0,00457788					
Mean absolute error = 0,000522494					
Durbin-Watson statistic= 2,125					
Residual Autocorrelation Lag 1 = -0,0661765					

Table 58: Anova test for N Korsmeyer.

Other studies have reported the possibility to elucidate the diffusional mechanism of the drug release with the β values of Weibull's function due to the demonstrated correlation

with N values of Korsmeyer function (Papadopoulo V.et al., 2006). The obtained values in this study (table 59) show a high correlation ($R^2= 0,8401$) between them, and then the β values confirm the difference of the mechanism of drug release of the same two group of microspheres. The group of microspheres with β values between 0,39 and 0,69 will release the drug by diffusion in fractal or disordered substrate different from the percolation cluster (slow flow of fluids through porous networks) and that formulations with β values between 0,75 and 1 by diffusion in normal Euclidian substrate with contribution of another release mechanism (Papadopoulo V.et al., 2006). Furthermore, studying the influence of factors on β values by ANOVA test, the results obtained show how glutaraldehyd also influence increasing it like on N-values ($P>0,05$). Moreover, it has been reported that K_h values > 1 mean that the drug release follows Fick's law (Higuchi T., 1963) but taking into account AIC values and considering Korsmeyer-Peppas as the best model fitting data, it is possible to accurate the drug release mechanism as explained above. In the present study all the values are bigger than 1 (table 60).

Microspheres	Kormeyer-Peppas	Weibull	Composition		
	N	β	% v/v Gluta	% w/w Gluta	% w/v Chitosan
E3	0,3696 \pm 0,0135	0,5401 \pm 0,0291	1	0,3	3
E5	0,3792 \pm 0,0494	0,5420 \pm 0,0125	1	1	1
E14	0,4134 \pm 0,0577	0,5430 \pm 0,0334	1	0,3	3
E7	0,4037 \pm 0,0749	0,5433 \pm 0,0323	1	0,3	1
E16	0,4751 \pm 0,0195	0,5559 \pm 0,0519	1	1	1
E10	0,4402 \pm 0,0385	0,5840 \pm 0,0062	1	1	1
E1	0,4306 \pm 0,0167	0,5847 \pm 0,0541	3	1	3
E9	0,4695 \pm 0,0695	0,6103 \pm 0,0635	2	1	2
E13	0,4882 \pm 0,0485	0,6113 \pm 0,0639	1	0,3	3
E17	0,4842 \pm 0,0124	0,6114 \pm 0,0182	3	1	3
E12	0,4905 \pm 0,1008	0,6321 \pm 0,0275	3	1	3
E4	0,4752 \pm 0,0722	0,6377 \pm 0,0514	3	1	3
E8	0,4456 \pm 0,0399	0,6389 \pm 0,0777	1	0,3	3
E11	0,5581 \pm 0,0894	0,7848 \pm 0,0509	3	3	1
E2	0,5115 \pm 0,0586	0,7984 \pm 0,0588	3	3	1
E6	0,5828 \pm 0,0829	0,8145 \pm 0,0695	3	3	1
E15	0,6402 \pm 0,0308	0,8876 \pm 0,0541	3	3	1

Table 59: N and β values of microspheres in increasing order of β and % v/v of glutaraldehyd and w/w of glutaraldehyd/chitosan and %w/v of chitosan in the formulations.

There is a clear correlation between the % w/w glutaraldehyd/chitosan in front of β values ($R^2=0,915605$) (figure 97).

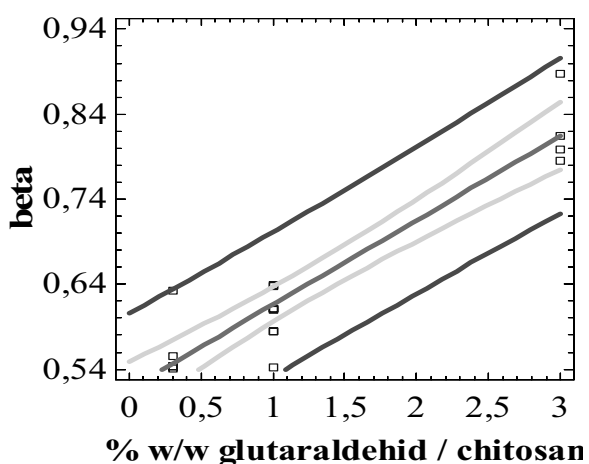


Figure 97: Correlation graph between β values and % w/w glutaraldehyd/chitosan % respectively.

Curiously, among the microspheres which showed N and β values higher (additional mechanism of release) (see table 59) microspheres **E6**, **E11** and **E15** also showed a higher percentage of drug released, 83,90 %, 91,62 % and 84,51

To rule out the possibility of the presence of porous in the surface of this similar group of microspheres and then its influence in the drug release mechanism, one sample (**E6**) is studied under SEM by Hitachi S-4300. This microscope has a higher resolution than Hitachi 2300 which has been used in the characterization of microspheres. As can be seen in the figure 98, the surface is totally smooth without the presence of porous.

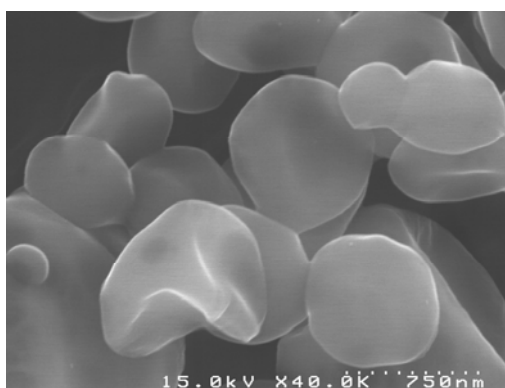


Figure 98: Microspheres E6 under SEM.

B.8.3. Drug release kinetics

MICROS.	Zero order		First order		Higuchi		Weibull			Korsmeyer-Peppas		Mechanism drug release
	K_0 (h ⁻¹)	K_1 (h ⁻¹)	K_h (h ^{-1/2})	β	dt (h)	K_k (h ⁻ⁿ)	K_k (h ⁻ⁿ)	K_k (h ⁻ⁿ)	K_k (h ⁻ⁿ)	K_k (h ⁻ⁿ)	K_k (h ⁻ⁿ)	
E1	1,0513 ± 0,0543	0,5253 ± 0,2756	4,8377 ± 0,4360	0,5847 ± 0,0167	4,8082 ± 3,2221	0,2847 ± 0,0750	0,2847 ± 0,0750	0,2847 ± 0,0750	0,2847 ± 0,0750	0,2847 ± 0,0750	0,2847 ± 0,0750	Fickian release
E2	1,0998 ± 0,0351	0,4526 ± 0,0656	5,0941 ± 0,1807	0,7984 ± 0,0586	2,6611 ± 0,2578	0,2904 ± 0,0289	0,2904 ± 0,0289	0,2904 ± 0,0289	0,2904 ± 0,0289	0,2904 ± 0,0289	0,2904 ± 0,0289	Non-Fickian release
E3	0,8744 ± 0,0180	0,6619 ± 0,1071	4,0545 ± 0,0414	0,5401 ± 0,0135	3,6327 ± 0,6751	0,3058 ± 0,0140	0,3058 ± 0,0140	0,3058 ± 0,0140	0,3058 ± 0,0140	0,3058 ± 0,0140	0,3058 ± 0,0140	Fickian release
E4	0,9020 ± 0,0505	0,3657 ± 0,1225	4,0618 ± 0,3187	0,6377 ± 0,0722	7,2100 ± 5,9801	0,2397 ± 0,0366	0,2397 ± 0,0366	0,2397 ± 0,0366	0,2397 ± 0,0366	0,2397 ± 0,0366	0,2397 ± 0,0366	Fickian release
E5	1,0521 ± 0,0443	0,5863 ± 0,1042	4,8533 ± 0,2578	0,5420 ± 0,0494	4,7930 ± 2,0180	0,3127 ± 0,0297	0,3127 ± 0,0297	0,3127 ± 0,0297	0,3127 ± 0,0297	0,3127 ± 0,0297	0,3127 ± 0,0297	Fickian release
E6	1,0813 ± 0,0281	0,3074 ± 0,0771	4,8620 ± 0,1865	0,8145 ± 0,0829	3,9563 ± 0,5080	0,2371 ± 0,0433	0,2371 ± 0,0433	0,2371 ± 0,0433	0,2371 ± 0,0433	0,2371 ± 0,0433	0,2371 ± 0,0433	Non-Fickian release
E7	0,8837 ± 0,1070	0,4873 ± 0,1338	4,0280 ± 0,5296	0,5433 ± 0,0749	7,2902 ± 3,8656	0,2657 ± 0,0439	0,2657 ± 0,0439	0,2657 ± 0,0439	0,2657 ± 0,0439	0,2657 ± 0,0439	0,2657 ± 0,0439	Fickian release
E8	0,9305 ± 0,0522	0,4810 ± 0,2518	4,2617 ± 0,3377	0,6389 ± 0,0399	4,6297 ± 2,5147	0,2946 ± 0,0711	0,2946 ± 0,0711	0,2946 ± 0,0711	0,2946 ± 0,0711	0,2946 ± 0,0711	0,2946 ± 0,0711	Fickian release
E9	0,9768 ± 0,0238	0,3288 ± 0,0945	4,3661 ± 0,1597	0,6103 ± 0,0695	6,7777 ± 1,5599	0,2559 ± 0,0371	0,2559 ± 0,0371	0,2559 ± 0,0371	0,2559 ± 0,0371	0,2559 ± 0,0371	0,2559 ± 0,0371	Fickian release
E10	0,9628 ± 0,0771	0,3752 ± 0,0514	4,3457 ± 0,3683	0,5840 ± 0,0385	6,4441 ± 2,7687	0,2544 ± 0,0241	0,2544 ± 0,0241	0,2544 ± 0,0241	0,2544 ± 0,0241	0,2544 ± 0,0241	0,2544 ± 0,0241	Fickian release
E11	1,0790 ± 0,0403	0,3064 ± 0,0517	4,8559 ± 0,1941	0,7848 ± 0,0894	4,1870 ± 1,0677	0,2648 ± 0,0184	0,2648 ± 0,0184	0,2648 ± 0,0184	0,2648 ± 0,0184	0,2648 ± 0,0184	0,2648 ± 0,0184	Non-Fickian release
E12	0,8137 ± 0,0137	0,3127 ± 0,0956	3,6252 ± 0,0292	0,6321 ± 0,1008	6,7722 ± 1,3539	0,2297 ± 0,0289	0,2297 ± 0,0289	0,2297 ± 0,0289	0,2297 ± 0,0289	0,2297 ± 0,0289	0,2297 ± 0,0289	Fickian release
E13	0,8639 ± 0,0775	0,2827 ± 0,0566	3,8294 ± 0,3550	0,6113 ± 0,0485	8,1990 ± 2,3504	0,2185 ± 0,0250	0,2185 ± 0,0250	0,2185 ± 0,0250	0,2185 ± 0,0250	0,2185 ± 0,0250	0,2185 ± 0,0250	Fickian release
E14	1,0028 ± 0,0710	0,4464 ± 0,0871	4,5435 ± 0,3074	0,5430 ± 0,0577	6,9071 ± 2,4016	0,2780 ± 0,0204	0,2780 ± 0,0204	0,2780 ± 0,0204	0,2780 ± 0,0204	0,2780 ± 0,0204	0,2780 ± 0,0204	Fickian release
E15	1,1258 ± 0,0298	0,2855 ± 0,0389	5,0404 ± 0,1907	0,8876 ± 0,0308	3,8572 ± 0,4642	0,2196 ± 0,0292	0,2196 ± 0,0292	0,2196 ± 0,0292	0,2196 ± 0,0292	0,2196 ± 0,0292	0,2196 ± 0,0292	Non-Fickian release
E16	0,8260 ± 0,0398	0,3110 ± 0,0803	3,6721 ± 0,2223	0,5559 ± 0,0195	10,3708 ± 3,0155	0,2044 ± 0,0298	0,2044 ± 0,0298	0,2044 ± 0,0298	0,2044 ± 0,0298	0,2044 ± 0,0298	0,2044 ± 0,0298	Fickian release
E17	0,8569 ± 0,0663	0,3017 ± 0,0480	3,8168 ± 0,3290	0,6114 ± 0,0124	7,1382 ± 1,6616	0,2205 ± 0,0297	0,2205 ± 0,0297	0,2205 ± 0,0297	0,2205 ± 0,0297	0,2205 ± 0,0297	0,2205 ± 0,0297	Fickian release

Table 60: Values of K_0 , K_d , K_h , β , dt and K_k for the microspheres of the experimental design and its mechanism of meglumine antimoniate release.

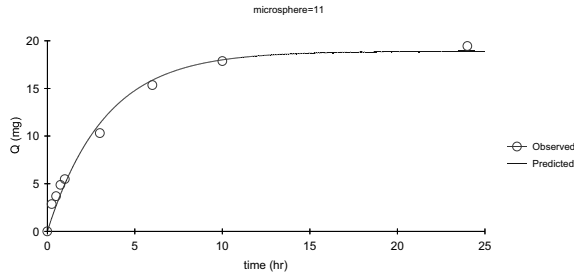


Figure 99: Quantities of drug released from microspheres 11 fit in first-order model.

Once the drug release mechanism has been elucidated, it is necessary to study its kinetics. Experimental data are also fitted in zero-order, first-order and Higuchi’s models. The highest R^2 and the smallest AIC values indicate that first order is the function which, statically explain better the MGA release kinetics following Korsmeyer model, nevertheless Higuchi’s

function also shows a good correlation values (table 60).

Although zero order is the worst model fitting the experimental data, the K_0 values in increasing order will be shown in the table 61 because they reflect the influence of percentage of the chitosan polymer in the kinetic release of the microspheres clearly. Moreover, they reflects that the microspheres **E11**, **E6**, **E2** and **E15** show the higher values of K_0 , ones which would show a different kind of drug release mechanism.

Microspheres	K_0	Composition		
		% v/v Gluta	% w/w Gluta	% w/v Chitosan
E12	0,8137 ± 0,0137	1	0,3	3
E16	0,8260 ± 0,0398	1	0,3	3
E17	0,8569 ± 0,0663	3	1	3
E13	0,8639 ± 0,0775	3	1	3
E3	0,8744 ± 0,0180	1	0,3	3
E7	0,8837 ± 0,1070	1	0,3	3
E4	0,9020 ± 0,0505	3	1	3
E8	0,9305 ± 0,0522	3	1	3
E10	0,9628 ± 0,0771	1	1	1
E9	0,9768 ± 0,0238	2	1	2
E14	1,0028 ± 0,0710	1	0,3	1
E1	1,0513 ± 0,0543	1	1	1
E5	1,0521 ± 0,0443	1	1	1
E11	1,0790 ± 0,0403	3	3	1
E6	1,0813 ± 0,0280	3	3	1
E2	1,0998 ± 0,0351	3	3	1
E15	1,1258 ± 0,0298	3	3	1

Table 61: K_0 values and composition of microspheres in increasing order.

Main factors	K _k	K ₁	K _h
A: % v/v Glutaraldehyd	- *	-	+*
B: % w/v Chitosan	- *	-	-*
C: Pump	-	-	+*
D: Flow rate	- *	-	-*
E: Inlet temperature	- *	-	-*
AB	+*	+	-*
AC	-	+	-
AD	+	+	+*
AE	-	-	-*
BC	+	-	+
BD	-*	-	-*
BE	-	-	-
CE	+	+	-*
CD	-	+	+*
DE	+*	+	+*

Table 62: Influence of the factors established in the experimental design and their interactions in the kinetics constants of Korsmeyer equation, First-order, and Higuchi's function. (-) negative influence, (+) positive influence. * significant influence P<0,05.

Microspheres (**E1-E17**) showed K_k, K₁, K_h values significantly different between them (P<0,05), for this reason the influence of the different factors of the experimental design on each one is studied. In the table 62 the influence of the main parameters and their interactions are shown.

ANOVA test, including all the possible interactions, shows that all the main factors (flow rate, % v/v glutaraldehyd, inlet temperature, % w/v chitosan and pump) influence negatively on K₁. It means that if these parameters are higher, K₁ values will be smaller, then the drug release slower. The same main parameters, except pump, influence significantly reducing the K_k values. It is worth pointing out that percentage of glutaraldehyd reduces the K_k. Then, it could justify why during the first 3 h of study, microspheres with higher proportion of cross-linking, drug release is slower besides to appear an anomalous drug release

mechanism in this group of microspheres in 24 h. The interactions DE (flow rate and inlet temperature) and AB (glutaraldehyd and chitosan) influence significantly increasing this parameter, BD (chitosan and inlet temperature) reduces it.

Some differences exist in K_h case in respect with the other constants, more interactions influence significantly and % of glutaraldehyd and pump variables affect increasing constant values.

ANOVA of the **dt** (63,2% drug released) obtained by Weibull's equation does not show significant differences among their values (P>0,05). However, it is clear the significant influence of the concentration of polymer on **dt** (P<0,05). It means that when high concentrations of chitosan is used higher is the time to dissolve the drug. The mean **dt** is 5,861 h ± 1,997 h and the range of values is from 2,661 h (microspheres **E2**) to 10,371 h (microspheres **E16**) (see table 60).

B.8.4. Amodelistic parameters

Although all the microspheres fit better in the same kinetic model (Korsmeyer), amodelistic parameters have been calculated. In the table 63, Mean Disolution Time (**MDT**) values and Dissolution Efficiency (**DE**) are shown in increasing order.

Microspheres	MDT (h)	Microspheres	DE (%)
E2	3,0969 ± 0,1098	E16	74,7951 ± 2,9929
E3	4,1362 ± 0,4910	E13	75,7482 ± 2,5550
E6	4,1489 ± 0,2159	E17	76,5253 ± 2,1965
E11	4,1769 ± 0,6764	E12	77,2781 ± 1,9003
E15	4,2175 ± 0,5492	E9	77,6975 ± 2,9537
E5	4,2287 ± 0,8793	E14	78,5994 ± 0,7665
E1	4,2675 ± 1,9348	E4	78,8978 ± 5,5488
E8	4,2755 ± 2,0171	E10	79,0898 ± 1,9836
E7	4,8758 ± 0,9742	E7	79,6841 ± 4,0591
E10	5,0234 ± 0,4847	E8	82,1856 ± 8,4048
E4	5,0645 ± 1,3317	E1	82,2189 ± 8,0616
E14	5,2778 ± 0,4140	E5	82,3803 ± 3,6637
E9	5,3526 ± 0,7089	E15	82,4272 ± 2,2881
E12	5,4533 ± 0,4561	E11	82,5964 ± 2,8182
E17	5,6378 ± 0,5225	E6	82,7128 ± 0,8995
E13	5,8204 ± 0,6132	E3	82,7657 ± 2,0460
E16	6,0008 ± 0,6379	E2	88,2529 ± 1,5565

Table 63: MDT and DE values of microspheres.

It can be find microspheres with **MDT** from 3 to 6 h with a mean value of 4,788 h ± 0,776. The minimum value of **MDT** is obtained by microspheres **E2** which has the maximum **DE** (88,252 %).

5.4.4. Investigation of microsphere surface characteristics on macrophage uptake using quantum dots (QD) assisted imaging

5.4.4.1. Characterization of QD solution

5.4.4.1.1. Concentration

The UV-vis spectra obtained by UV-vis scanning from 300 to 800 nm shows an inflexion point of absorbances values at 576 nm, the first excitonic absorption pick (figure 100). From this wavelength, the particle size is deduced by extrapolation in the figure 101 obtaining a value of 3,5 nm. The correspondent molar extinction coefficient is $1,5 \cdot 10^5 \text{ L/mol}_{\text{particle}} \cdot \text{cm}$.

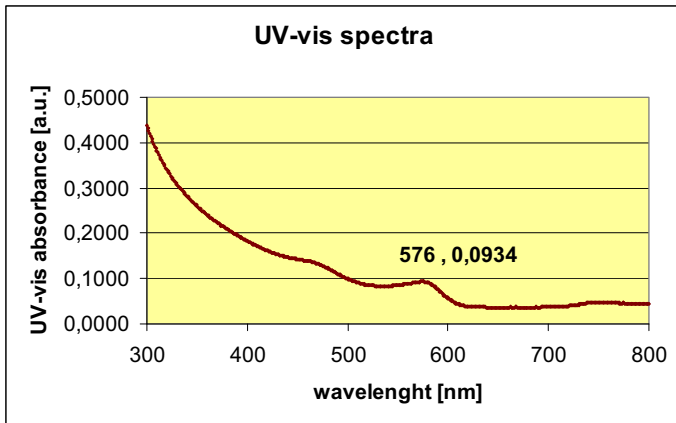


Figure 100: CdSe/ZnSe QD UV-vis absorption spectra

Using Beer-Lambert law it is possible to obtain the concentration of the solution of QD which is pretended to be encapsulated into microspheres. Beer-lambert law is: $A = \alpha l c$

Where, A is 0,0934

l is considered 1 cm

α is $3,27 \cdot 10^3 \text{ L/mol}_{\text{particle}} \cdot \text{cm} \cdot \text{nm}$

α has been obtained using the next

formula:

$$\alpha = \frac{4\pi k}{\lambda}$$

Where k is $1,5 \cdot 10^5 \text{ l/mol}_{\text{particle}} \cdot \text{cm}$ and λ

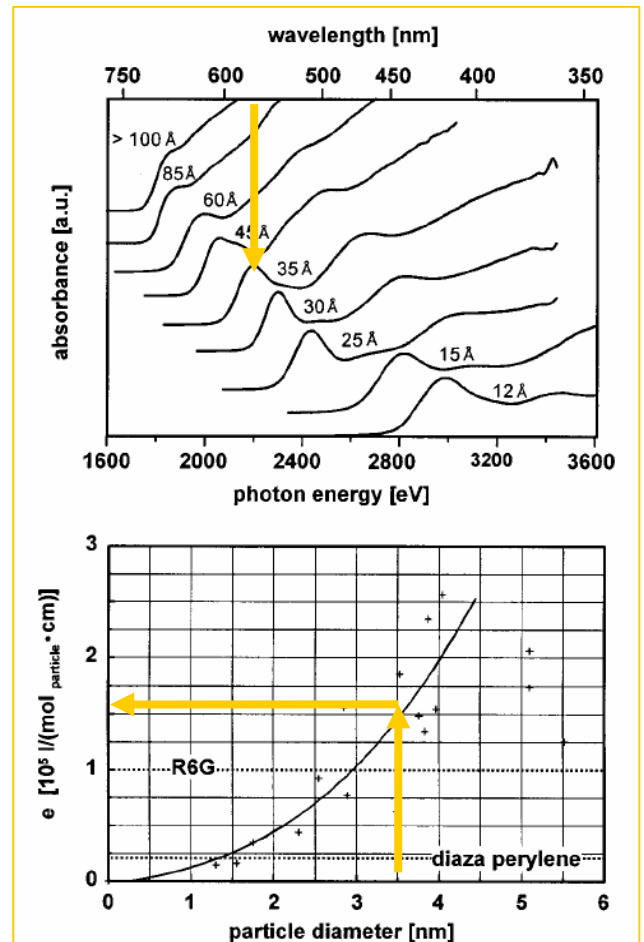


Figure 101: The upper graph (A) shows a set of CdSe nanocrystals in a size regimen of 1-10 nm diameter. The QDs used are marked with a gold arrow. The lower graph (B) shows their molar extinction coefficients at their first absorption maximum (Schmelz O. et al., 2001).

is 576 nm, and then the concentration obtained is $1,62 \cdot 10^{-4}$ mol/L.

5.4.4.1.2. Fluorescence

Under normal light illumination CdSe/ZnS QD solution produce bright orange fluorescence light emission. Emission spectrum shows a pick at 600 nm under a constant excitation of Xe lamp at 360 nm (figure 102).

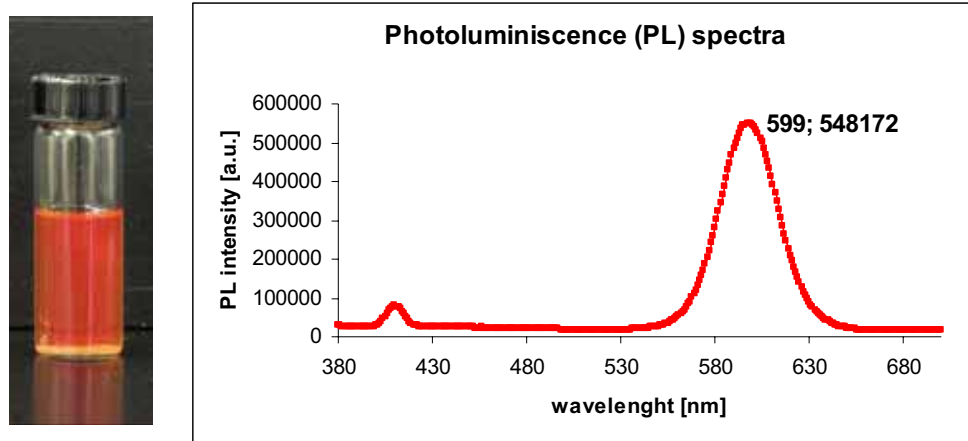


Figure 102: Fluorescence light emission from red QDs and QD emission spectra.

5.4.4.2. Encapsulation of QD in microspheres

5.4.4.2.1. Characterization of microspheres

A) Particle size and Z-potential

As can be seen in the table 64, all microspheres used for encapsulation of QDs have similar mean particle size (range of 2.0 to 5.0 μm) measured by Accusizer® 780 A Autodiluter, and Z-potential varies from strong positive (chitosan) to weak negative (PLGA) in Zetaplus® apparatus.

	Mean (μm)	Z-potential (mV)
N°		
F1	$4,963 \pm 1,671$	$56,08 \pm 1,35$
F2	$3,650 \pm 0,278$	$49,85 \pm 2,51$
F3	$1,813 \pm 0,148$	$50,11 \pm 0,72$
F4	$1,760 \pm 0,101$	$100,16 \pm 1,52$
F5	$5,137 \pm 0,362$	$-6,15 \pm 1,56$
F6	$3,843 \pm 0,042$	$-3,20 \pm 6,33$

Table 64: Particle size and Z-potential of chitosan microspheres and PLGA microspheres

B) SEM

1% Chitosan microspheres (without lipids) (F1 and F2) are smooth in appearance, whereas the O/W emulsion chitosan microspheres (F3 and F4) have a rough porous wrinkled appearance under SEM (figure 103).

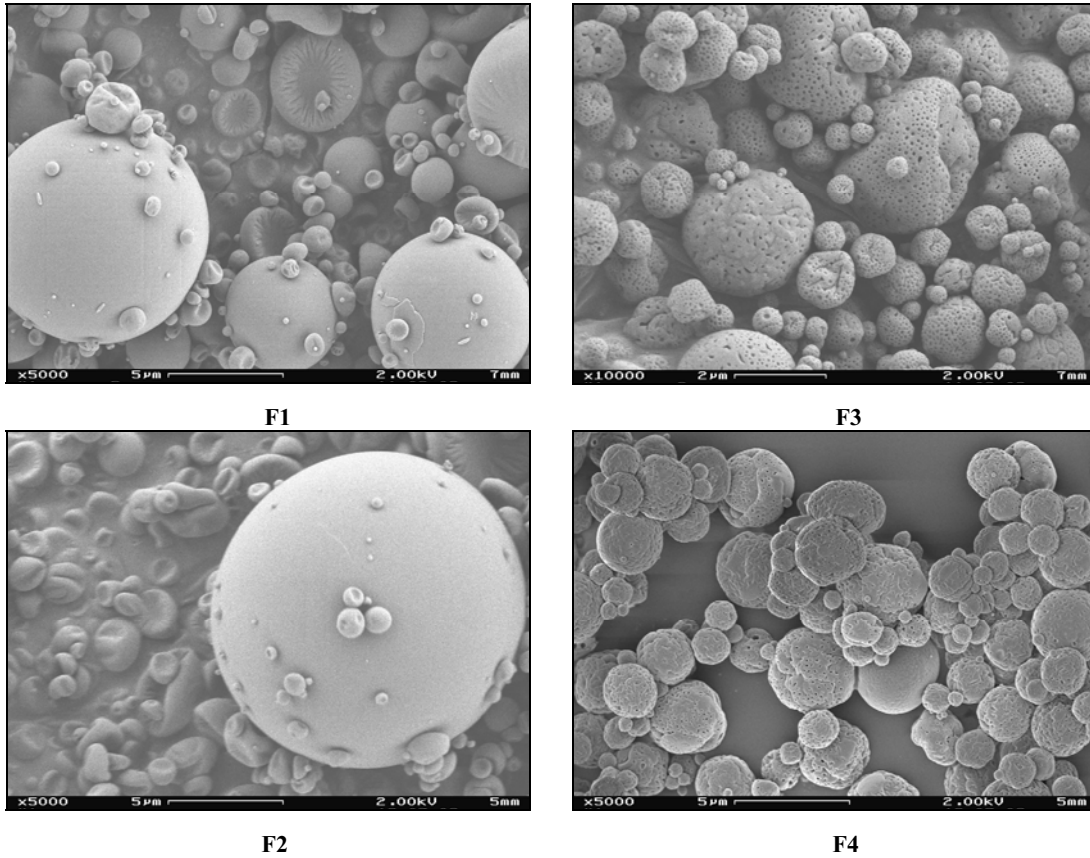


Figure 103: Chitosan microspheres without lipids (left) and O/W emulsion chitosan microspheres (right). N° F1 and F3 do not contain QDs and N° F2 and F4 contain red QDs.

The topography of the O/W chitosan microspheres suggested the presence of lipids on the particle surface (figure 104).

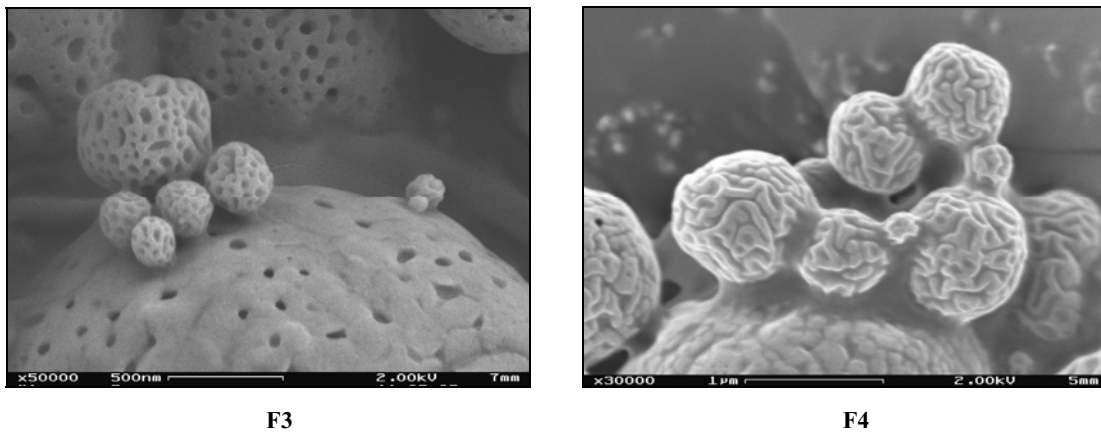


Figure 104: Pictures of stucked O/W chitosan microspheres by the presence of some lipidic component in the surface.

The PLGA microspheres are also smooth in appearance and they have spherical shape under SEM. Exceptionally, some of these microspheres appear folded inward with smaller microspheres inside (figure 105):

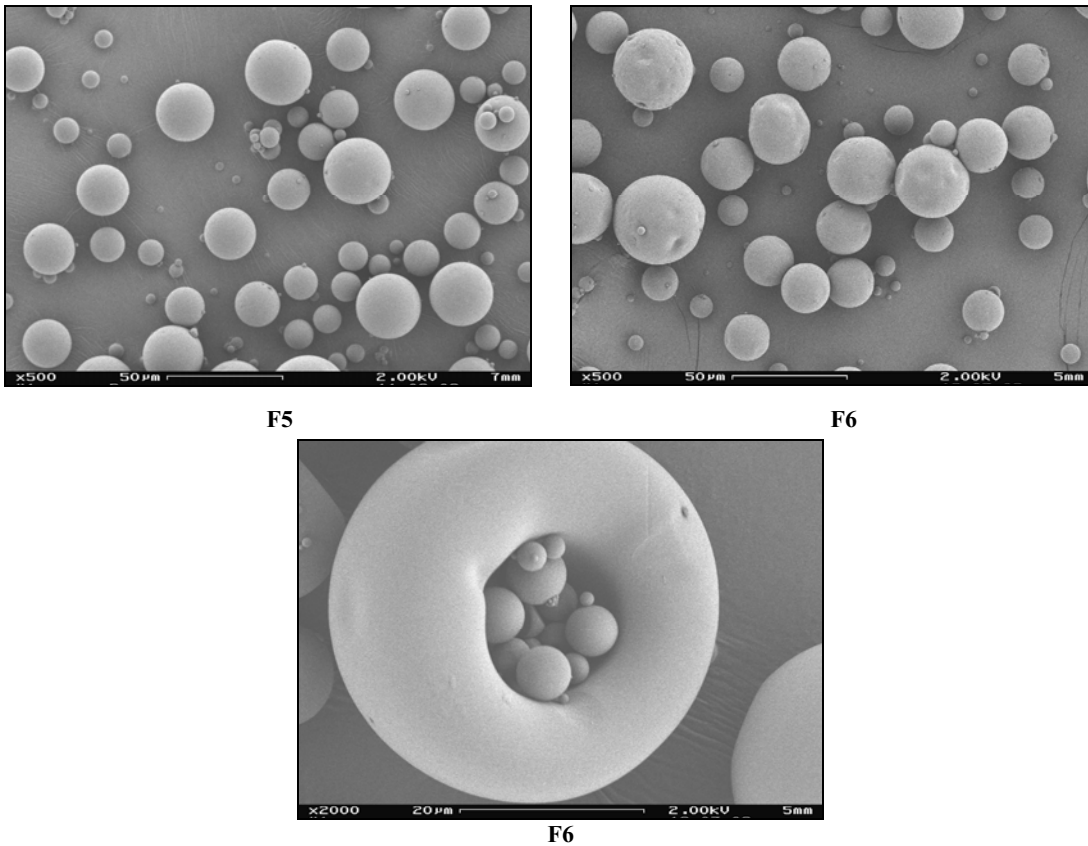


Figure 105: PLGA microspheres by solvent evaporation technique: F5 free-qd and F6 qd-loaded PLGA microspheres

C) Confocal microscopy

The used Leica SP2 laser spectral confocal microscope (LSCM) has not the possibility to excite at 365 nm (the best wavelength for the excitation of QDs) however 488 nm is used due to QDs can be excited for any wavelength. Bright orange fluorescence signal from the solution of QDs is obtained as shown in figure 106. It is necessary to rule out some light emission from the components of the microspheres because it would not make possible to study the encapsulation of the QDs. For this reason, QDs-free microspheres were prepared and examined under LSCM.

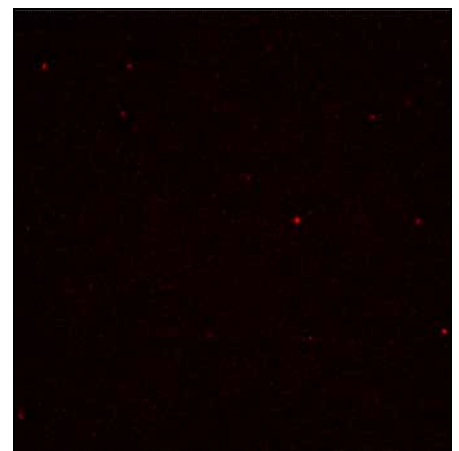


Figure 106: Aqueous solution of QDs in glass slide under LSCM at 488 nm.

No fluorescence signal is received from QDs-free microspheres and then QDs-loaded microspheres are studied. In all cases, red fluorescence is detected (figure 107).

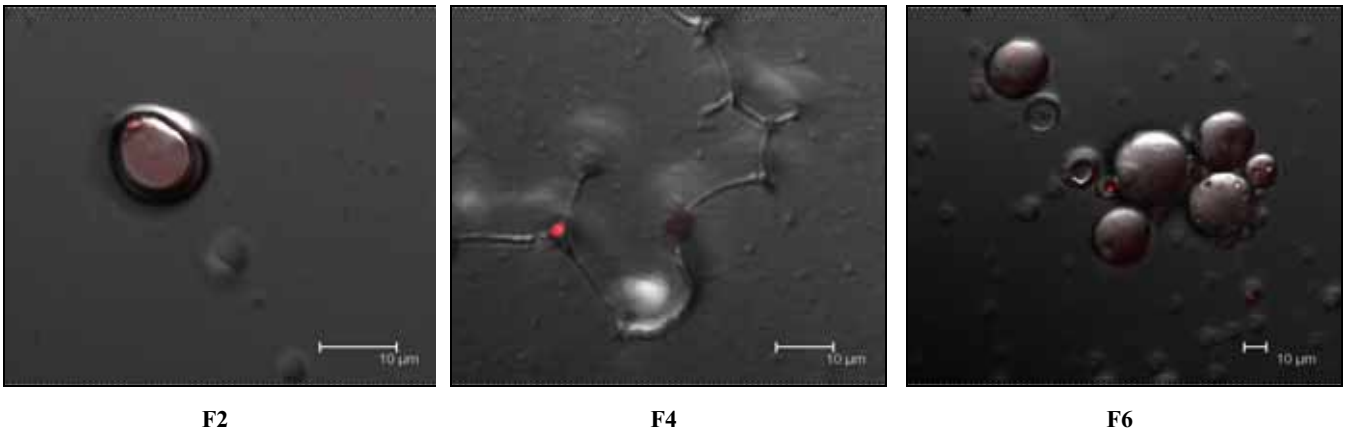


Figure 107: QD-loaded chitosan microspheres without lipids (F2) and lipids (F4) and QD-loaded PLGA microspheres (F6) in glass slide under LSCM at 488 nm.

Moreover, Z-section studies show that the QDs were internalized in all types of microspheres and verify that they are not only in the surface. The Z-section studies of chitosan microspheres F2 and F4 are composed by 10 sections along 7,20 µm and 14,4 µm of depth respectively (figure 108). In PLGA microspheres case, Z-section study is composed by 16 sections along 13,50 µm of depth (figure 109).

For each sample, a delimited coloured area of the first section image is selected in order to quantify the fluorescence intensity in that, then this same area will be used to analyse the same region of all the other Z-sections of that sample. Once these intensities are plotted it can be seen how fluorescence is distributed across the microspheres and higher intensities are from inside of the microspheres.

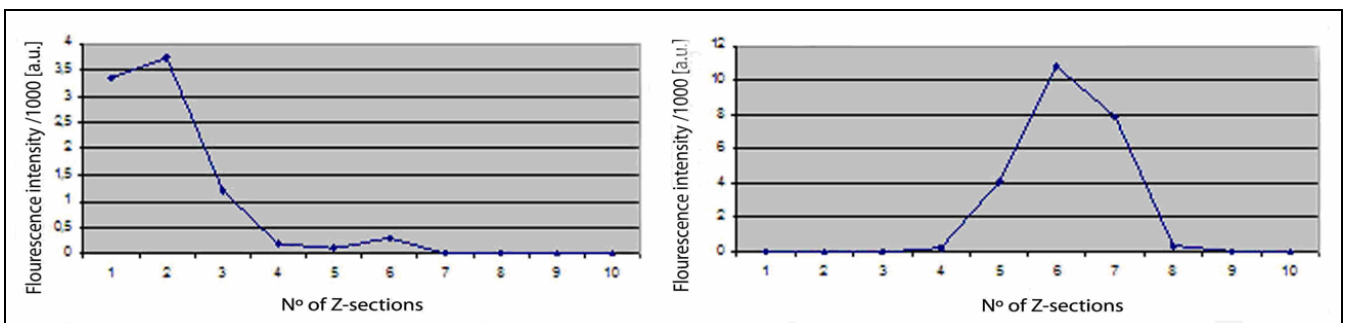


Figure 108: Graphs representing the fluorescence intensities of one selected area of Z-sections of F2 (left) and F4 (right) microspheres under LSCM at 488 nm.

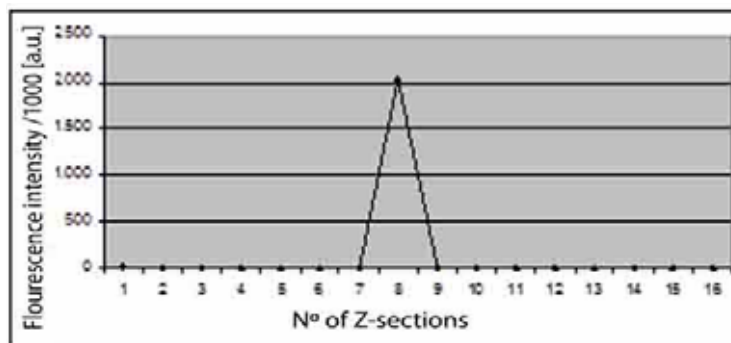


Figure 109: Graphs representing the fluorecence intensities of one selected area of Z-sections of F6 microspheres under LSCM at 488 nm.

5.4.4.2.2. Uptake studies

Once it has been reported that QDs are entrapped in the microspheres, uptake studies with MHS and RAW 264,7 cells can be started. Firstly, the photoluminescence of the own cells is studied in order to rule out any interference. No colour emission light is captured from the cells alone and their morphology can be seen in the figure 110.

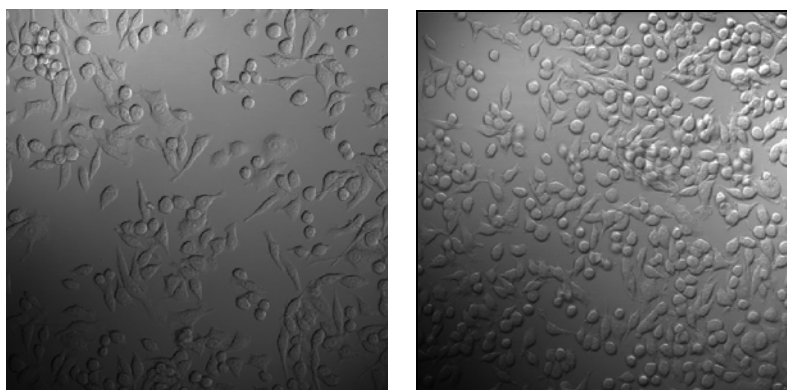


Figure 110: MHS cells (left) and RAW 264,7 cells (right).

The entrapped QDs allow visualization of the microspheres for long-term imaging in the macrophage uptake studies.

A) MHS cells

Following 1 h of transfection, uptake into MHS cells is investigated washing to remove material that was not internalized, and observing under LSCM. QDs in the presence of Lipofectamine 2000 form aggregates as a result of charge interactions. It has been reported that QDs alone are relatively unsuccessful in penetrating the cells (Srinivasan C., et al., 2006). The red channel image shows the aggregates inside the cell (figure 111).

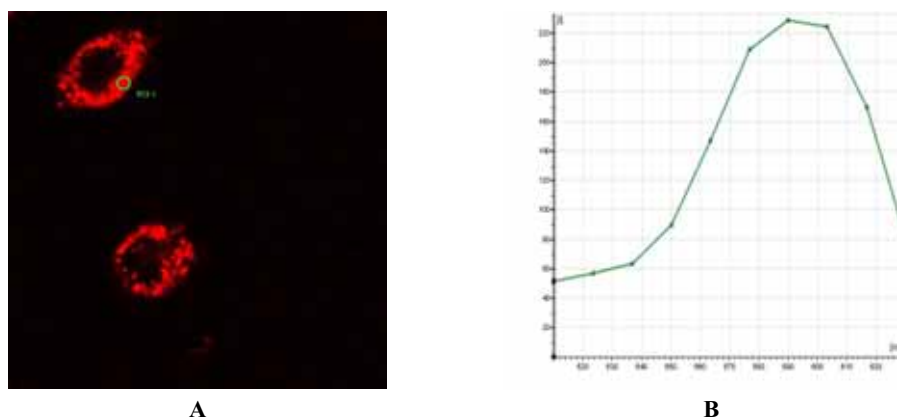


Figure 111: Cellular uptake studies of QDs after 1h incubation material in MHS cells. A) orange bright QDs in the presence of Lipofectamine2000 (green excitation filter). B) Graph representing fluorescence intensity of QDs which were exposed at 488 nm. QDs were added as $8,1 \times 10^{-6}$ mol per $0,8 \times 10^5$ cells per well.

Cellular uptake studies of microspheres which contain orange bright QDs inside after 1h incubation material in MHS cells are performed under LSCM with a green excitation filter. Overlapping the images obtained from the red channel with the transmitted image, it is possible to see how microspheres have been internalized in the cells (figure 112).

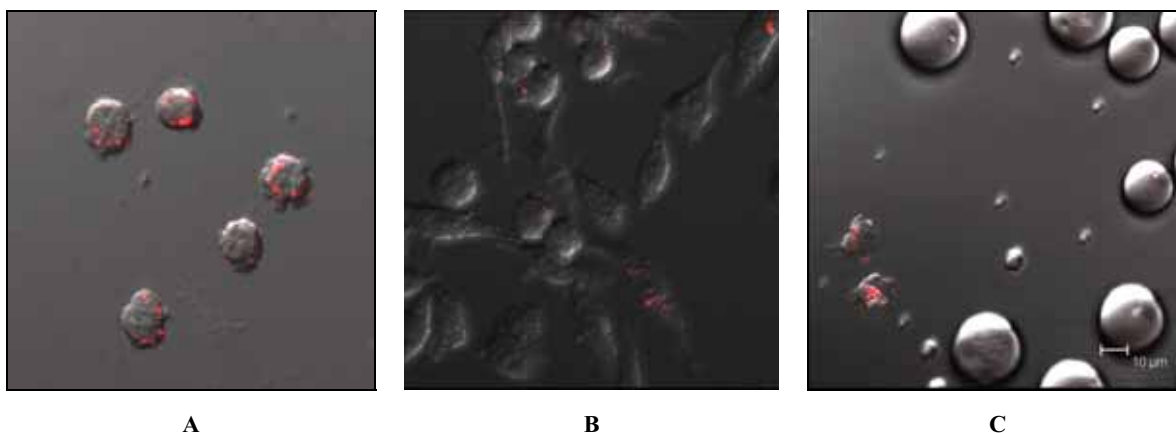


Figure 112: Cellular uptake studies of microspheres which contain orange bright QDs after 1h incubation material in MHS cells (green excitation filter). A) Chitosan microspheres (no lipids) B) Chitosan microspheres (with lipids) and C) PLGA microspheres. Microspheres were added as A) 125 μg, B) 1250 μg C) 2500 μg per $0,8 \times 10^5$ cells per well

Apparently, chitosan microspheres are more phagocytosed than PLGA microspheres and comparing between uptake results of the two kinds of chitosan microspheres, a negative influence of lipids could be deduced. It is noteworthy that these studies were started using suspensions at 2,5 μg/ml (125 μg of microspheres per well) but in chitosan microspheres with lipids and PLGA cases were necessary to increase it until 25 μg/ml and 50 μg/ml respectively for a correct study of the fluorescence.

The fact that the intensity of fluorescence was lower in the cells with chitosan microspheres with lipids could be, probably, due to an incorrect encapsulation of the components, and then their presence in the surface (detected under SEM) could be avoiding microspheres take into the cells. The component likely disrupter of the phagocytosis could be polyoxyl 40 hydrogenated castor oil (polyoxyethylene castor oil derivative) due to be a hydrophilic material and produce a steric repulsive effect to particle-macrophage adhesion. This effect has been used in order to redirect particles to the bone marrow and minimize or prevent their interaction with the reticuloendothelial elements of the liver and the spleen (Porter C.J.H., 1992). In other studies, the inclusion of surfactants at the surface of inhaled particles has been found to lead to a significant decrease in the phagocytic uptake of the inhaled particles (Hadinoto K. et al., 2007).

The internalization of chitosan microspheres in MHS cells is verified using a Z-section study (see figure 113). The results does not correspond to one study where chitosan microspheres appeared to remain located mainly at the cell surface rather than being internalized (Luzardo-Alvarez A. et al., 2005). The justification of a better chitosan microspheres uptaking than that from PLGA microspheres could be the fact that macrophages have the ability to recognize the size of foreign materials by an unknown mechanism. In the present case, PLGA microspheres look bigger than chitosan particles hence to affect uptaking. Moreover, it has been reported that both negatively and positively charged particles, the extent of phagocytosis was increased with increasing zeta potentials, and was the lowest when zeta potential was zero (Ahsan F. et al., 2002). In this case, the PLGA microspheres are weak negatively charged and chitosan strongly positively. Chitosan provides other advantages on phagocytosis due to its characteristics as has been explained previously (see 5.2.1.2). Sometimes, chitosan is used to coat PLGA microspheres in order to bioconjugate various active ligands and enhance the phagocytosis (Fischer S. et al. 2004, 2006).

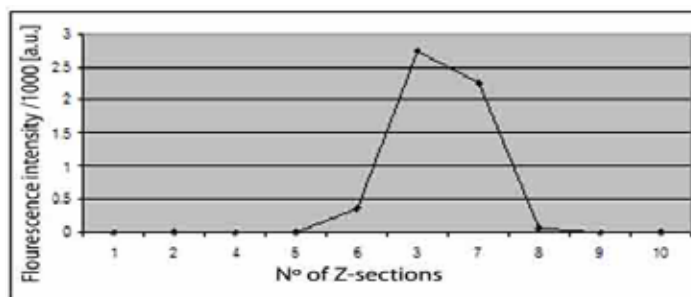


Figure 113: Graphs representing the fluorescence intensities of one selected area of Z-sections (18 μm of depth) of F2 microspheres inside MHS cells under LSCM at 488 nm.

B) RAW 264.7 cells

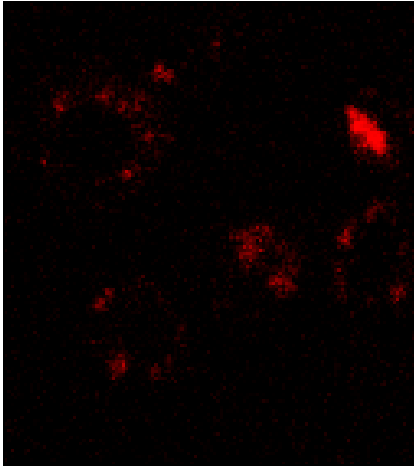


Figure 114: Cellular uptake studies of QDs after 1h incubation material in RAW 264.7 cells in the presence of Lipofectamine2000 (green excitation filter). QDs were added as $8,1 \times 10^{-6}$ mol per $0,8 \times 10^5$ cells per well.

Although RAW 264.7 cells and MHS cells are really similar some studies have been performed with this other cells. As in MHS cells uptake studies, after 1 h of transfection, uptake into RAW 264.7 cells is investigated washing to remove material that was not internalized, and observing under LSCM. Orange bright QDs in the presence of Lipofectamine2000 penetrate in the cells without problem as can be seen in the figure 114. Overlapped images obtained from the red channel with the transmitted images are shown in the figure 115. As expected, like in MHS cells, chitosan microspheres are more phagocytosed than PLGA microspheres and more fluorescence is detected inside. However, one study about the responses of cultured RAW 264.7 murine cells to PLGA and chitosan microspheres and the subsequent production of reactive oxygen intermediates (ROI), nitric oxide (NO), TNF- α and COX-2, do not appreciate differences in the efficiency of phagocytosis between both cases of microspheres (Luzardo-Alvarez A. et al., 2005) .

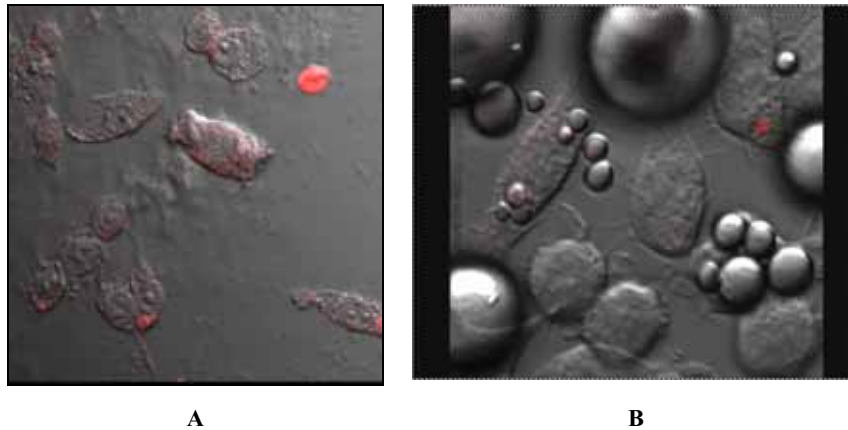


Figure 115: Cellular uptake studies of microspheres which contain orange bright QDs after 1h incubation material in RAW 264.7 cells (green excitation filter). A) Chitosan microspheres (no lipids) and B) PLGA microspheres. Microspheres were added as A) 2500 μ g, B) 2500 μ g per $0,8 \times 10^5$ cells per well.

In that way, it is confirmed that chitosan microspheres can be perfectly phagocytosed by macrophages cells.

5.4.5. In vitro parasitological studies

As can be seen in the previous results, chitosan microspheres, the new MGA delivery devices developed, showed a prolonged drug release and were perfectly phagocytosed by macrophages cells. During the development of these nano-microspheres by spray-drying, effectiveness and cytotoxicity studies have been performed. The results will be shown as follow: first those obtained from the main excipients used in the development and second the obtained from the two kinds of nano-microspheres prepared, with lipids (from O/W emulsion) or without lipids (from solutions). In all cases, the activity of the compounds was assessed in front of *Leishmania* promastigote forms so that, only those which showed effectiveness and were technological selected as the best, would be also tested against intracellular parasites (amastigote stage) afterwards. The fact that promastigote stage has been used as screening tool is due to the easy way to obtain and culture it. However, it is noteworthy that amastigotes stage is the clinical and relevant form of the parasite.

5.4.5.1. Study of the excipients

The main excipients used in the development of the new dosage form of MGA have been tested against *Leishmania* promastigote stage.

Among the different excipients tested, significant IC₅₀ value for chitosan was obtained for promastigotes assay ($112,64 \pm 0,53$ µg chitosan/ml), whereas the rest of the excipients did not show any activity. Afterwards, chitosan was tested in front of *Leishmania* amastigotes stages where the polymer also showed activity ($100,81 \pm 26,45$ µg chitosan/ml). None of the excipients were evaluated as cytotoxic (table 65). This aspect is important to rule out any possible damage into the cells where the effectiveness will be tested.

Formulation	IC ₅₀ µg/ml		CC ₅₀ µg/ml
	Promastigotes	Amastigotes	
MCT2	>25000	Na	> 25000
Polyoxyl 40 hydrogenated Castor Oil 1	>25000	Na	> 25000
Deoiled soy lecithin 1	>25000	Na	> 25000
Maltodextrin 19D/6D	>25000	Na	> 25000
Chitosan 1	$112,64 \pm 0.53$	$100,81 \pm 26.45$	> 25000

Table 65: *In vitro* activities and cytotoxicities of excipients against *L.infantum*.

Chitosan is a biopolymer which presents antimicrobial efficacy in pharmaceutical formulations against *P.aeruginosa* and *S.aureus* in emulsions, solutions (Jumaa M. et al.,

2002) and in wound dressing (Kim J. et al., 1999); it also presents activity against *E.coli* and *S.aureus* in artificial tears (Felt O. et al., 2000). Moreover, chitosan has been studied for its antifungal efficacy in front of *B.cinerea Pers.* and *Colletotrichum lagenarium* (Guo Z. et al., 2006) and its ability to induce resistance to viral infections in plants and inhibit viral infection in animal cells (Chirkov S. N., 2002). Nevertheless, the present dates report for the first time a novel *in vitro* activity of chitosan against *L. infantum* without cytotoxicity in macrophages assays in the concentrations tested. For this reason it has been protected under patent (PATENEP P200700968).

5.4.5.2. Study of meglumine antimoniate microspheres

Microspheres are suspended in water in a defined concentration (w/v) which will be used to calculate the IC₅₀ of the whole preparation. However, two components will be taking part of the possible activity, on one side antimony from MGA and chitosan as the excipient which has shown its own activity. For this reason, w/w percentages of microspheres components have been considered in the data processing to calculate IC_{50Sb^V and IC_{50chitosan. Previously, the compositions shown in the technical description of elaboration of microspheres by spray-drying (section 5.3.3.2.), are referred to the emulsion or solution before being atomized. The compositions of the microspheres in dry weight tested are shown in the table 66. The names given to each one are the same than that referred in their processes of elaboration.}}

Microspheres	% theoretical w/w components					
	MGA	Chitosan	Maltodextrin	MCT2	Polyoxyl 40 hydrogenated Castor Oil 1	Deoiled soy lecithin 1
A3	0	6,7	66,7	13,3	6,7	6,7
A4 ¹	33,3	6,7	33,3	13,3	6,7	3,3
A6	0	0	75,0	14,3	7,1	3,6
A9	11,7	5,9	58,8	11,7	5,9	5,9
A10	11,7	5,9	58,8	11,7	5,9	5,9
B8	11,7	5,9	58,8	11,7	5,9	5,9
C1	13,3	6,7	66,6	0	6,7	6,7
C2	12,5	6,3	62,4	12,5	0	6,3
C3	14,3	7,1	71,5	0	0	7,1
C4	12,5	6,3	62,4	12,5	6,3	0
C5	15,4	7,7	76,9	0	0	0
C6	0	9,1	90,9	0	0	0
D4	13,3	20	66,6	0	0	0
Experimental design 2⁵⁻¹						
E1, E2, E5, E6, E10, E11, E14 and E15	15,4	7,7	76,9	0	0	0
E9	14,29	14,29	71,43	0	0	0
E3, E4, E7, E8, E12, E13, E16 and E17	13,3	20	66,6	0	0	0

Table 66: Composition of the microspheres tested *in vitro*. (¹ A4 also contains 3,3 % of colloidal silice dioxide.)

5.4.5.2.1. *In vitro* studies of chitosan microspheres prepared from O/W emulsions by spray-drying

Among the first formulations of MGA microspheres prepared in the pre-formulation studies, **A3**, **A4**, **A6**, **A9** and **A10** are tested against *L. infantum*. The results of their activities and cytotoxicities and those of the reference compounds (Glucantime[®] and Sb^V solution), are depicted in table 67.

Sample	IC50 µg/ml						CC50 µg/ml
	Promastigotes			amastigotes			
	µg microsphere / ml	µg Sb ^V / ml	chitosan µg / ml	µg microsphere / ml	µg Sb ^V / ml	chitosan µg / ml	
A3	2473,85 ± 96,54	Not contain Sb	141,96 ± 4,20	2716,12 ± 24,47	Not contain Sb	212,91 ± 10,77	>25000
A4	2781,84 ± 15,80	214,90 ± 0,95	147,62 ± 0,63	Not technological well considered	Not technological well considered	Not technological well considered	>25000
A6	>25000	Not contain Sb	Not contain chitosan	Not activity in promastigotes	Not activity in promastigotes	Not activity in promastigotes	>25000
A9	116,78 ± 36,20	5,10 ± 1,72	8,30 ± 3,01	110,242 ± 16,30	3,19 ± 2,85	1,02 ± 1,21	>25000
A10	188,33 ± 48,89	8,29 ± 1,10	13,82 ± 2,15	133,513 ± 65,97	6,55 ± 2,54	11,89 ± 4,82	>25000
Reference products							
Sb (V)		7,05 ± 3,123			6,60 ± 3,58		>2000
Glucantime [®]		112,26 ± 12,74			176 ± 6,83		>25000

Table 67: *In vitro* activities and citotoxicities of microspheres and control drugs against *L.infantum*.

Microspheres **A3**, **A4**, **A9** and **A10** show activity in front of *Leishmania* promastigotes with different intensities, whereas **A6** did not show any. Moreover, it is worth to point out that microspheres **A3** although not contain MGA, produce a partial *L.infantum* growth inhibition either in promastigotes or amastigotes stages, so that *Leishmania* sensibility in front of chitosan is confirmed. As can be seen in previous table, microspheres **A4** are not tested in amastigotes, the reason is that this formulation has a high grade of particle size dispersity and it was ruled out to continue the studies.

The microspheres **A9** and **A10** give IC50 values (µg Sb^V/ml) lower to those obtained with Glucantime[®] solution against *Leishmania* amastigotes and promastigotes stages. Furthermore, besides to be the best technological sample in the pre-formulation studies, microspheres **A9** shows the lowest IC50 value among the first microspheres assessed. For this reason, it is selected to study in depth.

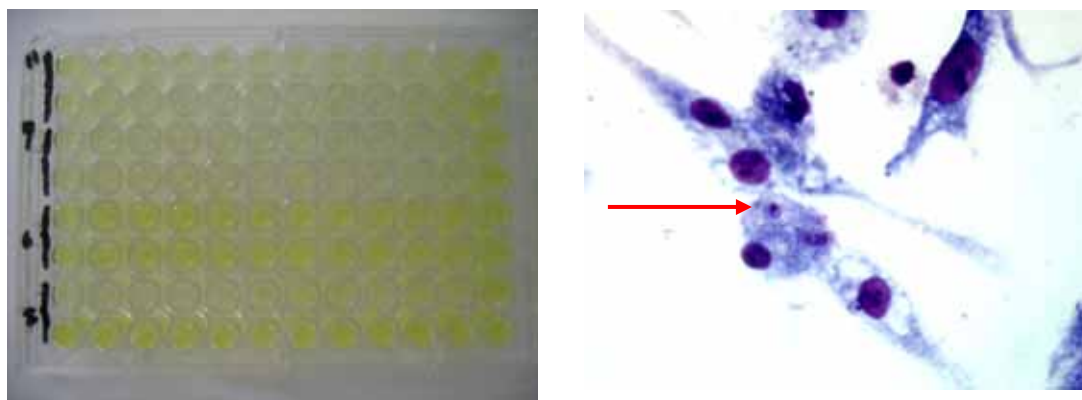


Figure 116: Illustrations of phosphatases assay performed in 96-well microtiter plate (left) and the first picture taken of peritoneal murine cells infected by *L.infantum* amastigotes (red arrow) under optical microscope (right).

Related to cytotoxicity assays, the security index (SI) ratio has been calculated dividing CC50 for murine macrophages by IC50 for protozoans. In the case of microspheres **A9**, gave a SI ratio higher than 1 (214 in assays on promastigotes and 19 in assays on amastigotes forms), indicating they are more selective against parasites than mammalian cells.

As a result of pre-formulation studies, high pressure homogenization was considered technological important and incorporated in the process of elaboration of microspheres so that, sample **B8** (idem that **A9** but adding high pressure homogenization) is selected to follow parasitic studies. As expected, antileishmanial activity against *Leishmania* promastigotes continues being present, although mean IC50Sb^V values ($3,80 \pm 0,34 \mu\text{g Sb}^{\text{V}}/\text{ml}$) do not show significant differences respected the previous sample **A9** ($5,10 \pm 1,72 \text{Sb}^{\text{V}}/\text{ml}$) ($P > 0,05$).

Next *in vitro* studies are performed with the group of microspheres (**C1 to C6**) which derive from the primary designed compound **B8** and have been designed modifying their lipidic composition in order to study its influence on the activity. All of them showed a high level of parasite growth inhibition with antimony IC50 values of 3,80 to 9,53 and chitosan IC50 values of 5,15 to 10,81 (table 68).

Formulation	IC50 $\mu\text{g Sb/ml}$	IC50 $\mu\text{g chitosan/ml}$
B8	$3,80 \pm 0,34$	$5,84 \pm 0,39$
C1	$4,20 \pm 0,85$	$6,36 \pm 1,52$
C2	$3,77 \pm 0,30$	$5,39 \pm 0,53$
C3	$3,83 \pm 0,44$	$5,15 \pm 0,93$
C4	$9,53 \pm 0,70$	$6,83 \pm 0,50$
C5	$7,45 \pm 1,12$	$10,35 \pm 1,63$
C6	Not contain Sb	$10,81 \pm 0,66$

Table 68: *In vitro* activities of different microspheres in front of *L.infantum* parasites

As can be seen in the table 66 (compositions) **C5** and **C6** are the first microspheres without lipids tested and, moreover, **C6** do not contain MGA. Although these samples are microspheres produced from solutions, both formulations also show activity as whole compounds. Therefore, chitosan continues being effective for itself. Moreover, following the same table, to study the influence of lipidic components, microspheres are grouped by percentages of MCT2, polyoxyl-40-hydrogenated castor oil 1 and deoiled soil 1 and mean IC50 values are calculated.

Considering P-values obtained by ANOVA tests in a 95 % confidence interval can be deduced that the different percentage of MCT2, polyoxyl 40 hydrogenated Castor Oil 1 and deoiled soy lecithin 1 (table 66) do not affect significantly the *in vitro* activity of SbV ($P > 0,05$). Nevertheless, chitosan activity was modified by the presence and difference percentage of deoiled soy lecithin 1 ($P < 0,05$). Error bar graph plots of MCT2 for IC50Sb^V and deoiled soy lecithin 1 for IC50chitosan are depicted in the figure 117.

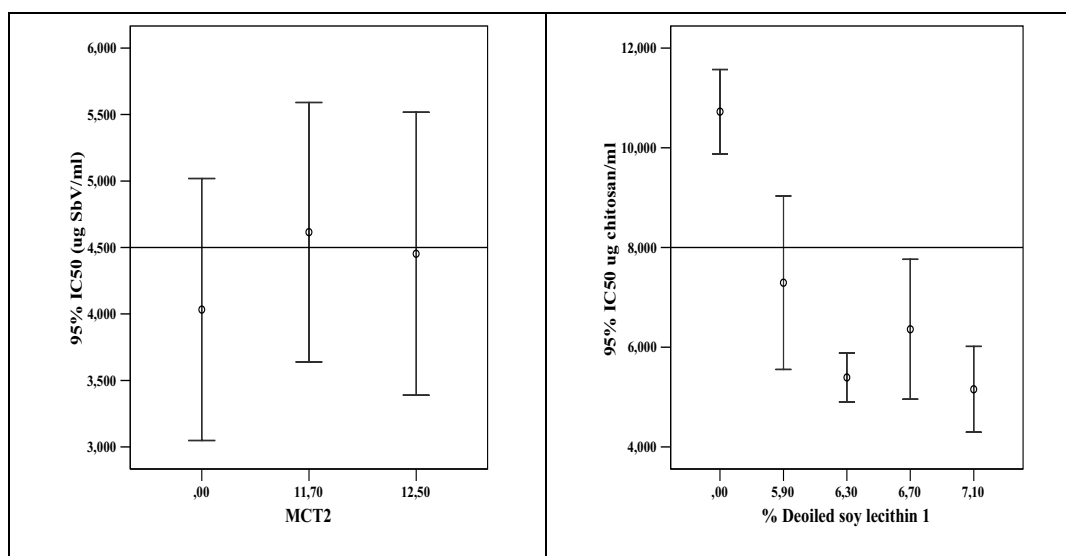


Figure 117: Error bar graph plots of MCT2 for IC50Sb^V (left) and deoiled soy lecithin 1 for IC50chitosan (right).

The addition of MCT and polyoxyl 40 hydrogenated Castor Oil, two compounds that are disrupters of PGPA, as excipients in microspheres did not produce any improvement in the activity on promastigotes when compared with microspheres without lipidic components, which were also resulted effective against *L. infantum*.

5.4.5.2.2. *In vitro* studies of chitosan microspheres prepared from solutions by spray-drying

In the last part of the previous section it has been shown that microspheres prepared from solutions by spray-drying (**C5** and **C6**) are also active in front of *Leishmania*. As these kinds of formulations have been technological improved, at the same time, more *in vitro* studies have been performed in order to complete their characterization. The sample **D4** was prepared in the pre-formulation studies of the optimization of chitosan microspheres preparing solutions by spray-drying (section 5.3.3.2.3). The original atomized solution had a 3 % chitosan concentration and then microspheres **D4** contain 20 % w/w of chitosan as can be seen in table 66 of compositions. The aim to increase chitosan proportion in this new MGA delivery device is to investigate how this increment of chitosan affects in the activity. The IC₅₀ Sb^V and IC₅₀ chitosan of microspheres **D4** are 5,43 and 12,650 µg/ml, respectively. Although, a little reduction of values can be noted comparing to the previous results, more studies are designed to draw conclusions.

A) Influence of technological factors on effectiveness of meglumine antimoniate microspheres against L.infantum

The following parasitological assays are performed using the samples obtained from the experimental design described in the section B in 5.3.3.2.3. The IC₅₀ values (µg/ml) of the whole compounds (microspheres suspensions), Sb^V and chitosan are shown in the table 69. Theoretical percentages of MGA lead to differentiate two groups of samples, one group contain 15,4 % w/w (highlighted in blue) and the other contain 13,3 % w/w (highlighted in yellow). In order to accurate the results, efficiencies of encapsulation of MGA into each microsphere have been considered to calculate IC₅₀ Sb^V. The richness of Sb^V of the MGA encapsulated is 26,6 % w/w.

Sample	Factors ¹					% MGA ²		IC50 µg/ml			
	A	B	C	D	E	% w/w A/B	% efficiency encapsulation	% found	whole compound	Sb ^V	Chitosan
E1	1	1	10	500	180	1	97,89	15,06	46,64 ± 1,79	4,60 ± 0,33	7,33 ± 0,36
E2	3	1	10	500	130	3	92,38	14,21	42,86 ± 10,42	4,15 ± 0,84	6,88 ± 1,46
E3	1	3	10	500	130	0,3	94,58	12,61	133,30 ± 9,54	8,87 ± 1,01	36,78 ± 0,61
E4	3	3	10	500	180	1	99,17	13,22	60,91 ± 3,32	6,32 ± 1,66	20,40 ± 3,20
E5	1	1	20	500	130	1	93,19	14,34	50,55 ± 30,16	4,62 ± 1,22	7,68 ± 2,60
E6	3	1	20	500	180	3	90,67	13,95	46,24 ± 23,54	4,63 ± 0,12	12,51 ± 7,96
E7	1	3	20	500	180	0,3	99,32	13,24	182,61 ± 38,26	10,59 ± 0,37	46,29 ± 5,78
E8	3	3	20	500	130	1	92,81	12,37	105,80 ± 49,66	7,00 ± 1,05	29,20 ± 9,44
E9	2	2	15	600	155	1	91,1	13,01	95,43 ± 17,83	7,84 ± 2,57	20,20 ± 3,71
E10	1	1	10	700	130	1	90,1	13,86	69,53 ± 55,13	5,47 ± 1,78	9,52 ± 4,21
E11	3	1	10	700	180	3	82,95	12,76	49,94 ± 8,61	5,48 ± 2,61	9,31 ± 3,78
E12	1	3	10	700	180	0,3	87,43	11,66	116,79 ± 65,72	7,78 ± 0,29	32,64 ± 10,75
E13	3	3	10	700	130	1	95,79	12,77	171,33 ± 124,66	8,33 ± 2,99	41,77 ± 23,75
E14	1	1	20	700	180	0,3	90,52	13,93	88,65 ± 6,57	6,35 ± 0,98	11,39 ± 1,56
E15	3	1	20	700	130	3	93,85	14,44	70,59 ± 31,63	6,54 ± 0,32	10,74 ± 0,65
E16	1	3	20	700	130	0,3	102,79	13,71	206,35 ± 126,34	11,84 ± 3,89	58,21 ± 14,54
E17	3	3	20	700	180	1	97,05	12,94	270,06 ± 164,69	14,85 ± 2,03	72,83 ± 17,42

Table 69: *In vitro* activities of chitosan microspheres against *L.infantum* promastigotes. Blue and yellow highlighted samples theoretically contain 15,4 % and 13,3 % of MGA, and 7,7 % and 20 % of chitosan, respectively.

¹ A: % v/v glutaraldehyd, B: % w/v chitosan, C: % pump, D: flow rate (l/h), E: inlet temperature (° C). ² Real percentages of MGA encapsulated in the microspheres.

In vitro activities of chitosan microspheres in increasing order according to IC50 microspheres, IC50 Sb^V and IC50 chitosan (µg/ml) are shown in table 70.

Sample	IC50 microspheres (µg/ml)	Sample	IC50 SbV (µg/ml)	Sample	IC50 chitosan (µg/ml)
E17	270,06 ± 164,69	E17	14,85 ± 2,03	E17	72,83 ± 17,42
E16	206,35 ± 126,34	E16	11,84 ± 3,89	E16	58,21 ± 14,54
E7	182,61 ± 38,26	E7	10,59 ± 0,37	E7	46,29 ± 5,78
E13	171,33 ± 124,66	E3	8,87 ± 1,01	E13	41,77 ± 23,75
E3	133,30 ± 9,54	E13	8,33 ± 2,99	E3	36,78 ± 0,61
E12	116,79 ± 65,72	E9	7,84 ± 2,57	E12	32,64 ± 10,75
E8	105,80 ± 49,66	E12	7,78 ± 0,29	E8	29,20 ± 9,44
E9	95,43 ± 17,83	E8	7,00 ± 1,05	E4	20,40 ± 3,20
E14	88,65 ± 6,57	E15	6,54 ± 0,32	E9	20,20 ± 3,71
E15	70,59 ± 31,63	E14	6,35 ± 0,98	E6	12,51 ± 7,96
E10	69,53 ± 55,13	E4	6,32 ± 1,66	E14	11,39 ± 1,56
E4	60,91 ± 3,32	E11	5,48 ± 2,61	E15	10,74 ± 0,65
E5	50,55 ± 30,16	E10	5,47 ± 1,78	E10	9,52 ± 4,21
E11	49,94 ± 8,61	E6	4,63 ± 0,12	E11	9,31 ± 3,78
E1	46,64 ± 1,79	E5	4,62 ± 1,22	E5	7,68 ± 2,60
E6	46,24 ± 23,54	E1	4,60 ± 0,33	E1	7,33 ± 0,36
E2	42,86 ± 10,42	E2	4,15 ± 0,84	E2	6,88 ± 1,46

Table 70: *In vitro* activities of chitosan microspheres are shown in decreasing order according to IC50 microspheres, IC50 Sb^V and IC50 chitosan (µg/ml).

The sample that has more activity against *L.infantum* is **E2**. Apparently, the composition of microspheres could influence in the IC50 values watching the results. Whereas, microspheres with high percentage of chitosan have higher IC50 values (highlighted in yellow), microspheres with lower chitosan percentage are located in the bottom of the table with the lowest IC50 values. Factorial ANOVA test has been used to analyze the results comparing the variances to the F-ratio values and study the influence of all the factors and their interactions. The results of ANOVA test for IC50 Sb^V are shown in the table 71.

Analysis of de la Variance for IC50Sb ^V					
Source	Sum of squares	Df	Mean square	F-Ratio	P-Value
A:Glutaraldehyd conc	0,496673	1	0,496673	2,06	0,3872
B:Chitosan conc.	71,1956	1	71,1956	295,67	0,0370
C:Pump	14,8514	1	14,8514	61,68	0,0806
D:Flow rate	15,7232	1	15,7232	65,30	0,0784
E:Inlet temperature	0,89823	1	0,89823	3,73	0,3041
AB	0,34545	1	0,34545	1,43	0,4429
AC	0,265483	1	0,265483	1,10	0,4845
AD	6,6861	1	6,6861	27,77	0,1194
AE	2,84344	1	2,84344	11,81	0,1803
BC	6,94191	1	6,94191	28,83	0,1172
BD	1,09464	1	1,09464	4,55	0,2792
BE	0,650846	1	0,650846	2,70	0,3479
CD	5,78523	1	5,78523	24,03	0,1281
CE	5,15631	1	5,15631	21,41	0,1355
DE	0,0385141	1	0,0385141	0,16	0,7578
Total error	0,240797	1	0,240797		
Total (corr.)	133,214	16			
R-squared = 99,8192 percent					
R-squared (ajusted for d.f.) = 97,1078 percent					
Standard error of Est. = 0,49071					
Mean absolut error = 0,0560069					
Durbin-Watson Statistic = 2,125					
Residual autocorrelation Lag 1 = -0,0661765					

Table 71: ANOVA results for IC50 Sb^V

Taking into account P-values, it is confirmed that chitosan concentration can be considered a factor which influences significantly in IC50Sb^V in a 95 % confidence interval ($P < 0,05$).

In the standardized pareto chart (figure 118) can be appreciate how glutaraldehyd concentration, although it does not influence significantly, is able to reduce slightly the IC50 Sb^V values. Chitosan is also a significant factor ($P < 0,05$) in IC50 microspheres and IC50 chitosan values.

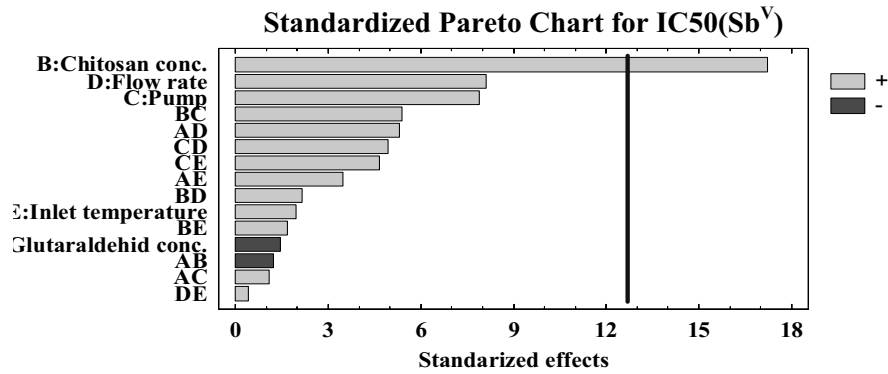


Figure 118: Standardized pareto chart for IC50Sb^V.

To study more properly the influence of the factors, the interaction DE has been included in the total error due to have an F-ratio near to 0. However, the results obtained after that (table 72) show that many factors and interactions do not influence significantly on IC50Sb^V because the probability of the differences was by chance, is higher than 10 % (highlighted in light grey). Therefore, they can be included in the experimental error and let us to accurate the results (table 73).

Analysis of de la Variance for IC50Sb ^V					
Source	Sum of squares	Df	Mean square	F-Ratio	P-Value
A:Glutaraldehyd conc	0,496673	1	0,496673	3,56	0,2000
B:Chitosan concentra	71,1956	1	71,1956	509,80	0,0020
C:Pump	14,8514	1	14,8514	106,34	0,0093
D:Flow rate	15,7232	1	15,7232	112,59	0,0088
E:Inlet temperature	0,89823	1	0,89823	6,43	0,1266
AB	0,34545	1	0,34545	2,47	0,2564
AC	0,265483	1	0,265483	1,90	0,3019
AD	6,6861	1	6,6861	47,88	0,0203
AE	2,84344	1	2,84344	20,36	0,0458
BC	6,94191	1	6,94191	49,71	0,0195
BD	1,09464	1	1,09464	7,84	0,1074
BE	0,650846	1	0,650846	4,66	0,1635
CD	5,78523	1	5,78523	41,43	0,0233
CE	5,15631	1	5,15631	36,92	0,0260
Total Error	0,279311	2	0,139655		
Total (corr.)	133,214	16			

R-squared = 99,7903 percent
R-squared (adjusted for d.f.) = 98,3226 percent
Standard error of Est. = 0,373705
Mean absolute error = 0,0741799
Durbin-Watson statistic= 2,19394 (P=0,0008)
Residual autocorrelation Lag 1 = -0,10876

Table 72: ANOVA results for IC50 Sb^V

Analysis of de la Variance for IC50Sb ^V					
Source	Sum of squares	Df	Mean square	F-Ratio	P-Value
B:Chitosan concentra	71,1956	1	71,1956	147,46	0,0000
C:Pump	14,8514	1	14,8514	30,76	0,0009
D:Flow rate	15,7232	1	15,7232	32,56	0,0007
AD	6,6861	1	6,6861	13,85	0,0074
AE	2,84344	1	2,84344	5,89	0,0456
BC	6,94191	1	6,94191	14,38	0,0068
BE	0,650846	1	0,650846	1,35	0,2837
CD	5,78523	1	5,78523	11,98	0,0105
CE	5,15631	1	5,15631	10,68	0,0137
Total error	3,37978	7	0,482826		
Total (corr.)	133,214	16			

R-squared = 97,4629 percent
R-squared (ajustado para g.l.) = 94,2009 percent
Standard error of Est. = 0,694857
Mean Error absoluto de la media = 0,364387
Estadístico Durbin-Watson = 2,50884 (P=0,0080)
Autocorrelación residual Lag 1 = -0,31928

Table 73: ANOVA results for IC50 Sb^V

That factors and interactions highlighted in dark grey can be considered influence parameters on IC50Sb^V values.

The minimum value of IC50Sb^V obtained in this experimental design is that produced by E2 microspheres (4,14 µg/ml). The mathematical optimized response given by the statistical program to minimize IC50Sb^V values is as follow: 2,807 µg/ml is the optimum value

Optimized answer			

Aim: minimum IC50Sb ^V			
Optimum value = 2,807 µg/ml			
Factor	Lower	Higher	Optimum

Glutaraldehyd conc.	1,0	3,0	2,399
Chitosan conc.	1,0	3,0	1,0
Pump	10,0	20,0	20,0
Flow rate	500,0	700,0	501,778
Inlet temperature	130,0	180,0	130,0

Table 74: Optimized answer to minimize IC50Sb^V

mathematically considered by the program and the conditions to obtain it: 2,399 % v/v glutaraldehyd concentration, 1 % chitosan concentration, 20 % of pump, 501,778 l/h of flow rate and 130 °C of inlet temperature (table 74). If these parameters are compared to the spray-drying conditions to obtain E2 microspheres, pump rate is not the same. E2 microspheres were produced at 10 % of pump. To study in depth the influence of pump rate on IC50Sb^V, the estimated response surface of the interactions between pump rate and chitosan concentration (BC) and pump and flow rate (CD) are analysed.

It can be seen in figure 119 that is possible to use both levels of pump rates, to obtain similar IC50Sb^V values than E2 microspheres (from 4µg/ml to 5 µ g/ml) in a range of chitosan concentration between 1 % to 1,5 %, approximately (maintaining 3 % v/v glutaraldehyd concentration, 500 l/h pump rate and 130 °C of inlet temperature).

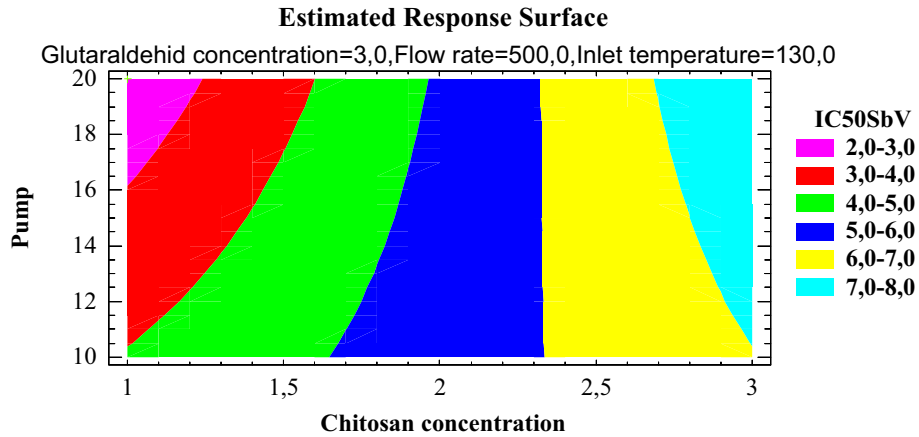


Figure 119: Estimated response surface for IC50SbV.

Analysing the interaction CD (pump and flow rate) (figure 120) it can be seen that working under 580 l/h of flow rate is possible to obtain IC50Sb^V values lower than 5 µg/ml in any pump range between 10 and 20 %.

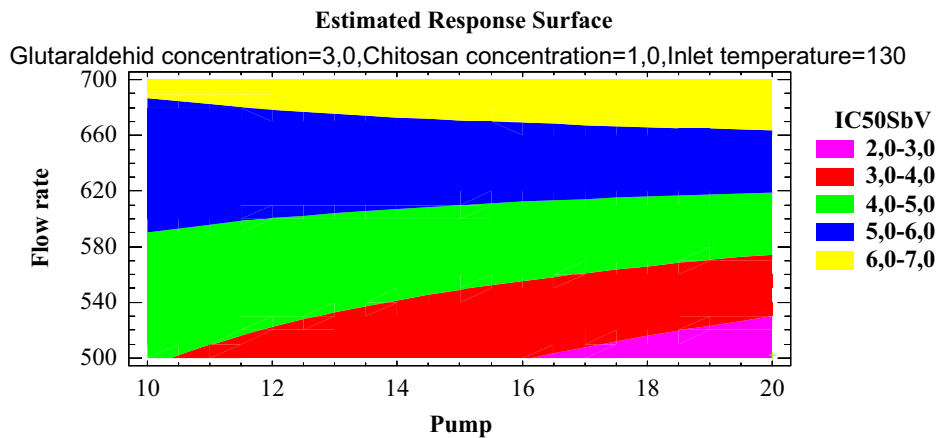


Figure 120: Estimated response surface for IC50SbV.

Summarising, the most adequate spray drying conditions to produce the most effective microspheres are those where chitosan concentration is 1 %, glutaraldehyd concentration is 3 % v/v and the inlet temperature is 130 °C. Maintaining the previous parameters pump rate could be between 10 % to 20 % and flow rate under 580 l/h (table 75).

Spray conditions	
Glutaraldehyd conc.	3 %
Chitosan conc.	1 %
Inlet temperature	130 °C
Pump rate	10-20 %
Flow rate	< 580 l/h

Table 75: Most adequate spray conditions to obtain the most active MGA chitosan microspheres.

Nevertheless, it is believed necessary to study the *in vitro* results of effectiveness and dissolution studies of the tested microspheres together, in order to elucidate why high chitosan concentrations increase $IC_{50}Sb^V$. For that, IC_{50} values will be related to the drug released in 24 h, the drug release mechanism and the drug release kinetics in the next sections.

B) Relation between effectiveness against L.infantum and dissolution studies of chitosan microspheres

B.1. IC_{50} vs. drug released in 24h

As can be seen in the section B.8 of the dissolution studies (5.3.3.2.3), those microspheres composed with greater quantities of chitosan release inferior quantities of drug in 24 h, probably due to a viscosity growth.

Antimony quantities released in 24 h (Q_{24h}) are fit in a lineal model to be related to IC_{50} microspheres, $IC_{50} Sb^V$ and IC_{50} chitosan. The next equations are obtained:

$$1. IC_{50} \text{ microspheres} = 707,78 - 7,5974 * Q_{24h}$$

$$2. IC_{50} Sb^V = 31,2779 - 0,3020 * Q_{24h}$$

$$3. IC_{50} \text{ chitosan} = 211,279 - 2,3466 * Q_{24h}$$

P-values are lower than 0,05 in each case and then a significant statistic relation between IC_{50} and Q_{24h} exists in a 95 % interval confidence. The correlation coefficients are $R^2_1 = -0,5935$, $R^2_2 = -0,5420$ and $R^2_3 = -0,6099$ respectively. The negative coefficient (slope) in the equations means that when greater is the quantity of Sb released lower are IC_{50} values. Moreover, this correlation increases when the study is made with the mean IC_{50} values of the groups of microspheres divided by chitosan percentage (% w/v) and

glutaraldehyd percentage (% v/v) (table 76). The correlation coefficients were $R^2_1 = -0,7897$, $R^2_2 = -0,7609$ and $R^2_3 = -0,7291$.

% chitosan	% glutaraldehyd	IC50 (μg microspheres/ml)	IC50 (μg Sb ^V /ml)	IC50($\mu\text{g}/\text{ml}$ chitosan)	Q24h
1	1	63,8426	5,25811	8,98074	78,2784
	3	52,4064	5,19945	9,8575	85,0831
3	1	159,761	9,77082	43,4802	74,2386
	3	152,025	9,1244	41,0507	77,7268
R²		-0,789695363	-0,760942686	-0,72912449	

Table 76: Mean IC50 values obtained by groups of microspheres according to chitsosan and glutaraldehyd percentages.

B.2. IC50 vs. drug release mechanism

Mean IC50 values of the microspheres with drug non Fickian release mechanism (diffusional exponent of Korsmeyer-Peppas equation (N) >0,5) were lower compared to the mean IC50 values obtained from the microspheres with normal drug Fickian release (N<0,5) (figure 121). It is believed that the additional mechanism of mass transport in the first group influences in the quantity of drug released. Thus, if the mean quantities of Sb released by groups are 85,08 % in the first case and 77,35 % in the second in 24 h, the sensibility differences shown by *L.infantum* are as expected .

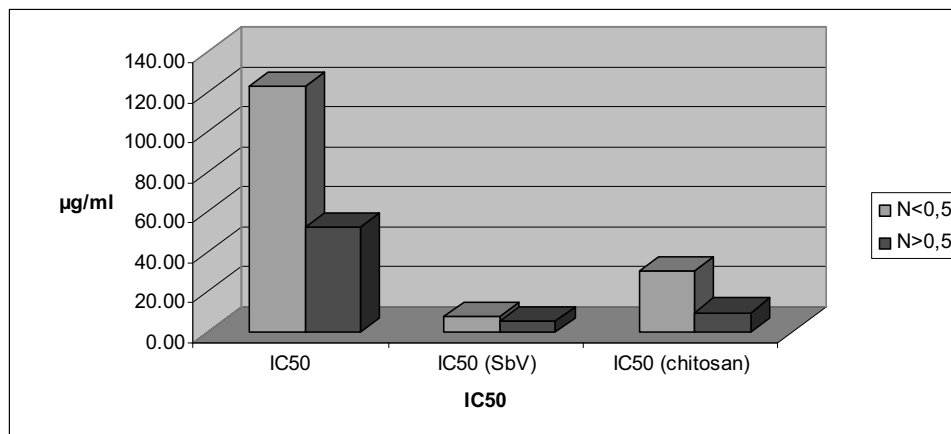


Figure 121: IC50, IC50 (Sb^V) and IC50 (chitosan) by groups of microspheres divided depending on drug release mechanism (N<0,5: normal Fickian diffusion, N>0,5: additional mechanism).

B.3. IC50 vs. drug release kinetics

Resorting to the results of dissolution tests, the constants obtained by the kinetic models named Korsmeyer-Peppas and first order, are fit in a lineal model to be related to IC50, IC50 (Sb^V) and IC50 chitosan. Korsmeyer-Peppas model was the function, statistically explained better the Sb release kinetics. The lineal equations obtained for this function are:

1. IC50 microspheres = 342,816 - 918,61*K_k
2. IC50 Sb^V = 18,0065 - 41,324*K_k
3. IC50 chitosan = 97,829 - 280,912*K_k

Taking account P- values obtained by ANOVA test a significant statistic relation between IC50s and K_k exists in 90 % interval confidence (P <0,10). The correlation coefficients are R²₁ = -0,4619, R²₂ = -0,4770 and R²₃ = -0,4700 respectively. There is not significant correlation between IC50 values and K₁.

Summarizing, the group of microspheres with antimony non-Fickian release (**E11**, **E2**, **E6** and **E15**) is among the more active samples against *L.infantum*. Even, **E2** is that produce lowest IC50 values although it does not release the maximum quantity of drug in 24 h (this was done by **E11** with 91,62 %). Paying attention to the previous data, common technological characteristics, low percentages of chitosan and high percentages of cross-linking, has been used to produce all of them.

These active microspheres showed a MGA release pattern characterized by an initial burst effect followed by a prolonged release and consequently, it is believe that the new MGA delivery device developed could be a good alternative to the treatment of leishmaniosis. Some authors believe that the success of antileishmanial therapy depends on maintaining sustained concentrations for most of the time. First studies developed with sodium stibogluconate in hamsters suggested that for eradicating the parasites *in vivo*, the peak concentration of Sb was more important than the area-under-the curve (AUC). However, this may not be the case since a short exposure of the parasites to a high concentration of Sb followed by a sharp decline (i.e. smaller AUC) would not ensure abating the parasites to the same extent as if a sufficiently high concentration is maintained for a reasonable length of time (i.e. larger AUC) (Al-Jaser et al., 1995). Similarly, the application of

microencapsulation to achieve a slow release of rifampicin to the treatment of *Micobacterium tuberculosis* (another intracellular organism) has demonstrated to be ideal to maintain both high drug level in alveolar macrophages and low drug level in blood (Makino K., et al. 2004).

5.5. CONCLUSIONS

1. A new meglumine antimoniate delivery device for the treatment of *leishmaniosis* has been properly developed using spray drying technique.
2. SEM and ICP-OES techniques confirm that meglumine antimoniate has been efficiently encapsulated in chitosan microspheres atomizing either an O/W emulsion or a solution by spray drying with high yield.
3. Using the method of meglumine antimoniate encapsulation developed, it is possible to achieve efficiencies of encapsulation higher than 90 % and process yields of 60 %.
4. Experimental designs have let to optimize the production of chitosan microspheres and study the influence of formulation and technological parameters on microspheres properties.
5. All the antimony IC₅₀ values from encapsulated meglumine antimoniate in the chitosan microspheres tested against promastigotes and amastigotes are considerably lower compared to the mean value of IC₅₀ in Glucantime[®] solution and give an Safety Index ratio higher than 1.
6. It is reported for the first time a novel *in vitro* activity of chitosan against *L.infantum* with a low cytotoxicity in macrophages assays (PATENEP P200700968).
7. Medium chain triglycerides and polyoxyl 40 hydrogenated Castor Oil, likely disrupters of P-gp, as excipients in microspheres do not produce any improvement in the activity on promastigotes of *L.infantum* when compared with microspheres without lipidic components.
8. QDs have been properly entrapped into chitosan and PLGA microspheres by spray drying and solvent evaporation techniques.

9. The targeting of chitosan microspheres to macrophages is proved by uptake studies using QDs assisted imaging. These studies confirm the better suitability of chitosan as polymer to target drugs to macrophages compared to the commonly used PLGA.
10. High percentages of chitosan in solutions to be spray-dried reduce the yield of the process, produce larger wrinkled microspheres but increase the efficiency of encapsulation.
11. A method to study meglumine antimoniate release profile from chitosan microspheres has been successfully developed.
12. Chitosan microspheres exhibit a biphasic prolonged release for 24 h, characterized by an initial burst effect followed by slow release. High polymer ratios reduce the drug release in all the study.
13. The model of Korsmeyer-Peppas is the one which, statistically, describes the best meglumine antimoniate release mechanism from chitosan microspheres. Two different kinds of meglumine antimoniate release mechanism have been found among chitosan microspheres; Fickian and Non-Fickian release.
14. High percentages of glutaraldehyd in chitosan microspheres tend to increase significantly the presence of Non-Fickian drug release mechanism. These microspheres show the slowest release for the first 3 h but the highest percentage of drug released at 24 h. Moreover, they are among the more active microspheres against *L.infantum*.
15. The minimum antimony IC50 value of chitosan microspheres is obtained using high percentages of glutaraldehyd, low percentages of chitosan and low inlet temperatures.
16. This new delivery system could offer a new pharmacological tool for treatment of leishmaniosis that reduces the doses required, lowering toxic side effects due to meglumine antimoniate.